

**METHOD OPTIMIZATION AND GENE EXPRESSION ANALYSIS  
FOR INTERFERON KAPPA mRNA IN HPV-ASSOCIATED  
CERVICAL DISEASE**

BY

CORRENE A DECARLO

A Thesis Submitted to the Faculty of Biology in Partial Fulfillment of the Requirements for the  
Degree of

MASTER OF SCIENCE

Department of Biology  
Lakehead University  
Thunder Bay, Ontario

©July 2008



Library and  
Archives Canada

Published Heritage  
Branch

395 Wellington Street  
Ottawa ON K1A 0N4  
Canada

Bibliothèque et  
Archives Canada

Direction du  
Patrimoine de l'édition

395, rue Wellington  
Ottawa ON K1A 0N4  
Canada

*Your file Votre référence*  
ISBN: 978-0-494-43420-8  
*Our file Notre référence*  
ISBN: 978-0-494-43420-8

**NOTICE:**

The author has granted a non-exclusive license allowing Library and Archives Canada to reproduce, publish, archive, preserve, conserve, communicate to the public by telecommunication or on the Internet, loan, distribute and sell theses worldwide, for commercial or non-commercial purposes, in microform, paper, electronic and/or any other formats.

The author retains copyright ownership and moral rights in this thesis. Neither the thesis nor substantial extracts from it may be printed or otherwise reproduced without the author's permission.

**AVIS:**

L'auteur a accordé une licence non exclusive permettant à la Bibliothèque et Archives Canada de reproduire, publier, archiver, sauvegarder, conserver, transmettre au public par télécommunication ou par l'Internet, prêter, distribuer et vendre des thèses partout dans le monde, à des fins commerciales ou autres, sur support microforme, papier, électronique et/ou autres formats.

L'auteur conserve la propriété du droit d'auteur et des droits moraux qui protègent cette thèse. Ni la thèse ni des extraits substantiels de celle-ci ne doivent être imprimés ou autrement reproduits sans son autorisation.

---

In compliance with the Canadian Privacy Act some supporting forms may have been removed from this thesis.

Conformément à la loi canadienne sur la protection de la vie privée, quelques formulaires secondaires ont été enlevés de cette thèse.

While these forms may be included in the document page count, their removal does not represent any loss of content from the thesis.

Bien que ces formulaires aient inclus dans la pagination, il n'y aura aucun contenu manquant.

■ ■ ■  
**Canada**

## **DEDICATION**

To my wonderful parents for their endless support and encouragement

## ACKNOWLEDGMENTS

First and foremost, I would like to thank my supervisor, Dr. Ingeborg Zehbe. I am forever grateful for this opportunity and it would not have been possible without your guidance, knowledge and support. This experience has made me want to be a researcher for life.

Thank you!

I would like to extend a big thank you to my supervisory committee, Drs Dave Law, Marina Ulanova and Kam Leung, for their helpful suggestions, advice and use of laboratory equipment.

To Christina Richard, a person whom I cannot give enough thank you's to. Its amazing how one person can completely change the environment in which one works and, in this case, it was for the better. Thank you for bringing fun into the lab (bully; "this cap doesn't close," "WA," "You want a Christmas card, HERE's your Christmas card" ). Thank you for always being a reliable source of support and for making me see that intelligence will always rise above politics and, above all, thank you for your friendship Tina!

To the group at Genesis Genomics; Kerry Robinson, Jen Maki, Andrea Maggrah, Caroline Karwinski, Orlanda DaSilva, and Brian Reguly. Thank you for your technical help and for representing a positive environment to work in.

To Dr. Julieta Werner and Jeff Werner, two people I value tremendously. Thank you so much for the many laughs (Courtyard, "Living without hair," "Vodka"), for being my qRT-PCR mentor (Julieta), for your support both in the lab and outside and for giving me home-cooked meals and the opportunity to meet your two little scientists at home, Erick and Ian (from whom I learned the intricacies of game cube and the history of dinosaurs, and whom I will never forget).

To the TBRHSC central laboratory staff (pathology/histology), Evelyn McLean, Tammy Wood and other supportive staff, the TBRHSC colposcopy clinic staff, Dr. Nick Escott, Dr. Glen Holloway (late) and colposcopy nurses Carol, Bonnie and Donna as well as Dr. Anthes in Radiation Oncology: Thank you so very much for help with obtaining patient tissue, for help with tissue processing and for providing me with valuable exposure to patients.

To Jessica Nehrebecky (aka Prettie): Thank you for your humor ("SHE JUS SHO UP," "Go update," "the Z, D&T comic strip," "the look," "Monkey"), ridiculous emails and Tx, of course, for your friendship! I will never forget our science experiments and your help with reverse transcription and my poster.

Thank you to all laboratory staff for your support throughout the past two years and specifically Kylie Funk-Williams, Alexis McEwan, Erin Karlsted, Andy Cumming, Marlon Haggarty and Caroline Chung for your friendship. Thank you to Kyle Cullingham for specimen collection. Thank you to NOSM research personnel; Dr. Neelam Khaper, Rebecca Barns, Sean Bryan, Pete Mitsopolous, Lindsay Sutherland, and Pam Tallon for your support and encouragement.

## **Personal Acknowledgments**

To my best friend Andrea: your insight, encouragement and endless support and friendship mean so much to me and has helped me through this entire process. I wouldn't have even dreamed about moving to Thunder Bay if you hadn't, one day, said "What about northern Ontario?" Best friends just know these things!

To James, thanks for being there for me and making sure there was always a smile on my face.

To Vic, the sweetest person from Cow-town. Thank you for your friendship, encouragement and story swaps. We both got through it alive!!

To my good friend Olga: My first friend in Thunder Bay. Thank you for all your helpful advice and discussions and the fun we had hanging out in T-Bay.

I want to thank the totally amazing roommates I had while living in Thunder Bay: Julie Rafaelli, Jen Clark, Alicia Kirkwood, Sandra Fortier, Roxanne Pellow and Erin Lynch, you all helped make me feel at home in northern Ontario and truly helped make this experience amazing. Thank you for being such awesome people to live with!

To Lisa Caruso and Yvette Cuthbertson, my crantini drinking, movie-watching, sing-star singing power squad. Thanks for giving me a second home in Thunder Bay and for lending me your ears on many occasions. Most of all, thank you for the ridiculous laughs and fun times ("Team Moo," "Keychain," Shags, ice cream runs, and so many more). I'm so glad I met you two!!

Lastly, the most important and influential people in my life must be thanked. Thank you to my parents for your infinite love and support through all of my decisions. You both mean so much to me and I am forever grateful for everything you have done for me, particularly within the past two years. I love you and thank you.

## TABLE OF CONTENTS

<b>DEDICATION.....</b>	<b>1</b>
<b>ACKNOWLEDGMENTS.....</b>	<b>2</b>
<b>TABLE OF CONTENTS.....</b>	<b>4</b>
<b>LIST OF FIGURES.....</b>	<b>8</b>
<b>LIST OF TABLES.....</b>	<b>10</b>
<b>LIST OF ABBREVIATIONS.....</b>	<b>11</b>
<b>ABSTRACT.....</b>	<b>13</b>
<b>1.0 INTRODUCTION.....</b>	<b>15</b>
1.1 Cervical Cancer and Cervical Precursor Lesions.....	15
1.2 Human Papillomavirus.....	15
1.3 Interferons.....	19
1.4 Novel Interferon Kappa.....	22
1.5 Interferon Induction Pathways.....	23
1.5.1 <i>Extracytoplasmic Pathogens Sensors</i> .....	23
1.5.2 <i>Cytoplasmic Pathogen Sensors</i> .....	25
1.6 Interferon Regulatory Factors.....	26
1.7 Interferon Signaling Pathways.....	26
1.8 Interferon Stimulated Genes.....	27
1.9 Human Papillomavirus and Interferon Interactions.....	27
1.10 Interferons and Cervical Disease.....	28
1.11 Method Development.....	29
1.12 Research Rationale.....	31

1.13 Hypotheses.....	31
1.14 Research Aims.....	32
<b>2.0 MATERIALS AND METHODS.....</b>	<b>33</b>
2.1 Sample Preparation.....	33
2.1.1 <i>Cell Lines</i> .....	33
2.1.2 <i>Biopsy Material</i> .....	33
2.1.3 <i>Peripheral Blood Lymphocytes</i> .....	34
2.2 DNA Extraction.....	34
2.3 Polymerase Chain Reaction.....	35
2.4 P16 Staining.....	36
2.5 Immunohistochemistry.....	36
2.6 RNA Extraction.....	36
2.7 Nucleic Acid Quantification and Integrity Assessment.....	37
2.8 Laser Capture Microdissection.....	38
2.9 Reverse Transcription and cDNA Amplification.....	38
2.10 Quantitative Real-Time Polymerase Chain Reaction.....	39
2.11 Statistical Analysis.....	40
<b>3.0 RESULTS.....</b>	<b>41</b>
3.1 Sample Size and Material Characterization.....	41
3.1.1 <i>RNA Integrity of Sample</i> .....	41
3.1.2 <i>HPV Typing</i> .....	41
3.1.3 <i>Infiltrating CD4/CD8+ Cell Status</i> .....	46
3.2 Method Development for IFN- $\kappa$ Detection in Cervical Material: DNA.....	50

3.2.1	<i>Optimal PCR conditions</i> .....	50
3.2.2	<i>DNA Extraction Methods: NIKS and Tissue Samples</i> .....	50
3.2.3	<i>DNA Extraction Methods: LCM material</i> .....	53
3.3	Method Development for IFN- $\kappa$ Detection in Cervical Material: RNA.....	53
3.3.1	<i>Sample Storage and RNA Extraction</i> .....	53
3.3.2	<i>RNA Integrity and Tissue Morphology of LCM Samples</i> .....	59
3.3.3	<i>Reverse Transcription</i> .....	59
3.3.4	<i>HKG for Normalization between Samples</i> .....	64
3.3.5	<i>cDNA Amplification</i> .....	64
3.3.6	<i>Sensitivity of qRT-PCR and LCM for IFN Detection</i> .....	64
3.4	Interferon Gene Expression Profile Normal, Dysplastic and Carcinoma Tissue.....	69
3.4.1	<i>IFN-<math>\kappa</math> Expression</i> .....	69
3.4.2	<i>IFN-<math>\beta</math> Expression</i> .....	69
3.4.3	<i>IFN-<math>\gamma</math> Expression</i> .....	76
3.4.4	<i>Relative Expression of IFNs</i> .....	76
3.4.5	<i>Cervical Carcinoma Tissue</i> .....	83
3.5	In Vitro IFN Expression.....	84
3.5.1	<i>Keratinocytes and Cervical Cancer-Derived Cell Lines</i> .....	84
3.6	Peripheral Expression of IFNs in Patients.....	84
3.6.1	<i>Peripheral Blood Lymphocytes</i> .....	84
3.7	LCM Analysis of IFN Expression in Cervical Tissue.....	87
3.7.1	<i>Microdissected Cervical Epithelium and Stroma</i> .....	87
3.8	IFN Gene Expression in Repeated LCM Samples..	90

<b>4.0 DISCUSSION.....</b>	<b>92</b>
4.1 Method Development.....	92
4.2 Interferon Expression in Patients.....	96
4.3 Interferon Expression in Cell Lines.....	101
4.4 Conclusions and Future Studies.....	102
<b>5.0 REFERENCES.....</b>	<b>105</b>
<b>6.0 APPENDIX A.....</b>	<b>116</b>
6.1 Survey of Innate Immune Response in Microdissected Cervical Material.....	116
6.1.1 <i>Individual Normal Cases (n=12)</i> .....	116
6.1.2 <i>Individual Dysplastic Cases (n=11)</i> .....	121
6.2 Prevalence of Gene Expression in LCM Cohort.....	126
6.3 Statistical Difference in Gene Expression in LCM Cohort.....	127
6.4 Cell-specific Gene Expression in Cervical Carcinoma Epithelium and Stroma.....	132
6.5 Inter-Individual Distribution of Innate Immunity Gene Expression.....	133

## LIST OF FIGURES

<b>Figure 1.</b> HPV genome.....	16
<b>Figure 2.</b> HPV viral life cycle and cervical epithelium.....	18
<b>Figure 3.</b> The cell cycle, Rb and p16 <sup>INK4a</sup> .....	20
<b>Figure 4.</b> Interferon induction and signaling pathways.....	24
<b>Figure 5.</b> RNA integrity of samples.....	43
<b>Figure 6.</b> HPV detection in cervical biopsy material.....	45
<b>Figure 7.</b> p16 immunohistochemistry for the detection of high risk HPV infection in cervical samples.....	47
<b>Figure 8.</b> Infiltrating CD4/CD8+ cells in the cervical microenvironment.....	48
<b>Figure 9.</b> Optimization of PCR conditions for beta-globin detection.....	51
<b>Figure 10.</b> HPV detection in cervical samples using agarose gel electrophoresis.....	54
<b>Figure 11.</b> Sensitivity of LCM for detection of quality DNA.....	55
<b>Figure 12.</b> RNA integrity of cervical tissue using different sample storage and extraction methods.....	57
<b>Figure 13.</b> RNA integrity and tissue morphology of laser capture Microdissected cervical tissue. ....	60
<b>Figure 14.</b> The effect of different RT primer pairs on HKG expression.....	62
<b>Figure 15.</b> Housekeeping gene suitability for normalization across cervical disease states.....	65
<b>Figure 16.</b> Uniform cDNA amplification in cervical samples.....	67
<b>Figure 17.</b> Sensitivity of qRT-PCR and LCM for the detection of interferon gene expression in dysplastic cervical tissue.....	70
<b>Figure 18.</b> IFN- $\kappa$ gene expression in cervical biopsy sections.....	73

<b>Figure 19.</b> Average IFN- $\kappa$ expression in normal, dysplastic and carcinoma full biopsy tissue...	75
<b>Figure 20.</b> IFN- $\beta$ gene expression in cervical biopsy sections.....	77
<b>Figure 21.</b> Average IFN- $\beta$ expression in normal, dysplastic and carcinoma full biopsy tissue...	78
<b>Figure 22.</b> IFN- $\gamma$ gene expression in cervical biopsy sections.....	79
<b>Figure 23.</b> Average IFN- $\gamma$ expression in normal, dysplastic and carcinoma full biopsy tissue...	80
<b>Figure 24.</b> All analyzed IFNs in cervical biopsy sections.....	81
<b>Figure 25.</b> Relative expression of all analyzed IFNs in cervical biopsy sections.....	82
<b>Figure 26.</b> IFN gene expression in whole carcinoma tissue.....	83
<b>Figure 27.</b> IFN gene expression in cell lines.....	85
<b>Figure 28.</b> IFN and TNF- $\alpha$ gene expression in peripheral blood lymphocytes.....	86
<b>Figure 29.</b> Cell type-specific IFN- $\kappa$ expression in normal, dysplastic and carcinoma tissue.....	88
<b>Figure 30.</b> Cell type-specific IFN- $\beta$ expression in normal, dysplastic and carcinoma tissue....	89
<b>Figure 31.</b> Cell type-specific IFN- $\gamma$ expression in normal, dysplastic and carcinoma tissue.....	91
<b>Figure 32.</b> Cell type-specific gene expression of IFNs and genes involved in innate immunity in individual normal HPV- cervical tissue samples.....	116
<b>Figure 33.</b> Cell type-specific gene expression of IFNs and genes involved in innate immunity in individual dysplastic cervical tissue samples.....	121
<b>Figure 34.</b> Summary of IFN gene expression as well as genes displaying significant differences in expression between normal and dysplastic cervical tissue.....	128
<b>Figure 35.</b> IFN expression in cervical carcinoma epithelium and stroma.....	132
<b>Figure 36.</b> A survey of gene expression in different tissue layers within 7 individual tissue samples.....	133

## LIST OF TABLES

<b>Table 1.</b> Case number, morphological diagnosis, use, and HPV status for cervical tissue samples utilized in this study.....	42
<b>Table 2.</b> Summary of the presence of CD4/CD8 positive infiltrating cells in tissue samples.....	49
<b>Table 3.</b> Summary of the prevalence of IFN- $\gamma$ , - $\beta$ , - $\kappa$ in normal, dysplastic and cervical carcinoma whole biopsy tissue samples.....	72
<b>Table 4.</b> Statistical test results for whole biopsy sections.....	74
<b>Table 5.</b> Summary of the prevalence of genes expressed in normal and dysplastic epithelium and stroma. ....	126
<b>Table 6.</b> Statistical differences in gene expression in LCM cohort.....	127

## LIST OF ABBREVIATIONS

28S	Large ribosomal RNA Subunit
18S	Small Ribosomal RNA Subunit
ANOVA	Analysis of Variance Statistical Method
$\beta$ 2M	Beta-2-Microglobulin
$\beta$ -globin	Beta Globin
$\beta$ -actin	Beta Actin
CARD	Caspase Recruiting Domain
CaSki	HPV 16+ and HPV18+ Cervical Cancer-Derived Cell Line
CBP/p300	CREB Binding Protein
cDNA	Complementary DNA
CD4	Cluster of Differentiation 4, a marker for cytotoxic T lymphocytes
CD8	Cluster of Differentiation 8, a marker for helper T lymphocytes
CIN	Cervical Intraepithelial Neoplasia
CpG	Cytosine/Guanine Rich Sequence
CREB	cAMP response element-binding protein
Ct	Threshold Cycle
C-33A	HPV Negative Cervical Cancer-Derived Cell Line
DAPI	4', 6-diamidino-2-phenylindole
DNA	Deoxyribonucleic Acid
dNTPs	Nucleotide Bases
dsRNA	Double Stranded RNA
E6	Early (6) oncogene of HPV
E7	Early (7) oncogene of HPV
eIF2	Eukaryotic Initiation Factor
EMCV	Encephalomyocarditis
ex vivo	Experiment done on living tissue outside an organism
FR	Frozen Tissue
FFPE	Formalin-Fixed, Paraffin Embedded Tissue
GAAANN	Guanine/Adenosine rich nucleotide sequences to which IRFs bind
GAS	Interferon Gamma Activated Sequences
GTPase	Enzyme that Hydrolyzes GTP
HeLa	Henrietta Lacks-Cervical cancer cell line
HKG	Housekeeping Gene
HPV	Human Papillomavirus
HPRT-1	Hypoxanthine-guanine phosphoribosyltransferase-1
HR HPV	High-Risk Human Papillomavirus
IFN	Interferon
IFNAR-1/2	Interferon Alpha Receptor
IFNGR-1/2	Interferon Gamma Receptor
IFN- $\alpha$	Interferon Alpha
IFN- $\beta$	Interferon Beta
IFN- $\epsilon$	Interferon Epsilon
IFN- $\kappa$	Interferon Kappa
IFN- $\gamma$	Interferon Gamma

IFN- $\omega$	Interferon Omega
ISGs	Interferon-stimulated genes
ILs	Interleukins
In vitro	Experiment in controlled cell culture environment
IPS-1	Interferon Beta Promoter Simulator
IRF	Interferon Regulatory Factor
ISRE	Interferon Stimulated Regulatory Element
JAK	Janus Kinase
L1	HPV Late Gene 1
LCM	Laser Capture Microscopy/Microdissection
LCR	HPV Regulatory Element
LR HPV	Low-Risk Human Papillomavirus
Me180	HPV39+ Cervical Cancer-Derived Cell Line
mRNA	Messenger RNA
MDA5	Melanoma Differentiation Associated Gene-5
MHC	Major Histocompatibility Complex
MxA	Interferon-Induced GTPase
MyD88	Myeloid Differentiation Primary Response Gene 88
NF- $\kappa$ B	Nuclear Factor of Kappa B
NIKS	Near-Diploid Immortalized Keratinocytes
OAS	Oligoadenylate Synthetases
OCT	Optimal Cutting Temperature
ODNs	Oligodeoxyribonucleotides
PAMPs	Pathogen-Associated Molecular Patterns
p16 <sup>INK4a</sup>	Cyclin Dependent Kinase Inhibitor
p48	Transcription Factor in IFN Stimulatory Complex, aka ISGF3
P53	Tumor Protein 53
PBLs	Peripheral blood lymphocytes
PBS	Phosphate Buffered Saline
PCR	Polymerase Chain Reaction
PKR	Protein Kinase R
PLA	Phospholipase A
PRR	Pattern Recognition Receptor
qRT-PCR	Quantitative Real-Time Polymerase Chain Reaction
Rb	Retinoblastoma Susceptibility gene
REST	Relative Expression Software Tool
RIG-1	Retinoic Acid Inducible Gene-1
RNA	Ribonucleic Acid
RNA pol II	RNA Polymerase II
rRNA	Ribosomal Ribonucleic Acid
RT	Reverse Transcription
SiHa	HPV16+ Cervical Cancer-Derived Cell Line
STAT	Signal Transducer and Activator of Transcription
T <sub>A</sub>	Annealing Temperature
TLRs	Toll-Like Receptors
TNF- $\alpha$	Tumor Necrosis Factor Alpha

## ABSTRACT

Interferons (IFNs) are a common biological treatment option for many cancers as well as for human papillomavirus (HPV)-associated diseases, but current IFN treatments have not been optimized as disease progression subsists and treatment-limiting side effects still exist. IFN kappa (IFN- $\kappa$ ), a novel type I IFN, principally expressed in keratinocytes, may offer improvements in current IFN treatment regimes. The goal of the current study was to characterize the IFN- $\beta$ , IFN- $\gamma$  and IFN- $\kappa$  mRNA levels in normal, dysplastic and cervical carcinoma tissue, as well as microdissected cervical epithelium and stroma, to determine the effects of HPV on IFN- $\kappa$  gene expression in relation to other common IFNs. Optimal sample handling techniques for tissue preparation and storage, RNA extraction and quantification, and target gene detection are crucial for reliable gene expression analysis. Methods for measuring mRNA levels of low-expressing genes, such as IFNs, in human cervical samples are not described in the scientific literature. Thus, we obtained normal and dysplastic frozen and formalin-fixed cervical biopsies from colposcopy. Histopathological diagnoses were performed by one pathologist. Cervical keratinocytes and stroma were isolated using laser capture microdissection. Immortalized keratinocytes transduced with or devoid of an HPV oncogene were used for initial method development. Human keratinocytes, cervical cancer-derived cell lines as well as patient-derived peripheral blood lymphocytes were used for supportive experiments. Here we report optimal methods for gene expression analysis of IFNs in cervical tissue as well as the comprehensive analysis of whole tissue and cell-specific IFN- $\gamma$ , - $\beta$  and - $\kappa$  gene expression in HPV-associated cervical disease. IFN- $\kappa$  gene expression increased with disease progression, while IFN- $\beta$  gene expression decreased with disease progression. IFN- $\gamma$  levels remained unchanged despite HPV infection. Furthermore, IFN- $\kappa$  expression in cervical

stroma cells was induced upon HPV infection, implicating the involvement of cervical stroma cells in the HPV-associated increase in IFN- $\kappa$  expression. The described optimized methods could lead to improvements in immunological profiling and disease diagnosis, techniques without which IFN- $\kappa$  would remain undetectable in cervical samples. Further, characterization of the IFN immune profile in patients with different stages of HPV-associated cervical disease, with emphasis on the novel IFN- $\kappa$ , could help develop patient-tailored IFN treatment regimes that lead to the promotion of viral regression in women suffering from cervical disease.

## 1.0 INTRODUCTION

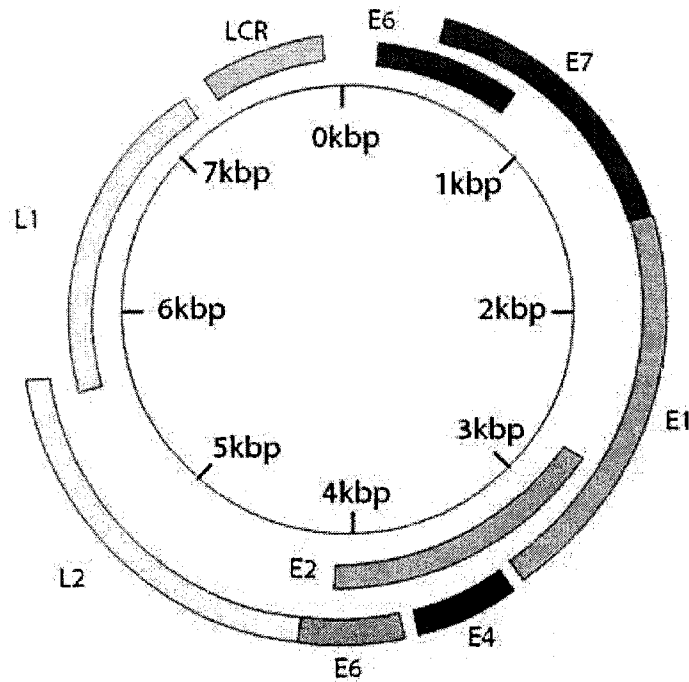
### 1.1 Cervical Cancer and Cervical Precursor Lesions

Cancer of the uterine cervix is one of the most common malignancies in women worldwide. Approximately 1,400 Canadian women are diagnosed with cervical cancer each year; however, this disease is much more prevalent in developing countries. Cervical cancer and its precursor lesions, cervical intraepithelial neoplasia (CIN) 1-3, are caused by high-risk human papillomavirus (HPV) infection<sup>1</sup>. HPV infection is required for the maintenance and propagation of the malignancy, but the infection is usually transient and most women can effectively clear it, resulting in lesion regression. A small percentage of women, however, cannot clear the infection, resulting in a persistent HPV infection which may lead to the formation of a cervical lesion and in some cases cervical cancer.

### 1.2 Human Papillomavirus

HPV is a DNA virus consisting of an 8,000 base pair, closed, double stranded, circular genome (**Figure 1**), surrounded by an outer shell consisting of capsid proteins but lacking an envelope. The HPV genome consists of three major regions: the early region consisting of early genes encoding proteins involved in viral transcription and transformation of the host cell, the late region encoding late genes encoding the capsid proteins and the regulatory element (LCR) required for viral transcription and replication. HPV directly infects the squamous epithelial cells of skin and mucosa and, in the cervix, initially infects the basal proliferating layer of the squamous epithelium present at the squamo-columnar junction where it is believed the virus enters at a site of wounding (reviewed in ref#2).

The viral life cycle relies heavily on the differentiation program of the host squamous epithelial cell, the keratinocyte. In the basal layer, the virus genome is present as a nuclear



<http://images.google.ca>

**Figure 1. HPV genome.** Circular genome consisting of early genes, late genes and a regulatory region. The early genes consist of E1, E4, E6, E7, the late genes consist of L1 and L2 and the regulatory element (LCR) stands alone.

plasmid and replicates itself approximately once every cell cycle by hijacking the host replication machinery<sup>3</sup>. As the basal cells divide, daughter cells destined for more superficial layers of the epithelium stratify and differentiate (**Figure 2**). It is in the differentiated cells that the virus enters the productive stage of its life cycle where a high copy number of viral DNA is produced and capsid production and viral assembly occurs<sup>4</sup>. Expression of HPV capsid proteins, namely L1 and L2, allows for the assembly of replicated viral DNA into virions. Production of virions constitutes a means of multiple host infections and maintenance of HPV DNA within the host. Interestingly, the development of prophylactic vaccines against HPV is based on the effects of L1 exposure to the host. The L1 capsid protein alone is able to form virus-like particles in the host that elicits production of B cell and T cell responses specific to HPV. These responses generate HPV type-specific neutralizing antibodies that, after immunization, would prevent persistent HPV infection. Maintenance of viral DNA in the host occurs through chromosomal viral genome integration during the progression of preneoplastic lesions to invasive cervical carcinoma<sup>4</sup>.

Many types of HPVs exist. Low risk types, such as HPV 6 and 11, are associated with benign lesions or genital warts, whereas the high risk types, such as HPV 16, 18, 31 and 33 are associated with anogenital and oropharyngeal cancers as well as > 90% of cervical cancers<sup>6</sup>. The involvement of papillomavirus DNA in cervical cancer was first described in 1974<sup>1</sup>. The ability of HPV to cause cancer is due to two oncoproteins it harbors. HPV E6 and E7 oncogenes are requisite factors for the malignant phenotype of HPV-positive cervical cancer cells<sup>7</sup>. In a healthy host cell, protein 53 (TP53; p53) is involved in the regulation of DNA repair, cellular apoptosis and cell cycle regulation. Upon HR HPV infection, HPV E6 renders p53 nonfunctional by targeting it for ubiquitin degradation. With the loss of p53, cells lose their ability to regulate

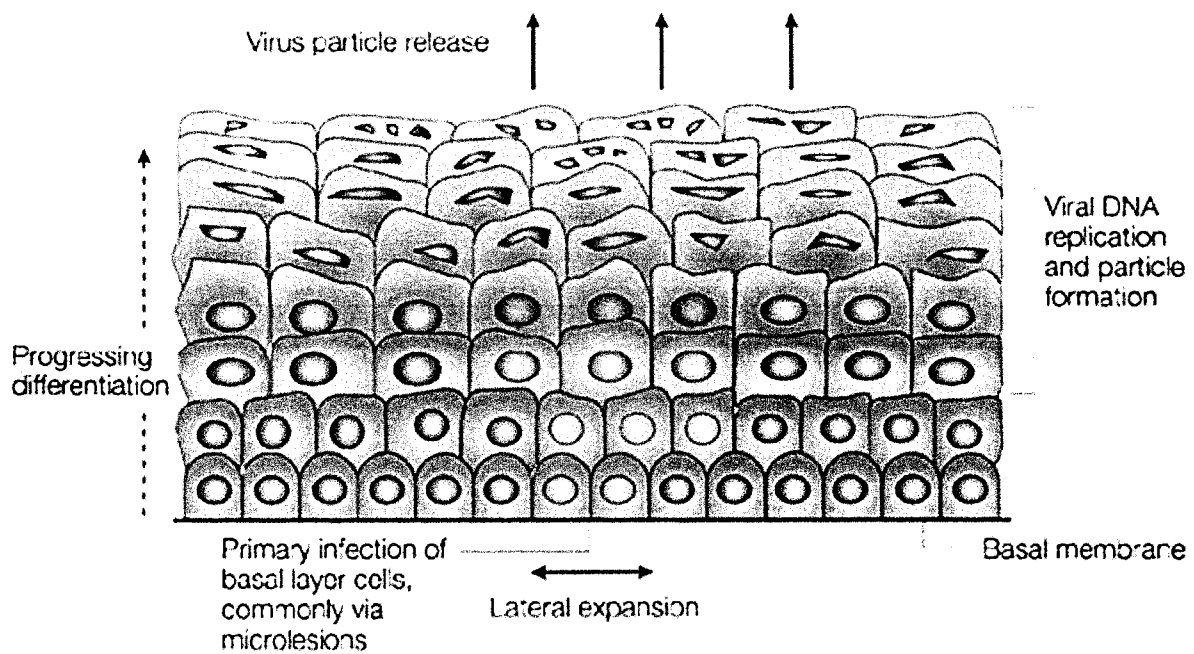
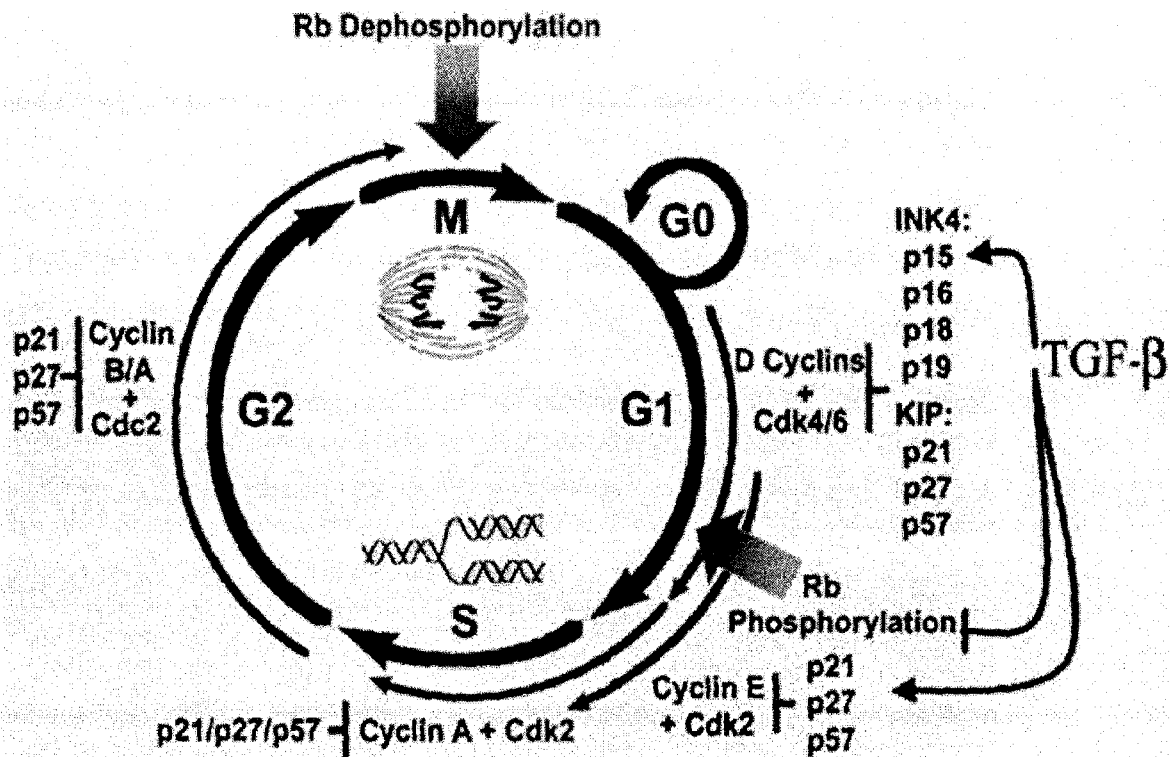


**Figure 2. HPV viral life cycle and cervical epithelium.** The basal membrane separates epithelium from stroma and is where the basal layer of epithelium rests which is the site of HPV infection via microlesions. Increasing vertical layers represents differentiating epithelial cells where enhanced viral DNA replication and particle formation occur. In the superficial epithelial layers is where the formed viral particles are released (ref #2).

cell proliferation and initiate programmed cell death in the presence of a stressor. Similarly, in a healthy cell, the Retinoblastoma (Rb) protein is involved in the regulation of normal cell cycle progression (**Figure 3**). Upon HR HPV infection, HPV E7 binds to Rb, rendering it nonfunctional and unable to regulate the cell cycle, resulting in the uncontrolled proliferation of squamous epithelium. Despite other cell cycle regulators that act to maintain normal levels of cellular proliferation, such as p16<sup>INK4a</sup> (**Figure 3**), without a functional Rb protein the cell cycle cannot be regulated. Incidentally, it has been proposed that p16 is an accurate biomarker for HR HPV infection in cervical squamous epithelium due to its upregulation upon HR HPV infection.

### 1.3 Interferons

Interferons (IFNs) belong to the family of vertebrate cytokines and, upon microbial infection, are produced by many cells and specialize in antitumor<sup>8</sup>, antiviral<sup>9</sup> and immunostimulatory<sup>10</sup> activity. IFNs were first described in 1957 when researchers noticed an interference effect caused by heat-inactivated influenza virus on the growth of the live virus; later described as a factor which blocks viral infection<sup>9</sup>. Type I IFNs include IFN alpha (IFN- $\alpha$ ), IFN beta (IFN- $\beta$ ), IFN-omega (IFN- $\omega$ ), IFN-epsilon (IFN- $\epsilon$ ) and IFN kappa (IFN- $\kappa$ )<sup>11</sup>, while type II IFNs consist solely of IFN- $\gamma$ <sup>12</sup>. Type I IFNs can be produced by all nucleated cells in response to microbial infections. Type I IFNs lack introns and their genes are located on the short arm of chromosome 9<sup>13</sup>. There are 13 different IFN- $\alpha$  genes but only one IFN- $\beta$  and IFN- $\omega$ <sup>11</sup>. Type I IFNs are strongly induced in virally infected cells and stimulate genes involved in fighting the infection, which acts to protect nearby uninfected cells. Type I IFNs also exhibit an ability to induce apoptosis in infected cells so as to limit the spread of the virus<sup>14</sup>.



<http://images.google.ca>

**Figure 3. The cell cycle, Rb and p16<sup>INK4a</sup>.** Rb exerts its action at the end of the G1 phase (prior to S phase entry) of the cell cycle and p16 acts as a negative regulator of Rb function during the same phase.

The type II IFN, IFN- $\gamma$ , is an immunomodulatory cytokine, mainly produced by lymphocytes and natural killer cells, and comprises the effective form of innate immunity against invading pathogens by being involved in the upregulation of MHC molecules<sup>15</sup>, by promoting the local formation of inflammatory agents, such as monocytes and activated T lymphocytes<sup>16</sup>. Unlike type I IFNs, IFN- $\gamma$  is encoded by a single gene present on chromosome 12. Similar to IFN- $\beta$ , IFN- $\gamma$  only has one active protein form; however, in contrast to type I IFNs, antigen-MHC complexes and other cytokines, such as IL-12 and IL-18, stimulate type II IFNs production<sup>17</sup>. Together the type I and II IFNs represent a bridge between innate and adaptive immunity by inducing a plethora of antiviral effects against invading pathogens.

IFNs, either used alone or in combination with other treatments, are an approved therapy for many diseases. IFN- $\alpha$  has shown some success for the treatment of chronic hepatitis B, hepatitis C and human herpes virus-8 infections as well as a small percentage of metastatic renal-cell carcinomas and has been employed in the treatment of HPV-associated conditions such as recurrent respiratory papillomatosis<sup>18</sup> and genital warts<sup>19</sup>. IFN- $\beta$ , in conjunction with other biological agents, is used with much success for treating multiple sclerosis, as it can decrease the rate of disease relapse and progression<sup>20</sup>. IFN- $\gamma$  has only been approved for treatment of chronic granulomatous disease, a rare congenital disorder. Furthermore, type I IFNs are a standard treatment for melanoma and some solid tumors<sup>21</sup>. Despite the proven therapeutic utility of type I IFNs, the existence of substantial side effects, such as fatigue, fever, malaise, myalgia and anemia<sup>22</sup> may limit the therapeutic potential of the type I IFNs currently in use. It is well documented that side effects from IFN treatment have been substantial enough to force patients to reduce or discontinue IFN therapy<sup>23-26</sup>.

## 1.4 Novel Interferon Kappa

Recently, a novel type I IFN, IFN-kappa (IFN- $\kappa$ ), that is expressed primarily in keratinocytes<sup>11</sup> has been identified. IFN- $\kappa$  exhibits 30% homology to other type I subtypes, however its gene is located on the short arm of chromosome 9, adjacent to the type I gene cluster<sup>11</sup> and is only expressed in epidermal keratinocytes, monocytes and monocyte-derived dendritic cells<sup>11</sup>. IFN- $\kappa$ , like other type I IFNs, contains a series of conserved cysteine residues in its amino acid sequence<sup>11</sup> as well as GAAANN elements which act to mediate IRF binding to its promoter in response to viral infection<sup>27</sup>. Unlike other IFNs, the IFN- $\kappa$  gene contains an intron within the 3' untranslated region<sup>11</sup> and the protein is slightly larger than other IFNs, where its mature size is 180 amino acids compared to 166 amino acids for IFN $\alpha$  and  $\beta$ <sup>11</sup>. IFN- $\kappa$  exhibits similar antiviral activity and utilizes the same receptor and regulatory element as other type I IFNs but differs in its expression and signaling characteristics. IFN- $\kappa$  and IFN- $\alpha$  display similar transcriptional activation potential, as transfection of either in HeLa cells resulted in a 20-fold increase in interferon stimulated regulatory element (ISRE) compared to a control<sup>28</sup>. Like other type I IFNs, transfection of IFN- $\kappa$  resulted in an increase in mRNA levels of the interferon-stimulated genes (ISGs), IFN-induced GTPase (MxA), protein kinase R (PKR) and oligoadenylate synthetases (OAS)<sup>11</sup>. Additionally, IFN- $\kappa$  and IFN- $\alpha$  both sustain cell viability against encephalomyocarditis (EMCV) infection in HeLa cells<sup>28</sup>. Following EMCV infection, the cell viability of HeLa cells is directly related to the number of cells expressing IFN- $\kappa$ , whereas viability is independent of the number of cells expressing IFN- $\alpha$ , indicating that the antiviral activity of IFN- $\kappa$  is cell-associated<sup>28</sup>. Furthermore, data suggest that monolayer cells only in close proximity to IFN- $\kappa$ -expressing cells are viable following EMCV infection<sup>28</sup>, suggesting that IFN- $\kappa$  signals in a discrete, autocrine manner different than the paracrine signaling usually

exerted by IFNs. Utilizing an antibody against the type I IFN receptor blocked IFN binding and completely abolished IFN- $\kappa$  signaling<sup>11</sup>, indicating that IFN- $\kappa$  signaling is initiated by the same receptor complex as the other type I IFNs. In addition, northern blot analysis of IFN- $\kappa$  mRNA levels in immortalized skin keratinocytes revealed that unlike IFN- $\beta$ , IFN- $\kappa$  mRNA is present in resting keratinocytes and, like other IFNs, is significantly upregulated upon dsRNA treatment<sup>11</sup>, indicating that IFN- $\kappa$  is present at a basal level in cells but can also be induced following dsRNA exposure. In a recent investigation into human cutaneous skin, IFN- $\kappa$  was found to be strongly expressed in allergic contact dermatitis and planus-affected skin, completely absent in healthy skin and weakly expressed in psoriatic and atopic dermatitis epidermis<sup>29</sup>. Both IFN- $\kappa$  and - $\beta$  stimulate cytokine production from both monocytes and dendritic cells and both bind to heparin, a member of the glycosaminoglycan family<sup>30</sup>.

Despite having many similarities to other type I IFNs in terms of signaling pathways and the activation of downstream antiviral genes, IFN- $\kappa$  represents a unique antiviral protein that is highly specific to epithelial cells and displays discrete signaling. Due to the distinct nature of its activity and overall potency of its antiviral effects, IFN- $\kappa$  could lead to an improvement in existing IFN treatment regimes by delivering more precise, local antiviral treatment, which may limit side effects.

## **1.5 Interferon Induction Pathways**

### ***1.5.1 Extracytoplasmic Pathogen Sensors***

The known extracytoplasmic pathway for IFN induction during RNA viral infection consists of the pattern recognition receptor (PRR/TLR) system (**Figure 4**). Toll-like receptors (TLRs) are membrane proteins, typically expressed on cells of the innate immune system, which have extracellular domains that search for pathogen antigens.

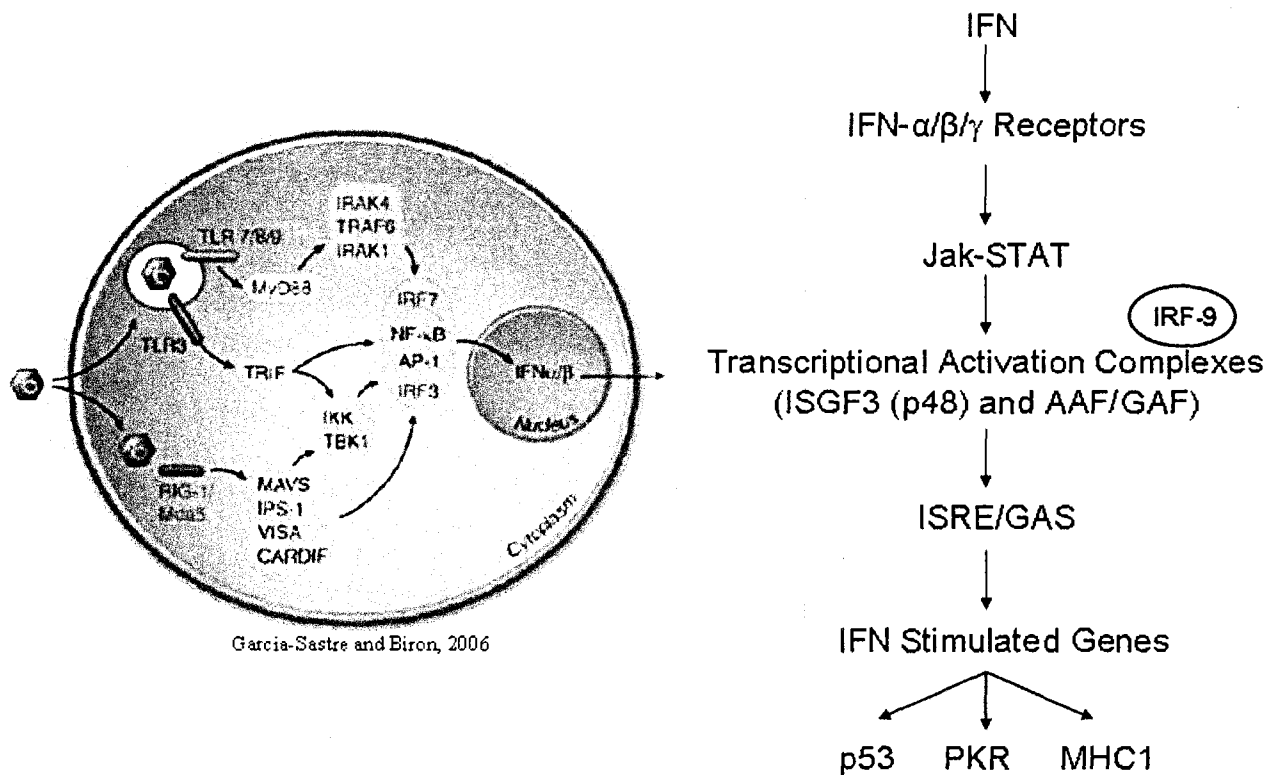


**Figure 4. Interferon induction and signaling pathways.** A microbial agent is recognized by an initial cells triggering a signaling cascade which leads to IFN gene transcription (left). Translated IFN proteins act on subsequent cells by binding to the IFN receptor and activating signaling cascades which lead to the activation of ISGs (right) (ref #109).

More specifically, TLRs recognize most types of viruses as well as components of gram-negative bacteria. It is important to note that while many TLRs are activated by single or double stranded RNA, DNA viral components can also activate TLRs. TLR9 senses DNA viruses, specifically DNA CpG motifs<sup>31</sup>, and it has recently been demonstrated that TLR3 is upregulated in response to HPV in *ex vivo* cervical keratinocytes (DeCarlo *et al.*, unpublished data). Some TLRs, such as TLR4, are present on the cell surface, however TLR 3,7,8 and 9 are localized in endosomes and recognize viral ligands once they are internalized.

### ***1.5.2 Cytoplasmic Pathogen Sensors***

The known cytoplasmic pathway for IFN induction during RNA viral infection consists of the retinoic acid inducible gene-1/melanoma differentiation associated gene 5 (RIG-1/Mda5) system and involves the intracellular recognition of viruses. Upon viral infection, dsRNA interacts with RNA helicase proteins which contain a caspase-recruiting domain (CARD). These helicases then interact with a mitochondrial resident protein which in turn interacts with the CARDS of the retinoic acid-inducible protein (RIG-1)<sup>32</sup> and the melanoma differentiation antigen 5 (MDA5). It is the CARD domains which are responsible for eliciting downstream signaling that leads to activation of downstream transcription factors governing IFN gene expression<sup>32</sup>.

Together, either extracytoplasmic or cytoplasmic pathogen sensors lead to activation of IFN regulators, such as NF- $\kappa$ B (Nuclear factor of kappa B) and IRF3 (Interferon regulatory factor-3), both of which are involved in IFN gene transcription regulation. Adaptor proteins, such as the interferon beta promoter stimulator 1 (IPS-1), mediate IFN gene upregulation by Mda and RIG through activation of IRF-3, IRF-7 and NF- $\kappa$ B transcription factors<sup>33</sup>. The IFN-induction pathways have not been characterized for IFN- $\kappa$ .

## 1.6 Interferon Regulatory Factors

Nine cellular IRF genes have been identified and their proteins represent major molecules involved in innate immunity; however only four forms play a role in IFN-mediated anti-viral defense (reviewed in ref#34). IRF-3 and IRF-7 are involved in a positive feedback loop responsible for massive IFN induction during a viral infection. Once pathogen sensor pathways elicit IRF-3, it translocates to the nucleus and induces IFN- $\beta$  transcription (**Figure 4**). The activation of IFN leads to the induction of IRF-7 expression through ISRE activation, which ultimately leads to a further increase in IFN- $\beta$  gene activation and more production of IRF-7<sup>35</sup>. Other IRF molecules play a vital role in IFN gene activation. IRF-9 is a component of ISGF3/p48 and is involved in the stimulation of ISG (Interferon Stimulated Gene) transcription<sup>36</sup>, while IRF-1 is a transcription factor present on the IFN- $\beta$  promoter<sup>37</sup> and is essential in the activation of various immune cells. While, IRF-1 has been shown to be induced upon IFN- $\kappa$  treatment<sup>11</sup>, similar to results found with IFN- $\beta$  and IFN- $\gamma$  treatment<sup>38</sup>, to this date no other transcription factors have been associated with IFN- $\kappa$  upregulation.

## 1.7 Interferon Signaling Pathways

Following IFN induction, the intracellular signaling cascades result in the transcription of genes responsible for anti-viral activity (**Figure 4**). Type I IFNs are associated with the IFN $\alpha/\beta$  receptor (IFNAR) which is composed of the two subunits IFNAR-1 and IFNAR-2<sup>39</sup>, whereas the IFN- $\gamma$  receptor (IFNGR) is composed of two subunits IFNGR-1 and IFNGR-2<sup>12</sup>. Activation of the IFN receptor complex by IFN binding results in the activation of the JAK-STAT pathway. These pathways differ slightly for type I and type II IFNs. The phosphorylation of STAT molecules in either pathway results in the formation of transcriptional activation complexes. The ISGF3 activation complex for type I IFNs, composed of STAT1, STAT2 and another

transcription factor, most commonly IRF-9 or p48<sup>40</sup>, binds to the IFN stimulated regulatory elements (ISRE) of downstream genes. In the type II IFN response, a separate activation complex is involved in binding to the IFN- $\gamma$  activated sequences (GAS) present on downstream genes<sup>41</sup>. Binding of ISRE or GAS results in the subsequent transcriptional activation of ISGs, which then evoke the anti-viral, anti-tumor and immunomodulatory activities associated with IFNs.

### **1.8 Interferon Stimulated Genes**

There are approximately 100 different ISGs, some of which represent genes most downregulated upon HR HPV infection<sup>42</sup>. Two well studied IFN-inducible proteins are protein kinase R (PKR) and 2'-5' oligoadenylate synthetases (OAS). PKR autophosphorylates when activated by dsRNA and continues to phosphorylate downstream substrates, one of which is the alpha subunit of initiation factor eIF2<sup>43</sup>. eIF2 forms a complex with GDP (eIFs-GDP-eIF2B), which results in an inhibition of cellular translation and termination of viral replication. OAS, another ISG, also recognizes dsRNA and in turn activates an endoribonuclease which degrades both viral and cellular RNAs<sup>44</sup>. OAS is significantly downregulated upon cellular exposure to HPV16 E6/E7 viral vectors<sup>42</sup>. Furthermore, many ISGs responsible for antiviral activity are also significantly perturbed by HPV, including p53, Rb, the TLR adaptor molecule MyD88, IFN-induced proteins IFIT1, IFI54 and ISG15 and the IFN induced GTPase Mx<sup>42</sup>. The human MxA GTPase exerts an antiviral function by interfering with viral protein transport within the cell<sup>45</sup>.

### **1.9 Human Papillomavirus and Interferon Interactions**

HPV directly interacts with and inhibits the function of many molecules involved in the interferon pathways which may, in part, explain why HPV infections can be sustained in the host without initiating an effective immune response. HPV interacts with both IFN gene regulation as

well as downstream IFN-elicited pathways. It has been shown that the HPV16 E7 protein inhibits type I IFN signaling by binding to p48, part of the IFN transcriptional activation complex<sup>46</sup>. The E7 protein can also recruit a histone deacetylase to the IFN- $\beta$  promoter, blocking IRF-1 activation and in turn IFN- $\beta$  transcription<sup>47</sup>. HPV16 E6 has also been found to impede IFN- $\beta$  transcription by binding and inhibiting IRF-3<sup>48</sup>. HPV 18 has been shown to eliminate expression of p48 as p48 transcription was absent in tumorigenic cervical cells<sup>38</sup>. HPV16 E6 protein has been found to degrade p53 by using a ubiquitin proteolytic pathway<sup>49</sup>. Therefore, E6-positive cells lose cell cycle regulation of p53, specifically at the G1 checkpoint<sup>50</sup>, rendering these cells resistant to p53-mediated apoptosis<sup>51</sup>. The HPV E6 protein represses p53 function by targeting CBP/p300 by inhibiting the CBP transcription adaptor motif TRAM in an interaction involving HPV E6 zinc fingers and CBP TRAM residues<sup>52</sup>. Furthermore, the HPV18 E6 oncoprotein impairs JAK/STAT activation by IFN- $\alpha$ <sup>53</sup>. These interactions demonstrate that HPV has evolved the ability to evade immune detection by inhibiting both the production and action of IFNs. However, it should be noted that the effects of HPV on IFN- $\kappa$  regulated and elicited pathways are currently unknown. Interestingly, in a recent study analyzing the effects of IFN treatment on HPV oncogene expression in cell lines, it was found that IFN- $\alpha$ , - $\beta$  and - $\gamma$  were effective at decreasing the level of oncogene transcripts in HPV18+ HeLa cells and IFN- $\gamma$  exerted the same effect in HPV16+ CaSki cells<sup>54</sup>. This evidence demonstrates that despite the detrimental interactions of HPV on the IFN pathways, IFN treatment can still be a useful option for HPV-associated cervical disease, including cervical carcinoma.

### **1.10 Interferons and Cervical Disease**

Multiple studies exist that attempt to correlate IFN expression alteration with cervical cancer. HPV16 has been shown to inhibit both IFN- $\alpha$  and IFN- $\beta$  in HPV16 + keratinocytes<sup>42</sup>.

Similarly, previous studies have concluded that IFN- $\gamma$  expression was significantly decreased in invasive carcinoma biopsies compared to premalignant tissue<sup>55</sup> and at lower frequencies in carcinoma versus dysplastic cervical tissue<sup>56</sup>. Further, IFN- $\gamma$  expression has been shown to be completely absent in a subset of cancer patients (stage II or III) displaying no defect in T cell infiltration, indicating that the alteration of IFN- $\gamma$  expression in these patients could be due to deactivation of T cells<sup>57</sup>. In a recent study conducted on TNF- $\alpha$  mediated IFN- $\beta$  signaling in cervical carcinoma cells, it was elucidated that TNF- $\alpha$ , a strong inducer of IFN- $\beta$ , was unable to induce IFN- $\beta$  activity in tumorigenic cells<sup>38</sup>. This indicates that the cross-talk between these two molecules is disturbed in cervical cancer<sup>38</sup>. In addition, IFN- $\beta$  and IFN- $\alpha$  transcription has been shown to be downregulated in keratinocytes infected with HPV16<sup>42</sup>. While convincing evidence exists illustrating the inhibitory effects of HPV on IFNs in cervical tissue, however, to date, there have been no investigations into IFN- $\kappa$  expression in the context of cervical carcinoma.

### **1.11 Method Development**

The use of quantitative real-time polymerase chain reaction (qRT-PCR) for the molecular analysis of disease is a powerful and widely used tool. Extraction of high-quality RNA for use in gene expression analysis techniques such as reverse transcription (RT), qRT-PCR and cDNA microarrays is of great importance. While obtaining high-quality RNA from cell lines is relatively straightforward, the complexity and heterogeneity of human tissue presents considerable challenges for linking gene expression patterns with disease state. Nonetheless, *ex vivo* studies utilizing human tissue samples are important for the validation of *in vitro* work and to closely mimic relevant biological processes. In recent years, the introduction of laser capture microdissection (LCM) has greatly enhanced the specificity of the molecular analysis of cell types within a sample. However, obtaining sufficient quantities of high quality RNA from

microdissected cells represents an additional obstacle. Performing reliable gene expression studies requires stringent monitoring of sample integrity during sample preparation, RNA extraction and qRT-PCR steps.

Poor tissue storage conditions can degrade RNA<sup>58</sup>. Formalin-fixed, paraffin-embedded (FFPE) tissue produces optimal morphology for histological assessment, but this technique may not preserve RNA integrity<sup>59</sup>. While the literature suggests that frozen (FR) tissue is optimal for the extraction of high quality RNA<sup>59,60</sup>, this has not been shown for FR cervical tissue. Numerous techniques and commercially available kits exist for RNA extraction from FR tissue<sup>61-64</sup> and some have been utilized for cervical specimen extraction<sup>65-67</sup>. However, the integrity of the RNA and the reproducibility of the techniques are often overlooked. Current literature does not provide a consensus for the optimal protocol for high quality RNA extraction, particularly from FR cervical specimens. In addition, the importance of LCM techniques for studying specific cell populations has resulted in the optimization of tissue preparation protocols specifically for LCM<sup>68-70</sup>, but it has not been demonstrated that these work well for cells obtained from cervical tissue.

The quality of data obtained from qRT-PCR experiments is greatly influenced by RNA integrity, RT conditions, housekeeping gene (HKG) selection and transcript abundance. The type of primers used for RT can also significantly alter the complementary DNA (cDNA) yield and specificity<sup>71</sup>. While normalization of qRT-PCR-derived expression levels requires an appropriate HKG for compensating for differences between samples<sup>72,73</sup>, HKG validation is required for each tissue type<sup>74</sup>. Furthermore, low transcript amounts represent an obstacle for simultaneous analysis of multiple targets or low-expressing genes and thus several methods exist for amplifying mRNA transcripts extracted from tissue samples<sup>75-78</sup>. However, none of these

parameters have been described or optimized for gene expression analysis in cervical samples.

### **1.12 Research Rationale**

Interferons are a common biological treatment option for many cancers as well as for HPV-associated diseases, but current IFN treatments have not been optimized as evidenced by the progression of the disease and the existence of treatment-limiting side effects. The novel IFN- $\kappa$  may improve upon existing therapeutics. Cervical tissue, the main constituent of which is the squamous keratinocyte, represents an ideal context in which to study IFN- $\kappa$  expression in response to a viral infection as HPV infects the squamous epithelium, the cell-type that chiefly expresses IFN- $\kappa$ . The requisite methods for detecting low-expressing IFNs in cervical samples and microdissected cervical epithelium are not described in current scientific literature, which made it necessary to develop and/or optimize these methods ourselves. To our knowledge, the expression of IFN- $\kappa$  in *ex vivo* cervical tissue has never been investigated. Further, the change of expression of this novel anti-viral mediator as a result of HPV infection has also never been examined in cervical tissue or isolated cervical epithelium and stroma. Together, with novel technological advancements for low-abundant gene expression analysis in cervical tissue, the detection and analysis of cell-specific IFN- $\kappa$  mRNA in HPV-associated cervical disease represents highly original research.

### **1.13 Hypotheses**

We expected a disparate IFN gene expression profile with disease progression resulting from an HPV-induced alteration in the host-cell antiviral activity and IFN- $\kappa$  to be expressed uniquely compared to other IFNs due to its distinct signaling characteristics. We also expected LCM to reveal the involvement of both cervical epithelium and stroma in the observed IFN expression patterns of IFNs.

## 1.14 Research Aims

- 1) To characterize tissue samples as morphologically normal, dysplastic or cervical carcinoma tissue, as well as to test samples for HPV in order to establish a HPV negative normal group and to determine HPV types present in dysplastic and carcinoma tissues.
- 2) To develop optimal methods for sample storage, RNA extraction, cDNA amplification and qRT-PCR for the detection of low-abundant interferon genes in cervical biopsy tissue and laser capture microdissected cervical keratinocytes.
- 3) To determine the effects of HPV on IFN gene expression in *ex vivo* cervical tissue by analyzing IFN mRNA levels in normal, dysplastic and malignant cervical tissue as well as LCM-derived HPV+ and HPV- cervical keratinocytes using qRT-PCR.
- 4) To establish the IFN mRNA profile using qRT-PCR in human primary keratinocytes, cervical cancer-derived cells lines and in the periphery of patients using human PBLs for supportive experiments.
- 5) To reveal the specific cell types involved in the observed IFN expression by analyzing the IFN mRNA levels using qRT-PCR in normal, dysplastic and carcinoma epithelium and stroma isolated using LCM.

## 2.0 MATERIALS AND METHODS

### 2.1 Sample Preparation

#### 2.1.1 Cell Lines

Near-diploid immortalized foreskin keratinocytes (NIKS)<sup>79</sup> in the presence or absence of the Human Papillomavirus type 16 (HPV16) E6<sup>80</sup> or E7 oncogene were used in initial experiments to mimic normal and diseased cervical tissue to assess HKG suitability and cDNA amplification uniformity. Cervical carcinoma cell lines HeLa (ATCC, CCL-2, HPV18+), SiHa (ATCC, HTB-35, HPV16+), CaSki (ATCC, CRL-1550, HPV16+ and HPV18+ related sequences), ME-180 (ATCC, HTB-33, HPV39+) and C-33 A (ATCC, HTB-31, HPV-) were used for supportive experiments. All cell lines were grown in culture to 70% confluency prior to harvesting.

#### 2.1.2 Biopsy Material

FR and FFPE normal and dysplastic cervical biopsies were obtained with written consent from women attending the Colposcopy Clinic at the Thunder Bay Regional Health Sciences Centre between November 2005 and November 2006. FR cervical carcinoma biopsies were obtained from the Cancer Centre at the Thunder Bay Regional Health Sciences Centre between November 2006 and December 2007 or the Ontario Tumor Bank in May, 2008. Biopsies were either snap frozen in liquid nitrogen and transferred to -80°C or immediately submerged in 10% (v/v) buffered formaldehyde solution for 3 hours at room temperature. The tissue was then dehydrated by submerging the tissue into ascending grades of ethanol (70%, 80%, 95% and 100% v/v in water), then with 100% (v/v) xylene followed by wax-impregnation with paraffin<sup>81</sup>. FR cervical tissue was sectioned on a cryostat (Leica CM1850, Leica Microsystems, Richmond Hill, ON, Canada), maintaining tissue temperature at -20°C using Tissue Tek™ embedding

medium (O.C.T. Compound, Sakura Finetek, Torrance, California, USA) while FFPE cervical tissue was sectioned using a microtome (Leica 1720 digital microtome, Leica Microsystems). Tweezers, brushes and surfaces were cleaned with DEPC-treated 70% (v/v) ethanol between specimens to reduce RNase activity and RNA cross-contamination. Ten micrometre thick tissue sections were processed for hematoxylin and eosin staining<sup>81</sup> and subsequent histopathological diagnosis by the same pathologist (Dr. Nicholas G. Escott). Additional 10 µm thick sections were used for HPV testing and stained immunocytochemically for p16 for detection of HPV infection. Tissue samples were diagnosed as morphologically normal, dysplastic or cervical carcinoma. Samples were grouped into the following categories; HPV negative normal tissue (n=12), low-grade dysplastic tissue (n=9), high-grade dysplastic tissue (n=10) and HR HPV positive cervical carcinoma tissue (n=2).

### ***2.1.3 Peripheral Blood Lymphocytes***

PBLs and monocytes were isolated from whole blood specimens using Ficoll separation (Ficoll-Paque<sup>TM</sup> PLUS; GE Health Care, Piscataway, New Jersey, USA) according to the specified protocol for lymphocyte isolation. Briefly, blood was layered on top of Ficoll and centrifuged at 1750 rpm for 40 minutes. Lymphocytes and monocytes were isolated from the Ficoll, plasma, and red blood cells, containing granulocytes layers and washed with PBS. Pellets were frozen at -20°C along with RPMI (RPMI 1640 medium, catalogue # 23400-021, Invitrogen, Burlington, Ontario, Canada), human serum and dimethyl sulfoxide (Sigma-Aldrich, Oakville, Ontario, Canada).

## **2.2 DNA Extraction**

Three methods were used to extract DNA from cell lines, cervical biopsy specimens and microdissected material. These include an in-house method, the Arcturus PicPure<sup>TM</sup> DNA

Isolation Kit (Arcturus Microgenomics, Molecular Devices, Sunnyvale, California, USA) and the Qiagen QIAamp® DNA micro kit (Qiagen, Mississauga, ON, Canada). The in-house method involved the addition of 50 µl of DNA digestion buffer (50 mM Tris-HCl, 1 mM EDTA, 0.5% (v/v) Tween 20, pH 8.5) to the samples along with 0.2 mg/ml proteinase K (Roche, Mississauga, ON, Canada) and incubation at 65°C for 4 hrs, 95°C for 5 minutes and then centrifugation at 13,000 rpm for 5 minutes. Isolation of DNA using the Arcturus and Qiagen methods followed the recommended protocols for isolation from cell pellets and/or tissue samples. All extracted DNA was stored at -20°C until used.

### **2.3 Polymerase Chain Reaction**

Approximately 100 ng of DNA extracted from NIKS was used to optimize PCR conditions for the detection of the  $\beta$ -globin gene for sample integrity monitoring. Various concentrations of MgCl<sub>2</sub>, nucleotide bases (dNTPs; dATP, dGTP, dCTP, dTTP) and primers were tested along with varying annealing temperatures until a discrete 110 bp  $\beta$ -globin band was visualized by agarose gel electrophoresis. Optimized PCR conditions for the detection of  $\beta$ -globin are as follows; 4.0 mM MgCl<sub>2</sub>, 200 µM dNTPs, 0.1 µM forward and reverse  $\beta$ -globin primers (PC03 [5116-035] and PC04 [5116-036] primers, Sigma-Aldrich), 1.25 units of Taq polymerase (Amplitaq DNA polymerase, Applied Biosystems, added to equal amounts of Taqstart Antibody ([S1476], Becton Dickinson and Company, Oakville, ON, Canada) and 1X PCR buffer (Applied Biosystems). PCR reactions of 25 µl diluted using nuclease free water (P1195, Promega Corporation, Madison, WI, USA) were incubated in a thermal cycler (2720 Thermal cycler, Applied Biosystems) under the following conditions; 94°C for 4 minutes, 40 cycles of 94°C for 1 minute, 60°C for 1 minute and 72°C for 2 minutes, and then 72°C for 7 minutes. PCR products were analyzed using a 1.5% (w/v) agarose (Certified PCR agarose 161-

3104, Bio-Rad Laboratories, Mississauga, ON, Canada) gel. DNA integrity from microdissected cervical epithelium was subsequently analyzed by amplifying the HKG  $\beta$ -globin using PCR from DNA extracted, as described above, from LCM material.

## **2.4 P16 Staining**

Sections from biopsy specimens were stained for p16 over-expression using the CINtec p16 immunocytochemistry staining kit (CINtec p16INK4a Cytology Kit; mtm laboratories, Westborough, MA, USA). Diffuse staining was considered p16 positive, while specimens displaying discrete focal positivity were deemed negative. A negative control was included in each case where the primary antibody was omitted to reduce false positive results.

## **2.5 Immunohistochemistry**

Samples used for LCM analysis were stained for CD4/CD8+ cells in the stroma epithelial layers. Primary antibodies specific for CD4/CD8 cell surface markers (MT310 (CD4), DK25 (CD8), DAKO, Glostrup, Denmark) were diluted in DAKO real antibody diluent (DAKO, S2022) at 1:100 in PBS and 100  $\mu$ l was added to the tissue section, then incubated for 1 hour at room temperature. Samples were then washed in ice cold 1X PBS. The secondary mouse antibody conjugated to an Alexa 594 fluorophore was diluted in antibody diluent 1:800 and then added to the section (100  $\mu$ l) and incubated in the dark for 30 minutes. Sections were washed in 1X PBS as before and mounted with medium containing DAPI.

## **2.6 RNA Extraction**

RNA was extracted from 10 x 10  $\mu$ m thick FFPE and FR cervical tissue sections as well as from 1 x 10<sup>6</sup> NIKS using three different methods: Sigma TriReagent® (Sigma-Aldrich), following the recommended protocol for extraction using 1 ml of TriReagent® with the addition of 20  $\mu$ g of RNase-free glycogen carrier (Fermentas Lifesciences, Burlington, ON, Canada) and

with 2 units of terminal DNase treatment (Ambion); the Ambion RNAqueous<sup>®</sup>-4PCR (Ambion Inc., Austin, Texas, USA), following the described method for extraction from FR tissue/cell pellets; and the Arcturus PicoPure<sup>™</sup> RNA Isolation kit following the protocol described for isolation from CapSure<sup>®</sup> Macro LCM Caps (Arcturus) with the addition of 13.6 Kunitz units of RNase-free DNase treatment (Qiagen, catalog# 79254) and slight modifications when using tissue sections<sup>82</sup>. Briefly, 100 µl of extraction buffer (XB) was added to samples and incubated at 42°C for 30 minutes. The addition of an extra 50 µl of XB made tissue homogenization more manageable when working with tissue sections. One hundred microlitres of 70% (v/v) ethanol was then added (1:1 ratio with XB) to the cell extract and RNA isolation was performed as described in the protocol. The Arcturus kit was also used for RNA extraction from microdissected samples using 8 µm thick FR tissue, following the recommended protocol for use with CapSure<sup>®</sup> Macro LCM caps (Arcturus)

## **2.7 Nucleic Acid Quantification and Integrity Assessment**

The quality and quantity of RNA extracted from cell lines and cervical tissue was assessed using the Bio-Rad Experion<sup>™</sup> Automated Electrophoresis System. RNA integrity from samples was assessed by visual inspection of the electropherograms<sup>83</sup> as well as the digital gel images. Samples possessing distinct 18S and 28S ribosomal peaks in the electropherogram<sup>83</sup> as well as sharp, abundant 18S and 28S ribosomal RNA (rRNA) bands in the gel images, were indicative of high RNA integrity. Calculated rRNA 28S/18S ratios did not always correlate with superior images<sup>84</sup> and are therefore reported here but were not used for sample integrity assessment.

High sensitivity chips (Experion<sup>™</sup> RNA HighSens Analysis Kit, Bio-Rad) were used to analyze RNA from LCM-obtained samples and from FFPE and FR cervical biopsy sections

whereas standard sensitivity chips (Experion™ RNA StdSens Analysis Kit, Bio-Rad) were used to assess RNA from cell lines. When specified, initial cell line cDNA was quantified using a Nanodrop spectrophotometer (ND-1000, NanoDrop Technologies, Thermo Fisher Scientific, Wilmington, Delaware, USA) and RNA integrity was later confirmed using the Experion™ (data not shown).

## **2.8 Laser Capture Microdissection**

The Arcturus Histogene™ Frozen Section Staining Kit was used to prepare samples for microdissection. FR biopsy sections were fixed, stained and dehydrated following the Arcturus method with slight modifications. Briefly, 1X ProtectRNA™ (ProtectRNA™ RNase Inhibitor 500x concentrate, catalog number R7397, Sigma-Aldrich) was added to the staining solution (Culling 1984) and tissue was dehydrated as normal with the addition of an extra 100% (v/v) ethanol step to acquire intact RNA<sup>68</sup>. Tissue sections were allowed to dry for up to 3 hours prior to capturing 5,000 to 25,000 cells in 1,000 to 5,000 captures using CapSure® Macro LCM caps. Typically one tissue section was adequate to obtain 1,000 LCM captures of cervical keratinocytes, while 4-5 sections were required to obtain 5,000 LCM captures. Five thousand captures were taken for IFN gene expression analysis. Macro caps were cleaned of unwanted debris using CapSure pads (Arcturus) prior to being deposited into 1.5 ml microfuge tubes for RNA extraction. The laser spot size was consistently 15 µm in diameter whereas the laser power and duration varied slightly between sections (ranging from 80 to 95 mW and 0.65 to 0.8 millisecond duration). LCM images were taken at 10X magnification.

## **2.9 Reverse Transcription and cDNA Amplification**

RNA isolated from samples was reverse transcribed to complementary DNA (cDNA) using the High Capacity cDNA Archive Kit (Applied Biosystems) according to the

manufacturer's directions with random hexamer primers. All RT reactions were performed in 18  $\mu$ l volume. RNA from cell lines whose cDNA was not amplified was reverse transcribed at 20 ng/ $\mu$ l while RNA from cell lines requiring cDNA amplification and cervical biopsy tissue was reverse transcribed at 4 ng/ $\mu$ l. RNA isolated from microdissected cervical samples was reverse transcribed at 0.06-2.8 ng/ $\mu$ l, depending on acquired LCM sample RNA concentration. Fifty nanograms of cDNA from NIKS and whole biopsy sections as well as between 0.75 and 35 ng of cDNA from microdissected tissue was amplified using the TaqMan® PreAmp Master Mix Kit (Applied Biosystems), unless otherwise specified. For amplification uniformity assessment, 7.5 ng of cDNA from NIKS and biopsy sections as well as 2.5 ng of cDNA from an LCM sample was amplified and compared to 7.5 ng of unamplified cDNA from NIKS and biopsy material and 1.8 ng of unamplified cDNA from the LCM sample. NIKS were used in initial experiments to determine the optimal amplification conditions. Uniform transcript amplification was assessed within each sample by comparing unamplified versus amplified gene expression between two genes using the  $\Delta\Delta$ Ct method, as described (Applied Biosystems TaqMan® PreAmp Master Mix Kit Protocol, Appendix A: checking preamplification uniformity). A  $\Delta\Delta$ Ct value of  $0 \pm 1.5$  indicated uniform amplification

## **2.10 Quantitative Real-Time Polymerase Chain Reaction**

Reactions were carried out according to the qRT-PCR protocol specified in the TaqMan® PreAmp Master Mix Kit. Amplified or unamplified cDNA (6.25  $\mu$ l) was added to each reaction. Triplicate reactions of 25  $\mu$ l volume were added to a 96-optical well plate (Applied Biosystems) and incubated at standard qRT-PCR conditions (50°C for 5 minutes, 95°C for 10 minutes and then cycled at 95°C for 15 seconds and 60°C for 1 minute for 40 cycles). TaqMan® gene expression assays for hypoxanthine phosphoribosyltransferase1 (HPRT1),  $\beta$ -actin, phospholipase

A (PLA), 18S ribosomal subunit (18S), beta-2-microglobulin (B2M), IFN- $\gamma$ , IFN- $\beta$  and IFN- $\kappa$  were used. Negative controls where cDNA was omitted or the enzyme was missing in the RT reaction were run to monitor for contamination or non-specific primer binding. A positive control was included on every plate to control for variation between runs. Candidate HKGs were chosen based on an extensive literature review. After demonstrating that its expression was unaffected by HPV infection, target Ct values were normalized to HPRT1. Relative quantification of target genes was performed using auto Ct and baseline settings and a threshold of 0.20 (Applied Biosystems 7300/7500/7500 Fast Real-Time PCR System Software).

### **2.11 Statistical Analysis**

The Relative Expression Software Tool (REST<sup>®</sup>)<sup>85-87</sup>, designed for highly sensitive quantification, was used for comparing gene expression between two groups when analyzing patient tissue, using reaction efficiencies set to 1. An efficiency value of 1 assumes all reactions are 100% efficient. Suitability of HKGs in patient tissue was assessed by setting target gene values to zero to measure only the HKG expression. Unpaired, two-tailed student's t-tests were used for cell line analysis as well as alongside REST when analyzing tissue samples. Student's t-tests appeared more appropriate when analyzing small sample sizes. ANOVA tests were used when analyzing gene expression in more than two groups. The Fisher's exact t-test was used when assessing the prevalence of gene expression between two groups. For all statistical tests, p-values  $\leq 0.05$  indicated a statistical difference in expression.

## 3.0 RESULTS

### 3.1 Sample Size and Material Characterization

#### 3.1.1 RNA Integrity of Samples

Samples used in this study were thoroughly tested for RNA integrity. Of all biopsy specimens tested, 79.4% displayed suitable RNA integrity and were therefore included in this study (**Table 1**). Cell lines were of the highest quality, as seen in **Figure 5**, where the Experion gel images (**Figure 5A**) show minimal degradation and distinct ribosomal subunit bands and the electropherogram (**Figure 5B**) showed a high 28S peak relative to 18S. Whole biopsy specimens also displayed good RNA integrity, as seen in **Figure 5C**, but with more degradation compared to cell lines. The whole biopsy electropherogram illustrated slight degradation with a lower 28S ribosomal subunit peak (**Figure 5D**). LCM samples also showed adequate RNA integrity as distinct ribosomal subunit bands still exist in the gel image with no appreciable amount of degradation (**Figure 5E**). However the LCM electropherogram demonstrated slightly more degradation from whole biopsy specimens with a lower 28S subunit peak (**Figure 5F**). PBLs isolated from patient blood specimens displayed high RNA integrity similar to cell lines (**Figure 5G**).

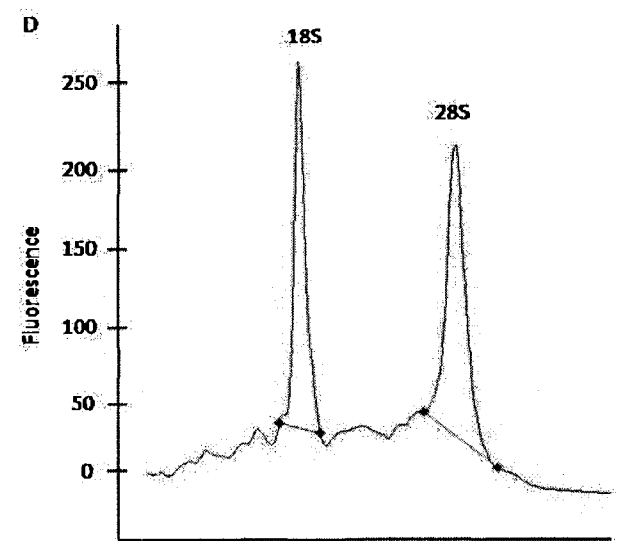
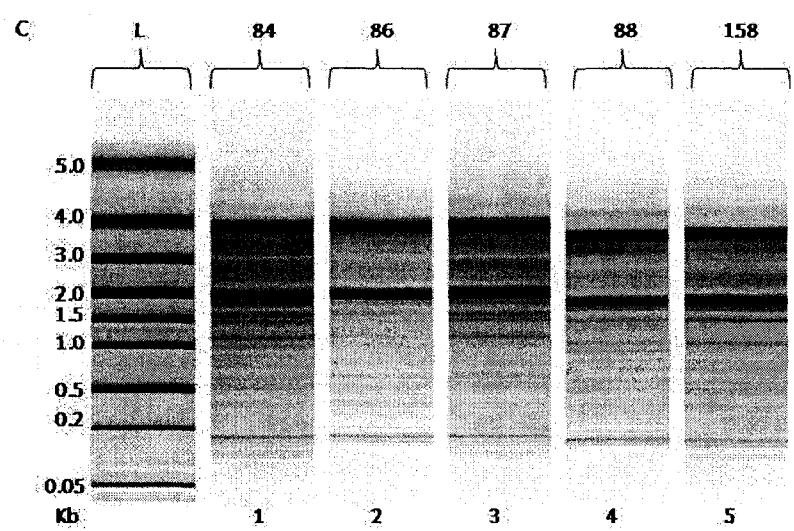
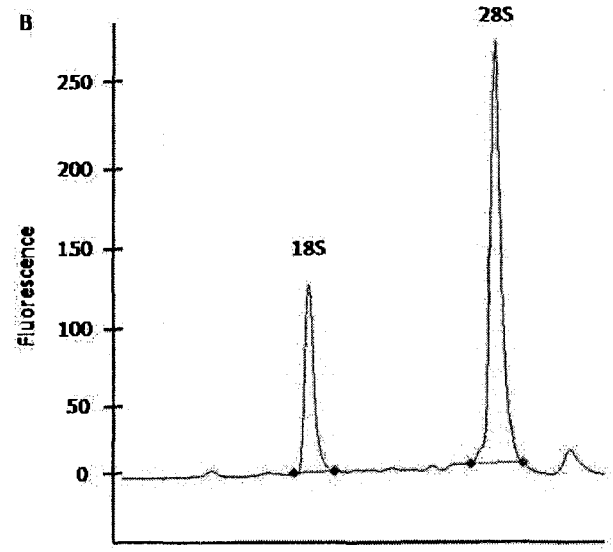
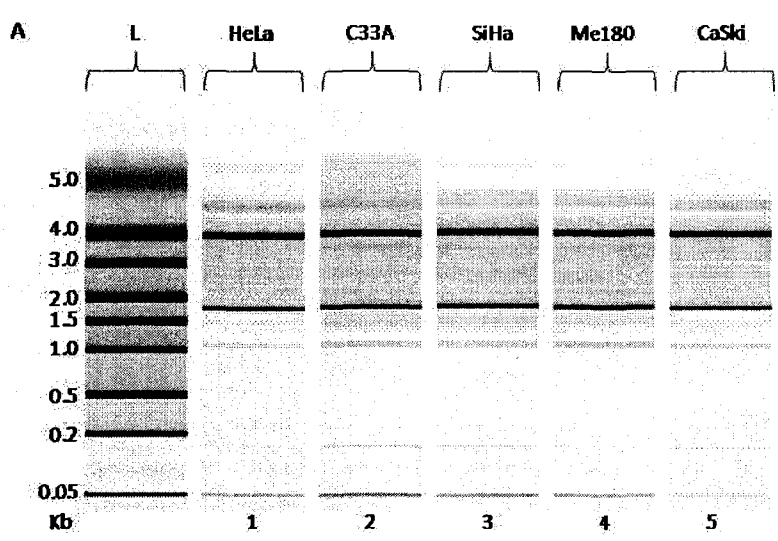
#### 3.1.2 HPV Typing

Of the 34 samples included in this study, 15 (45%) were infected with a HR HPV type. Of these 45%, 40% were infected with HPV16 detected using PCR and HPV16 E6 specific primers, as seen in **Figure 6A**. The remaining 60% were infected with an unknown HR HPV type. In the sample size, there were 13 samples (39.4%) that were HPV- when tested in a PCR using HPV-consensus primers (**Figure 6B**), HPV16-specific primers or stained for p16. Of these 13 samples, 12 were morphologically diagnosed as normal by pathologist Dr. Nicholas Escott. One low-grade sample (sample 80) was devoid of HPV infection with our tests. The one

**Table 1.** Case number, morphological diagnosis, use, and HPV status for cervical tissue samples utilized in this study

#	Case	Morphological Diagnosis	Whole Biopsy	LCM	HPV Consensus	HPV 16	P16	Overall HPV Status
1	75	normal	✓	✓	Negative	Negative	x	HPV-
2	79	normal	✓	✓	Negative	Negative	x	HPV-
3	81	normal	✓	✓	Negative	Negative	x	HPV-
4	82	normal	✓	✓	Negative	Negative	x	HPV-
5	83	normal	✓	✓	Negative	Negative	x	HPV-
6	161	normal	✓	✓	Negative	Negative	x	HPV-
7	165	normal	✓	✓	Negative	Negative	x	HPV-
8	166	normal	✓	✓	Negative	Negative	-	HPV-
9	815	normal	-	✓	Negative	Negative	-	HPV-
10	829	normal	-	✓	Negative	Negative	-	HPV-
11	831	normal	-	✓	Negative	Negative	-	HPV-
12	837	normal	-	✓	Negative	Negative	-	HPV-
13	88	lsil	✓	✓	Positive	Negative	+	HR HPV+
14	87	hsil	✓	-	Negative	Negative	x	HR HPV+
15	74	hsil	✓	x	Negative	Positive	+	HPV 16+
16	76	lsil	✓	-	Negative	Negative	+	HR HPV+
17	80	lsil	✓	x	Negative	Negative	x	HPV-
18	84	lsil	✓	✓	Positive	Negative	x	LR HPV+
19	86	hsil	✓	-	Negative	Negative	+	HR HPV+
20	87	lsil	✓	✓	Positive	Negative	+	HR HPV+
21	88	hsil	✓	-	Positive	Negative	+	HR HPV+
22	94	hsil	✓	-	Positive	Negative	+	HR HPV+
23	86	lsil	✓	-	Negative	Positive	+	HPV 16+
24	151	lsil	✓	-	Positive	Negative	-	LR HPV+
25	152	lsil	✓	-	Positive	Negative	-	LR HPV+
26	153	hsil	✓	✓	Negative	Negative	+	HR HPV+
27	158	hsil	✓	-	Positive	Positive	+	HPV 16+
28	166	hsil	✓	✓	Positive	Negative	+	HR HPV+
29	82	hsil	-	x	Negative	Positive	-	HPV16+
30	822	lsil	-	✓	Positive	Negative	-	HPV+
31	838	hsil	-	✓	Positive	Positive	-	HPV16+
32	839	hsil	-	✓	Positive	Negative	-	HPV+
33	C1D2	Carcinoma	✓	-	Positive	Positive	+	HPV16+
34	C1D4	Carcinoma	✓	✓	-	-	-	-

x = p16 negative, + = p16 positive, - =not analyzed for sample  
 lsil=low-grade epithelial lesion  
 hsil=high-grade epithelial lesion



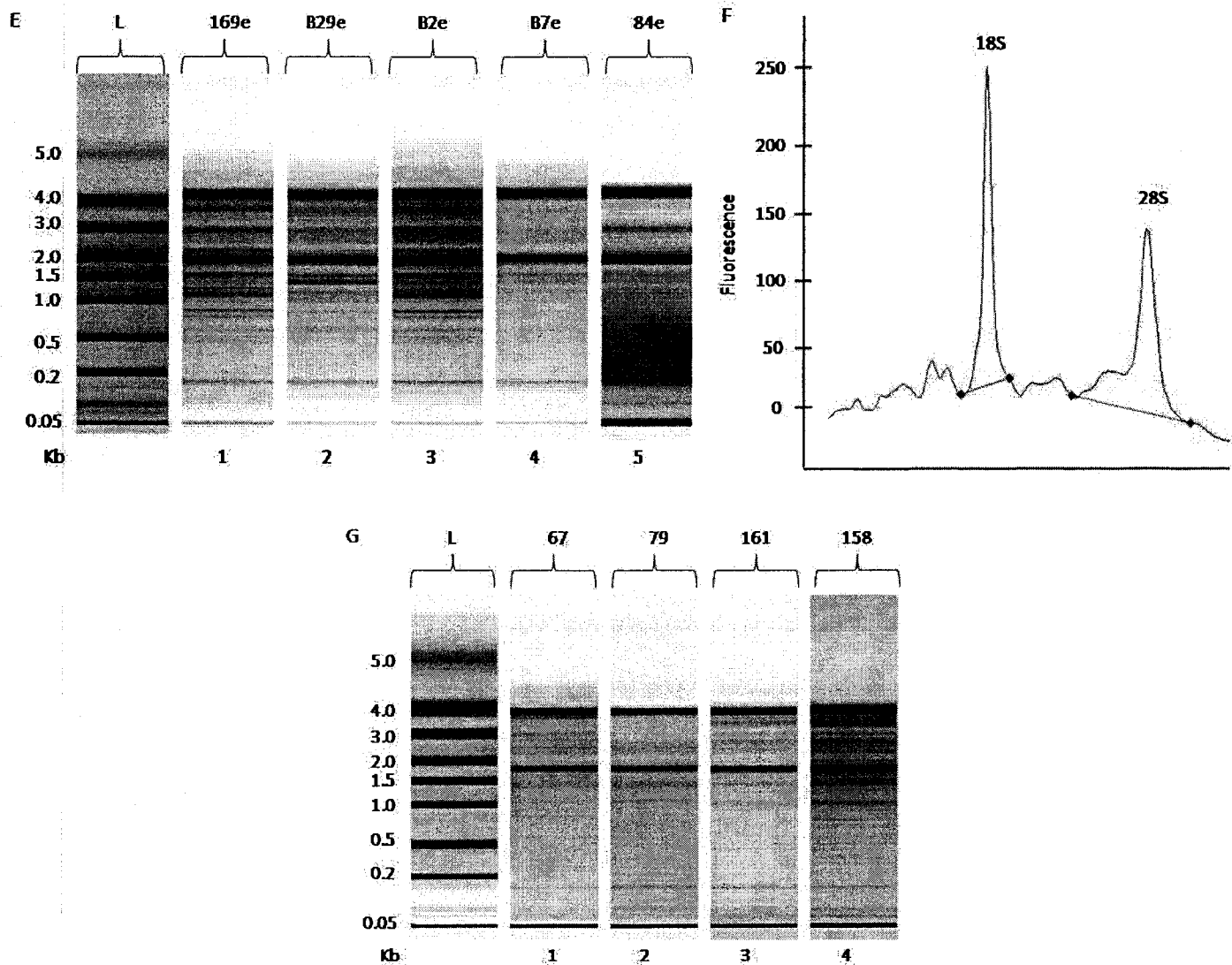


**Figure 5. RNA integrity of samples.** Experion™ gel images of ribosomal subunits for cell lines (HeLa, 28S/18S ratio 2.27; C33A, 1.95; SiHa, 1.95; Me180, 1.84; CaSki, 2.20)(A), full biopsy tissue (Sample 84, 1.12; 86, 1.20; 87, 1.06; 88, 0.90; 158, 1.21) (C), laser capture microdissected material (Sample 169e, 1.24; B29e, 1.24, B2e, 1.28; B7e, 0.00; 84e, 0.45) (E) and peripheral blood lymphocytes (Sample 67, 1.08; 79, 1.48; 161, 1.05; 158, 0.93) (G). The top thicker band represents the 28S ribosomal subunit while the lower thinner band represents the 18S ribosomal subunit. Representative Experion™ electropherograms of ribosomal subunit peaks in cell lines (B), full biopsy sections (C) and laser capture microdissected material (F). RNA from cell pellets (A and G) was extracted using the Ambion extraction method while RNA from tissue samples was extracted using the Arcturus method.

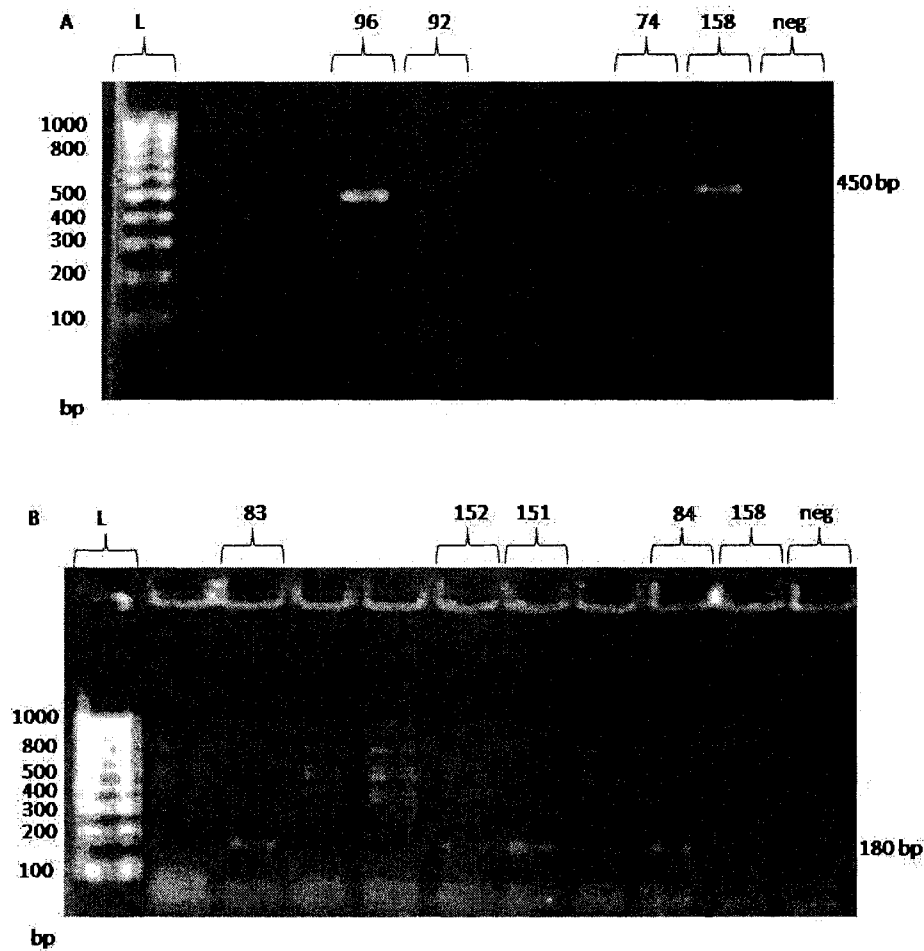


**Figure 6. HPV detection in cervical biopsy material.** HPV16 (A) and HPV consensus (B) sequence detection in FFPE cervical whole biopsy samples. Representative positive results shown for 3 HPV16+ samples (cases 96, 74, 158) and 5 HPV+ samples (cases 83, 152, 151, 84 and 158). DNA from FFPE biopsy tissue was extracted using the in house method and run in PCRs using HPV16 E6-specific primers (450 bp) as well as HPV consensus primers (180 bp) and run on a 1.5% (w/v) agarose gel. PCR conditions were as follows; 1x PCR buffer, 4 mM MgCl, 200  $\mu$ M dNTPs, 1  $\mu$ M HPV16 1/2 primers or 0.1  $\mu$ M HPV consensus primers, 1.25 units of Taq polymerase,  $T_A$  of 60°C.

carcinoma specimen HPV tested (n=1) in this study was HR HPV+. All samples were sent away for HPV genotyping to identify those with multiple HPV infections and to genotype the remaining 60% of HR HPV infected samples and the remaining carcinoma. P16 staining was used as a second analysis of HR HPV infection in case PCR primers were not sensitive enough to detect HPV sequences. Of the diseased cases stained for p16 positivity, 86.6% were positive for p16 overexpression, an example of which is shown in **Figure 7**. Furthermore, 100% (4/4) of HPV16+ samples (results obtained from PCR) stained for p16 resulted in positivity, indicating that p16 staining was a reliable measure of HR HPV infection in this study.

### **3.1.3 Infiltrating CD4/CD8+ Cell Status**

The cases used for LCM analysis of gene expression (n=25) (**Figure 29: Appendix A**) were stained for CD4/CD8+ positive infiltrating cells to reveal the extent of infiltrate in both the epithelium and stroma in these cases. CD4 and CD8 are cell surface markers on a range of leukocytes, including monocytes and dendritic cells, and are prominent markers for helper T and cytotoxic T lymphocytes, respectively. For microdissection, it was important to characterize the material excised in the epithelial layers and to know what kinds of cells were present in the dermis. Of the 24 cases analyzed, 100% of them showed CD4/CD8+ infiltrating cells in the epithelium and 96% showed positivity in the stroma. However, a range of positive CD4/CD8 infiltrate results existed within sample categories (**Figure 8, Table 2**). Some HPV- normal tissue exhibited a high amount of infiltrate in both the epithelium and stroma, whereas other normal HPV- specimens exhibited low levels of infiltrate. Two normal cases (75 and 169) exhibited substantially higher amounts of infiltrate in the epithelium than any of the diseased tissues. Many dysplastic cases showed a moderate amount of infiltrate in the epithelium and there seemed to be no correlation with amount of infiltrate and the grade of the lesion.



**Figure 7. p16 immunocytochemistry for the detection of high risk HPV infection in cervical samples.** Cervical tissue samples were stained for p16 overexpression (brown) using the CINtec p16INK4a cytology kit (ref #110). Negative cervical epithelium (left) shows no staining, whereas the presence of HR HPV infection in a cervical lesion (right) is indicated by diffuse brown staining.

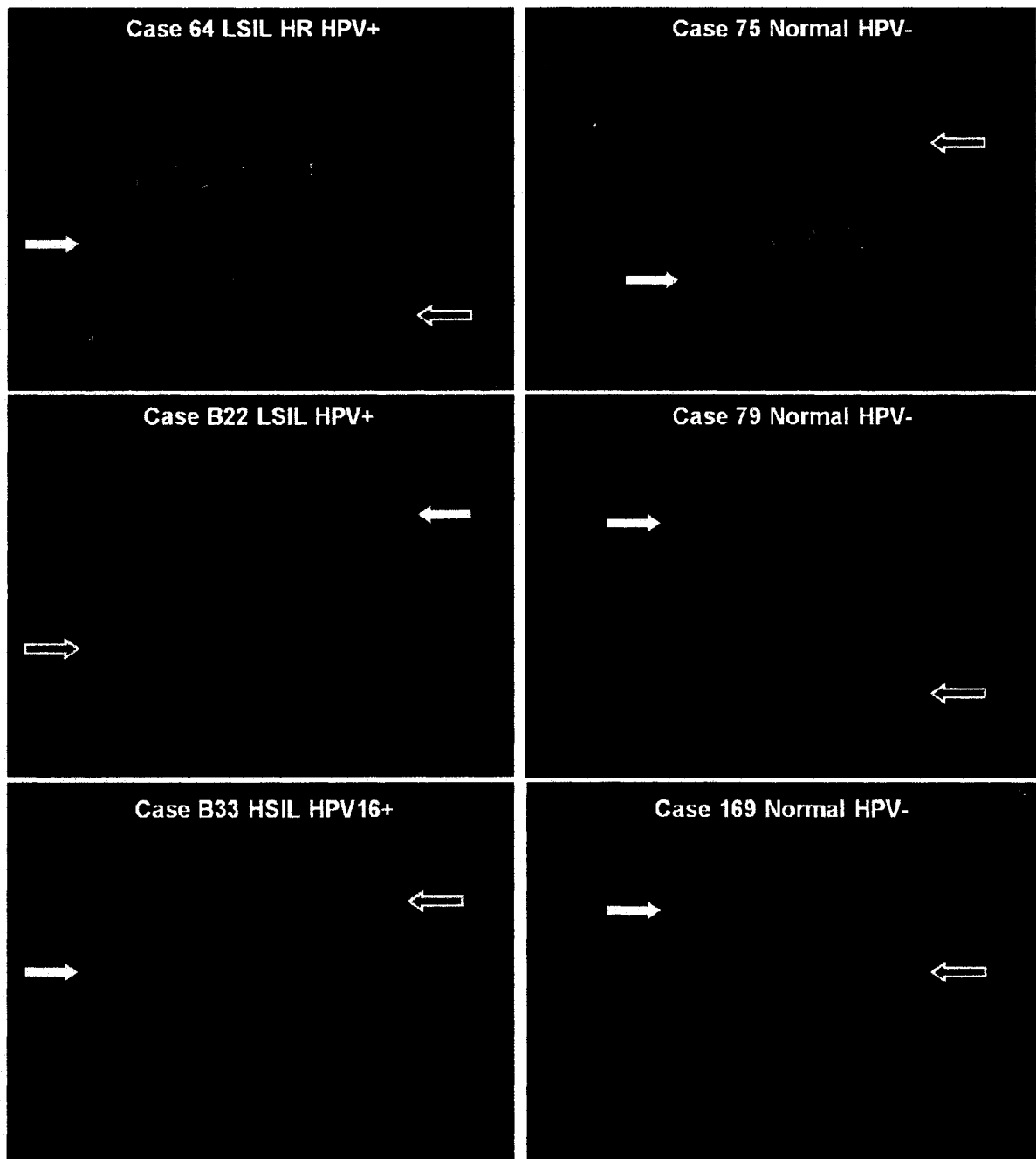


**Figure 8. Infiltrating CD4/CD8+ cells in the cervical microenvironment.** Sections of three normal and three dysplastic cervical tissue stained for infiltrating CD4/CD8+ lymphocytes (red). Cervical cell nuclei are shown in blue (DAPI stain). White arrows denote the cervical squamous epithelium while the grey arrows denote the underlying stroma. Images are at 20X magnification.

**Table 2.** Summary of the presence of CD4/CD8 positive infiltrating cells in tissue samples.

ICM Sample Information		CD4/CD8 Positive Infiltration	
Case	Diagnosis	Epithelium	Stroma
75	Normal	++	++
79	Normal	+	++
81	Normal	+	+
92	Normal	+	++
93	Normal	+	+
100	Normal	+	-
161	Normal	+	+
169	Normal	++	++
B15	Normal	+	+
B29	Normal	+	++
B31	Normal	+	++
B37	Normal	+	++
64	Lsil	+	++
74	Hsil	+	++
80	Lsil	+	++
84	Lsil	+	+
87	Lsil	++	++
153	Hsil	+	+
166	Hsil	+	+
B2	Hsil	+	++
B22	Lsil	+	++
B33	Hsil	+	++
B39	Hsil	+	n/a
CC04	Carcinoma	--	--

+ = positive staining  
 ++ = strong positive staining  
 n/a = no tissue to examine  
 -- = not examined yet

## **3.2 Method Development for IFN- $\kappa$ Detection in Cervical Material: DNA**

### **3.2.1 Optimal PCR conditions**

For the process of HPV typing cervical samples, the integrity of sample DNA must be monitored to control for false negative results. The HKG  $\beta$ -globin was used to monitor DNA integrity in samples. To obtain a highly specific  $\beta$ -globin band, standard PCR conditions were modified to yield an optimal reaction. Increasing the  $MgCl_2$  concentration (**Figure 9A**), decreasing the dNTP concentration (data not shown), increasing the annealing temperature ( $T_A$ ) to 60°C (data not shown), and decreasing the primer concentration (**Figure 9B**) generated a specific  $\beta$ -globin product in cell lines. The optimal PCR conditions for  $\beta$ -globin detection are: 50-100 ng DNA, 1x PCR buffer, 4 mM  $MgCl$ , 200  $\mu$ M dNTPs, 0.1  $\mu$ M primers, 1.25 units of Taq Polymerase and a  $T_A$  of 60°C, incubated at 94°C for 4 minutes and then 40 cycles of 94°C for 1 minute, 60°C for 1 minute and 72°C for 2 minutes, and then 72°C for 7 minutes.

### **3.2.2 DNA Extraction Methods: NIKS and Tissue Samples**

Four extraction methods were used to extract DNA from NIKS. This was initially done to obtain an optimal extraction technique that could be extended to cervical biopsy sections for the purposes of HPV typing. The extraction techniques tested included an in-house method (consisting of a home-made buffer composed of 50 mM Tris-HCl [pH 8.5], 1 mM EDTA and 0.5% Tween20 (v/v)), the Qiagen QIAamp DNA mini kit, the Arcturus Pico Pure DNA Isolation kit and the Qiagen QIAamp Micro kit. Extending from preliminary results (data not shown), two dilution series were performed using two of the extraction techniques, the home-made buffer technique and the Arcturus Pico Pure DNA Isolation Kit, to assess the sensitivity of the extraction methods. DNA was extracted from  $10^6$  NIKS transfected with different HPV16 E6 variants and serial diluted 1:10 seven times to yield a DNA dilution series from approximately



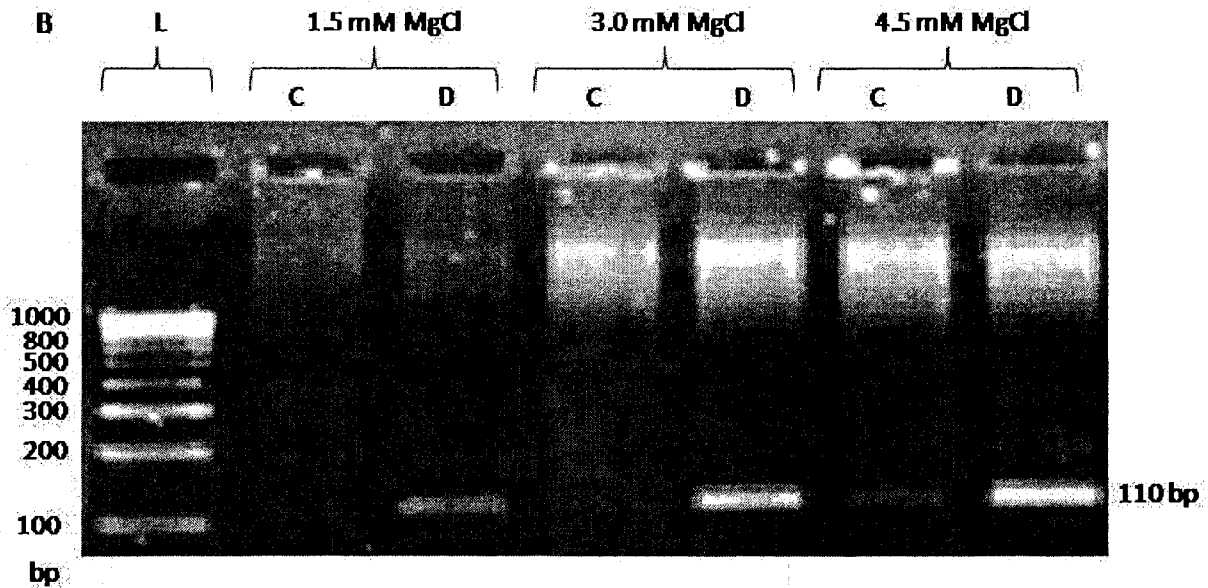


**Figure 9. Optimization of PCR conditions for beta-globin detection.** 1.5% (w/v) agarose gels show increasing the annealing temperature [ $\text{MgCl}_2$ ] plus decreasing the nucleotide concentration and primer concentration increases the specificity of the PCR reaction for the 110 bp beta globin band. **A.** Products were run with a 1  $\mu\text{M}$  primer concentration and different  $\text{MgCl}_2$  concentrations. **B.** Products were run with 0.1  $\mu\text{M}$  beta globin primer pair and the same  $\text{MgCl}_2$  concentrations as in gel A. Products run in pairs; PCR products obtained from DNA extracted from approximately 1,000 (Lanes A & C) and 100,000 (Lanes B & D) NIKS transfected with the 14/78/83 E6 gene. DNA was extracted using the home-made extraction buffer technique. Lane L represents the 100 bp DNA ladder.

$10^6$  cells to one cell.  $\beta$ -globin bands were obtained from DNA extracted from the 5<sup>th</sup> dilution (~100 cells) using the Arcturus method. The in-house method yielded  $\beta$ -globin bands from the 6<sup>th</sup> dilutions (~10 cells), as seen in **Figure 10**. The results indicate that to obtain optimal DNA yield from a small amount of cells, our in-house extraction method is optimal for extracting DNA from NIKS. This technique was extended for DNA extraction from FR and FFPE cervical biopsy tissue with much success, as demonstrated in **Figure 6**.

### ***3.2.3 DNA Extraction Methods: LCM material***

Extracting high quality DNA from LCM samples allows for HPV testing to be performed on isolated cell populations. Cervical biopsy tissue prepared for LCM using the Arcturus method described for DNA extraction allows for quality DNA isolation from 1, 10, 100 and 1,000 LCM captures (representing approximately 5, 50 500 and 5,000 cells respectively), as demonstrated in **Figure 11**. Both the home-made extraction buffer technique and the QIAamp micro DNA extraction kit were used to extract DNA from LCM cervical tissue. The QIAamp kit generated  $\beta$ -globin bands at a lower-limit of 1 LCM capture (**Figure 11**) while the home-made buffer failed to generate a band using material from one LCM capture (data not shown). This indicates that despite optimal DNA extraction results using the home-made extraction buffer for NIKS (**Figure 10**), the Qiagen QIAamp micro kit is the optimal method for extracting high quality DNA from LCM-excised cervical tissue. Furthermore, the sensitivity of LCM for analyzing DNA integrity is demonstrated by the presence of a  $\beta$ -globin band in just one LCM capture (lane 2; approximately 5 cells).

## **3.3 Method Development for IFN- $\kappa$ Detection in Cervical Material: RNA**

### ***3.3.1 Sample Storage and RNA Extraction***

RNA degradation, resulting from inadequate tissue storage and/or extraction techniques

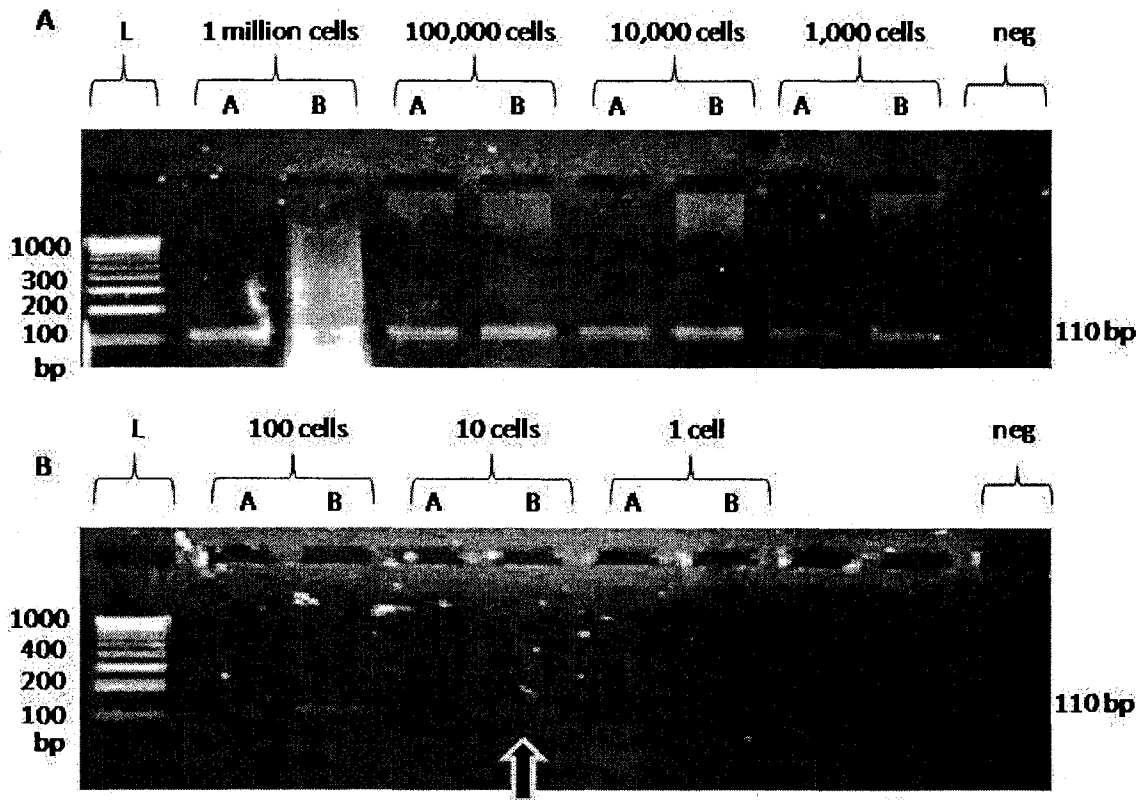


**Figure 10. HPV detection in cervical samples using agarose gel electrophoresis.** 1.5% (w/v) agarose gels show the 110 bp beta globin gene in a DNA dilution series using a combination of NIKS + HPV16 E6 variant cells. DNA was extracted using a home-made extraction method. Lane L represents a 100 bp DNA ladder. **A.** Lanes represent PCR products obtained from DNA extracted from approximately  $10^6$  to  $10^3$  NIKS using  $1\mu\text{l}$  (A) or  $8\mu\text{l}$  (B) DNA input. **B.** Lanes represent PCR products obtained from DNA extracted from approximately  $10^2$  to 1 cells using  $1\mu\text{l}$  (A) or  $8\mu\text{l}$  (B) DNA input. All PCR products were generated using same conditions; 1x PCR buffer, 4 mM MgCl, 200  $\mu\text{M}$  dNTPs, 0.1  $\mu\text{M}$  primer pair, 1.25 units Taq polymerase,  $T_A=60^\circ\text{C}$ .

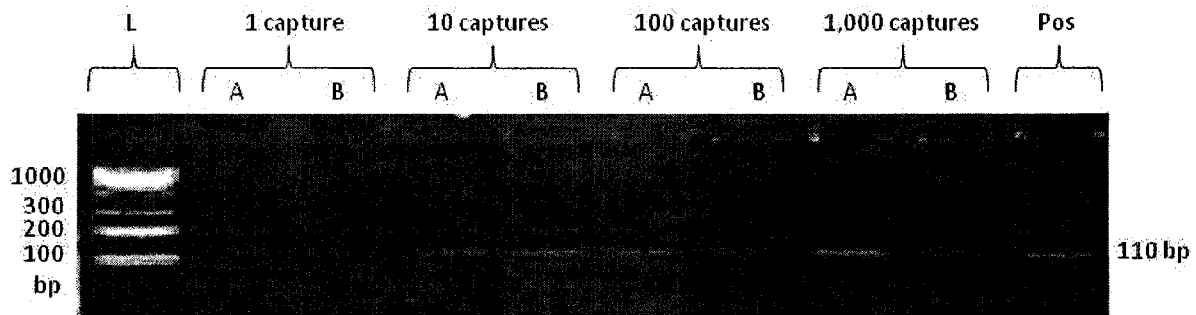


**Figure 11. Sensitivity of LCM for detection of quality DNA.** A 2.0 % (w/v) agarose gel showing the 110 bp beta globin gene from LCM captured cervical cells extracted using the Qiagen QIAamp micro kit. Products are presented in pairs with 1 $\mu$ l (A) and 8 $\mu$ l (B) DNA input. From left to right, lanes represent PCR products obtained from DNA extracted from 1 capture to 1,000 LCM captures. The last lane (Pos) represents a positive control for beta globin. All PCR products were generated using same conditions; 1 x PCR buffer, 4 mM MgCl, 200  $\mu$ M dNTPs, 0.1  $\mu$ M primers, 1.25 units Taq polymerase,  $T_A=60^\circ\text{C}$ .

could significantly alter the resulting transcript profile within a sample. Several methods exist to assess RNA integrity, including denaturing gel electrophoresis, UV spectrophotometry and microfluidics. Traditional gel electrophoresis requires large amounts of RNA to visualize ribosomal bands while UV spectrophotometry assesses sample purity not RNA integrity. Microfluidic gel electrophoresis, such as the Bio-Rad Experion™, permits integrity assessment of small amounts of RNA. This system was therefore used to assess RNA integrity in cervical biopsies, stored in different conditions, and extracted using various techniques as well as in laser capture microdissected cervical epithelium.

RNA extracted from FR cervical biopsy tissue showed higher integrity than RNA extracted from FFPE cervical tissue (**Figure 12A**). Using standard sensitivity Experion™ chips (lanes 1-6), RNA integrity was assessed between two FR samples (lanes 1-2) and 4 FFPE samples (lanes 3-6). No visible rRNA bands were found in the FFPE samples. However, as seen in lanes 7 and 8, the accuracy of the integrity assessment was greatly improved for the intact FR samples when high sensitivity Experion™ chips were used as demonstrated by the more pronounced rRNA bands shown. This data demonstrates that FR tissue specimens preserved the integrity of RNA whereas formalin-fixation procedures degraded it. However, out of all FR biopsy specimens tested, only 74% yielded high-quality (data not shown), indicating that RNA integrity is not equal between samples despite identical extraction and storage conditions. The Arcturus isolation method was optimal for the extraction of high quality RNA from small amounts of FR cervical biopsy tissue (**Figure 12B**) compared to the Sigma and Ambion methods. No visible rRNA bands were present when the Ambion or Sigma methods were used for extraction. Conversely, RNA yield and quality from NIKS was highest when using the Ambion method, as seen in **Figure 5A**.



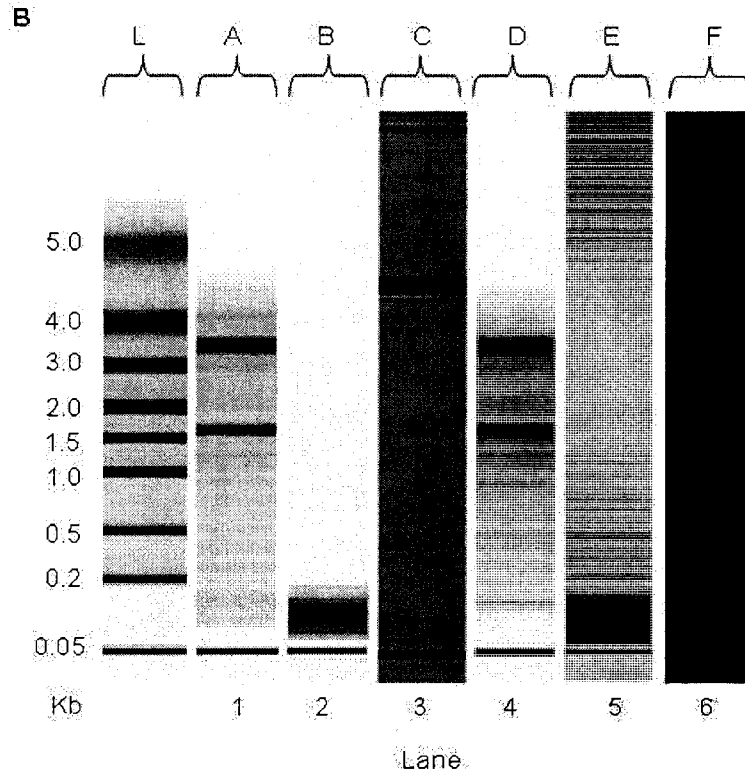


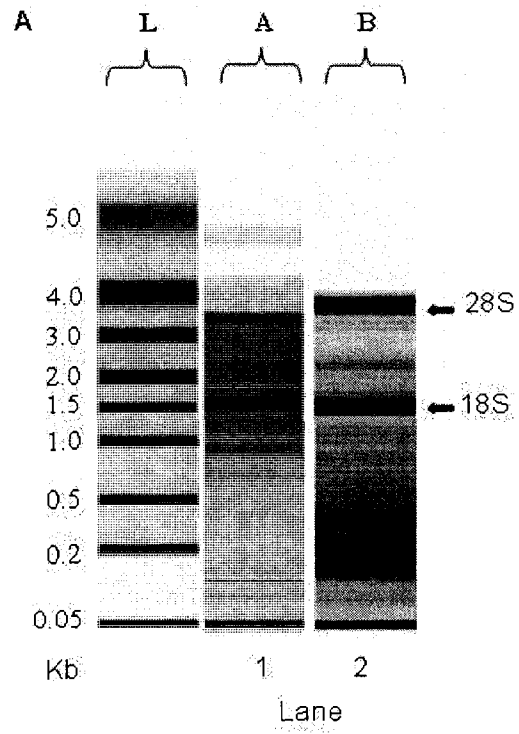
**Figure 12. RNA integrity of cervical tissue using different sample storage and extraction methods.** **A.** Integrity of RNA in FR versus FFPE cervical tissue. RNA was extracted from FR cervical biopsy sections (Lanes 1, 2, 7, 8) and FFPE cervical sections (Lanes 3, 4, 5, 6) using the Arcturus PicoPure™ RNA Isolation Kit. RNA in lanes 1 through 6 was measured using standard sensitivity Experion™ chips. RNA from FR samples A and B were re-measured using an Experion™ high sensitivity chip (lanes 7 and 8) resulting in 28S/18S rRNA ratios of 0.83 and 1.49 respectively. **B.** Integrity of RNA from 6 frozen cervical biopsies extracted using three different extraction kits. The Arcturus (lanes 1 and 4), Sigma (lanes 2 and 5) and Ambion (lanes 3 and 6) extraction kits were tested. Experion™ standard sensitivity chips (lanes 3 and 6) and high sensitivity chips (lanes 1, 2, 4, 5) were used. “L” represents the RNA ladder (Kb). Representative gel images are shown. 28S/18S rRNA ratios for samples A and D were 1.49 and 0.83 respectively. Two bands represent the 28S (top) and 18S (bottom) rRNA.

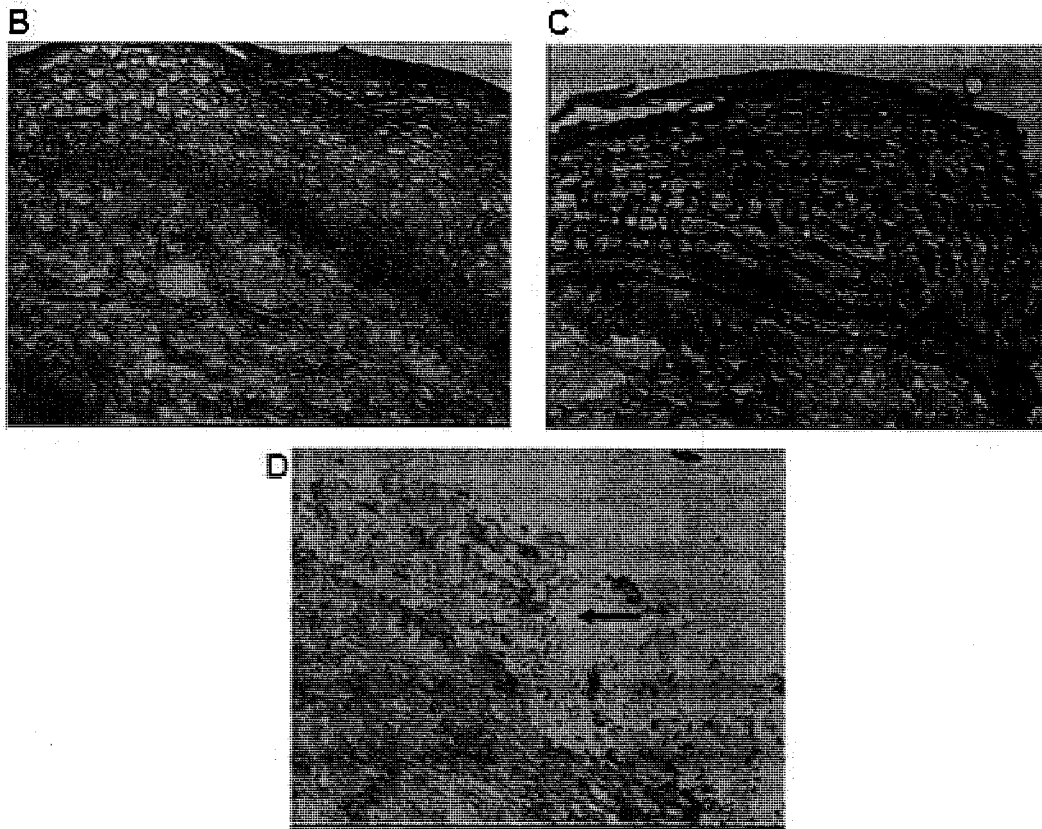
### **3.3.2 RNA Integrity and Tissue Morphology of LCM Samples**

LCM selects for specific cells within a heterogenous cell population. When target genes of interest are cell-type specific, such as IFN Kappa (IFN- $\kappa$ ), which is mainly expressed in epithelial cells<sup>31</sup>, it is crucial to isolate only those cells of interest to gain an accurate assessment of the gene expression profile within a tissue microecology. Obtaining intact RNA from microdissected samples is equally as important for accurate gene expression analysis. Cervical biopsy tissue prepared for LCM using the Arcturus method allowed isolation of high quality RNA from cervical keratinocytes using 1,000 or 5,000 LCM captures (**Figure 13A**), as distinct 28S and 18S rRNA bands can be seen in both LCM samples. Furthermore, the morphology of the tissue was adequate for differentiation between cell types within the tissue (**Figure 13B-D**), as cervical keratinocytes were easily differentiated from surrounding stroma. These data demonstrate that LCM tissue preparation using the reported method provides suitable tissue morphology and high-quality RNA for use in downstream applications.

### **3.3.3 Reverse Transcription**

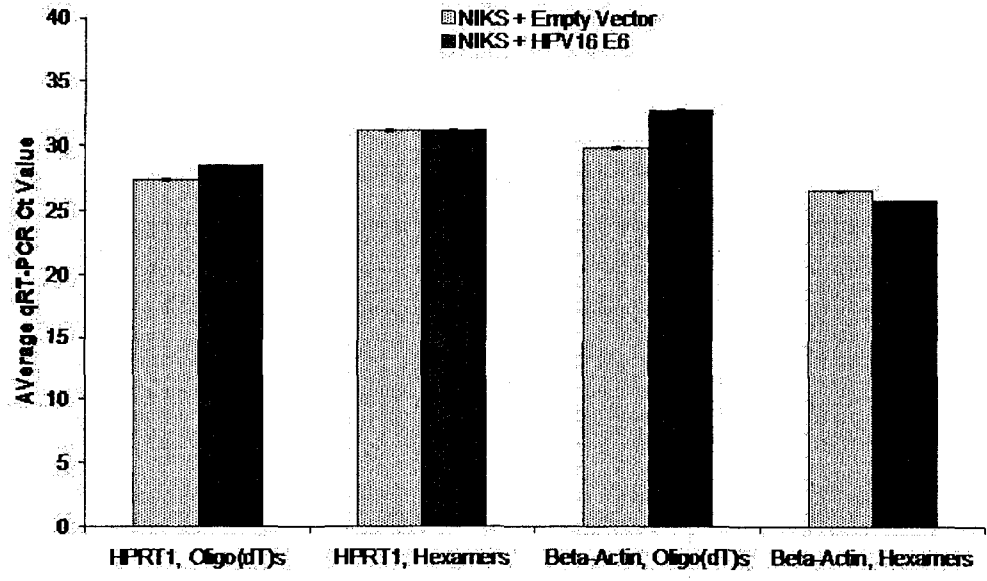
Random hexamer primers were more suitable for RT than oligo(dT) primers. HPRT-1 and  $\beta$ -actin gene expression was analyzed in NIKS transduced with the HPV16 E6 oncogene or an empty vector. Differences between the two conditions for both HPRT1 and  $\beta$ -actin were smaller (student's t-test,  $p=0.011$  and  $p=0.039$  respectively) when using random hexamer primers compared to oligo(dT)s, as shown in **Figure 14A**. RT primer pairs were also assessed in normal and dysplastic cervical biopsy tissue (**Figure 14B**). Similar to cell lines, random hexamer primers produced more favorable results as smaller differences in HPRT1 and  $\beta$ -actin mRNA levels exist between normal and dysplastic tissue when random hexamers were used (student's t-test,  $p= <0.0001$  and  $p= <0.0001$  respectively).





**Figure 13. RNA integrity and tissue morphology of laser capture microdissected cervical tissue.** **A.** Intact RNA obtained from 1000 (lane 2; 190 pg/ $\mu$ l RNA, 28S/18S= 0.38) and 5000 (lane 3; 630 pg/ $\mu$ l, 28S/18S= 1.50) laser capture microdissected cervical keratinocytes. Two bands represent 28S (top) and 18S (bottom) rRNA. **B.** Cervical biopsy section illustrating cervical keratinocytes (top arrow) and stroma (bottom arrow). **C.** 1,000 LCM captures before film was lifted from slide. **D.** Excised epithelial region after film was lifted from slide (black arrow). Representative gel and histological images are shown.

**A**



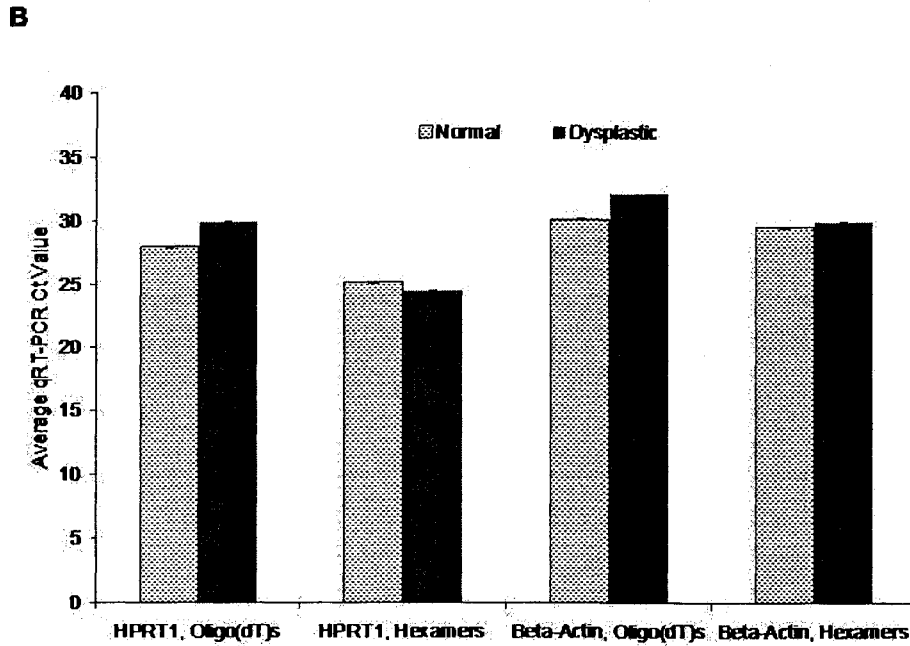


**Figure 14. The effect of different RT primer pairs on HKG expression. A.**  $\beta$ -actin and HPRT1 gene expression measured by qRT-PCR in NIKS +/- the HPV16 E6 oncogene with cDNA reverse transcribed using random hexamer or oligo(dT) primers. RNA was extracted from NIKS using the Ambion RNeasy<sup>®</sup>-4PCR kit. cDNA was quantified using a Nanodrop. **B.**  $\beta$ -actin and HPRT1 gene expression measured in normal and dysplastic cervical biopsy tissue with cDNA reverse transcribed using random hexamer or oligo(dT) primers. RNA was extracted from tissue sections using the Arcturus PicoPure<sup>™</sup> RNA Isolation Kit. Values represent raw qRT-PCR Ct value  $\pm$  SD. cDNA values were obtained from initial RNA values measured using the Experion<sup>™</sup>.

### **3.3.4 HKG for Normalization between Samples**

The use of HKGs for normalization between samples is critical, especially when using heterogeneous tissue samples. While all qRT-PCR studies utilize HKGs for normalization between samples, few studies determine an optimal reference gene for specific tissues. Expression of the HKGs HPRT1,  $\beta$ -actin, 18S, B2M and PLA was analyzed in NIKS in the presence or absence of an HPV16 oncogene (**Figure 15A**). HPRT1, B2M and PLA mRNA levels were statistically similar (student's t-test,  $p \geq 0.05$ ) between the two cell lines. By contrast, expression of  $\beta$ -actin and 18S genes was significantly different between the two cell lines (student's t-test,  $p < 0.05$ ). The expression of HPRT1 and PLA was significantly similar (REST,  $p=0.955$  and  $p=0.367$  respectively) between normal ( $n=4$ ) and dysplastic ( $n=12$ ) cervical whole biopsy tissue, as demonstrated in **Figure 15B**.

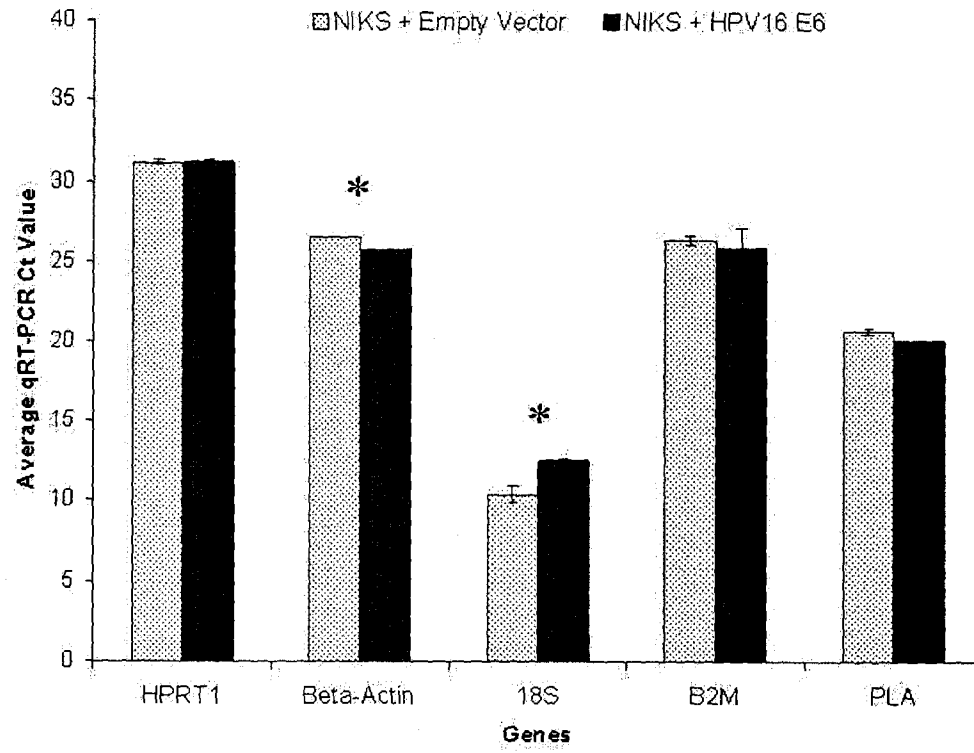
### **3.3.5 cDNA Amplification**

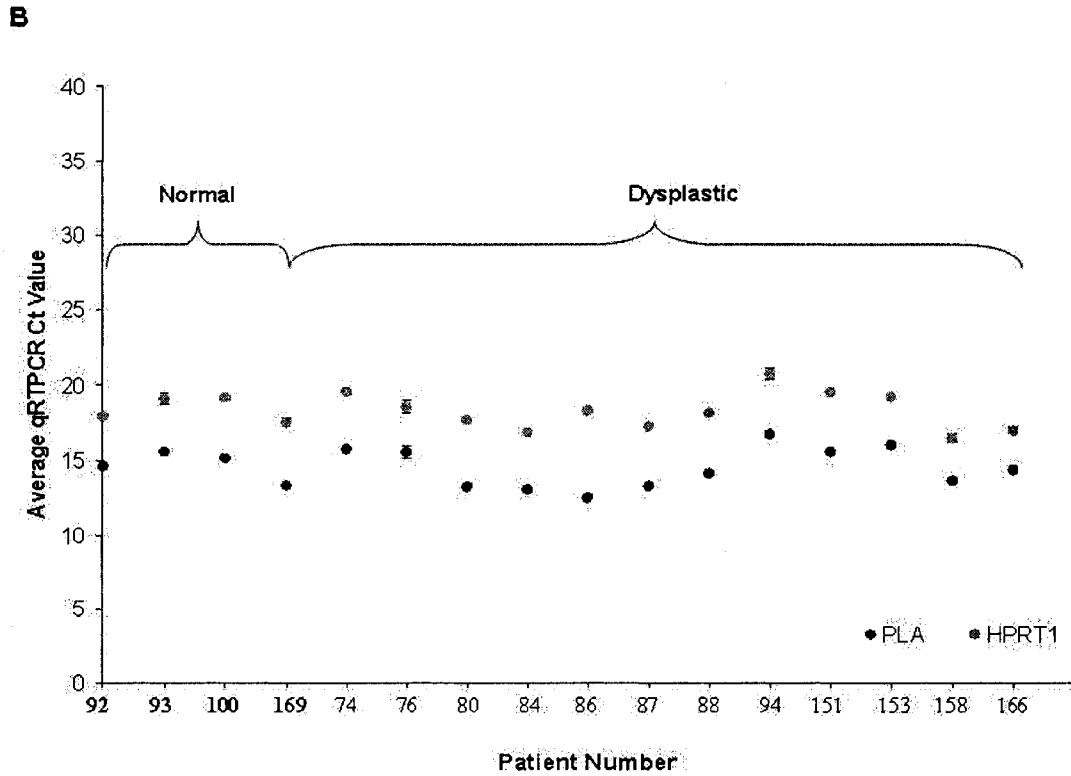
cDNA amplification involves the uniform amplification of specific target genes of interest within a sample and increases the ability to detect low expressing gene transcripts within a suitable range using qRT-PCR. The Taqman<sup>®</sup> PreAmp Master Mix Kit (Applied Biosystems) uniformly amplified cDNA transcripts within NIKS, whole cervical biopsy sections and microdissected cervical epithelium (**Figure 16A**) as all  $\Delta\Delta C_t$  values were less than 1.0. Using NIKS, the optimal cDNA amplification conditions were determined to be 14 cycles using 50 ng of cDNA template since the  $\Delta\Delta C_t$  value still indicated amplification uniformity for genes when the cDNA concentration was lowered and the cycle number was increased (**Figure 16B**).

### **3.3.6 Sensitivity of qRT-PCR and LCM for IFN Detection**

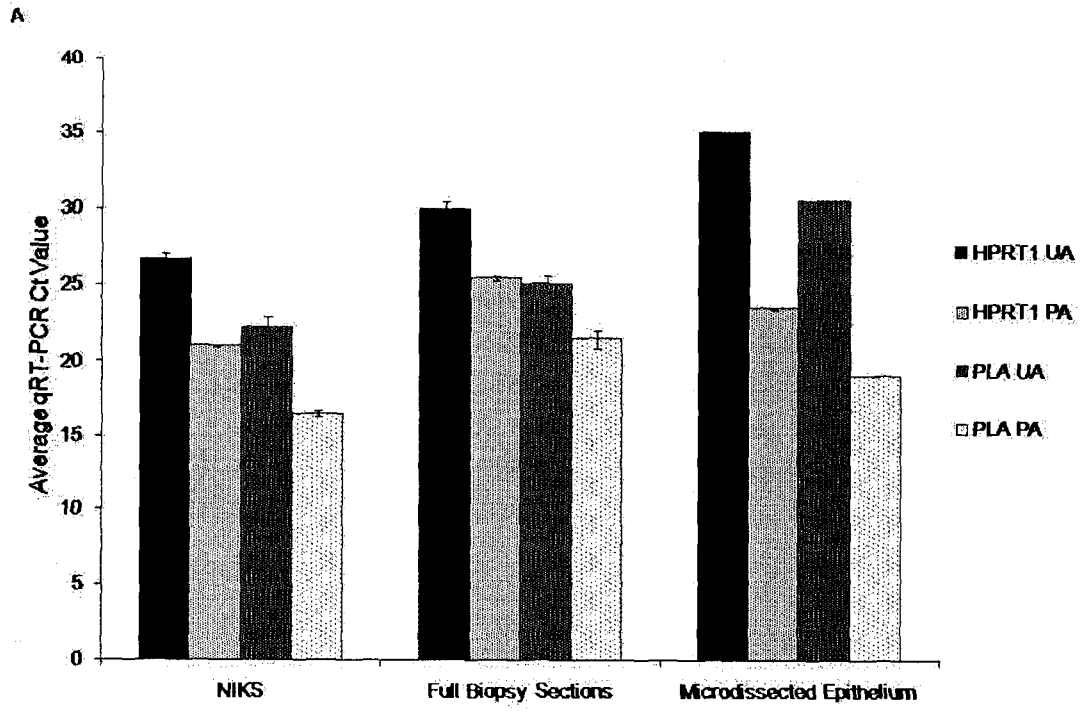
qRT-PCR allows for the simultaneous detection, real-time amplification and quantification of RNA transcripts. Utilizing the TaqMan<sup>®</sup> (Applied Biosystems) methodology

**A**





**Figure 15. Housekeeping gene suitability for normalization across cervical disease states. A.** HPRT1,  $\beta$ -actin, 18S, B2M and PLA housekeeping gene expression in NIKS +/- HPV16 E6 measured using qRT-PCR using unamplified cDNA. HPRT1 ( $p=0.955$ ), B2M ( $p=0.367$ ) and PLA ( $p=0.065$ ) were expressed the same between the cell lines. cDNA was quantified using a Nanodrop. Asterisks indicate significant difference in expression ( $p \leq 0.05$ ) between the cell lines. cDNA input concentrations were determined using the Experion™ and were not always equal between genes.**B.** HPRT1 and PLA housekeeping gene expression in normal ( $n=4$ ; patients 92, 93, 100, 169) and dysplastic ( $n=12$ ; patients 74-166) cervical tissue. HPRT1 ( $p=0.796$ ) and PLA ( $p=0.728$ ) are expressed the same between the control and dysplastic group. Values represent raw average qRT-PCR Ct value  $\pm$  SD using amplified cDNA.



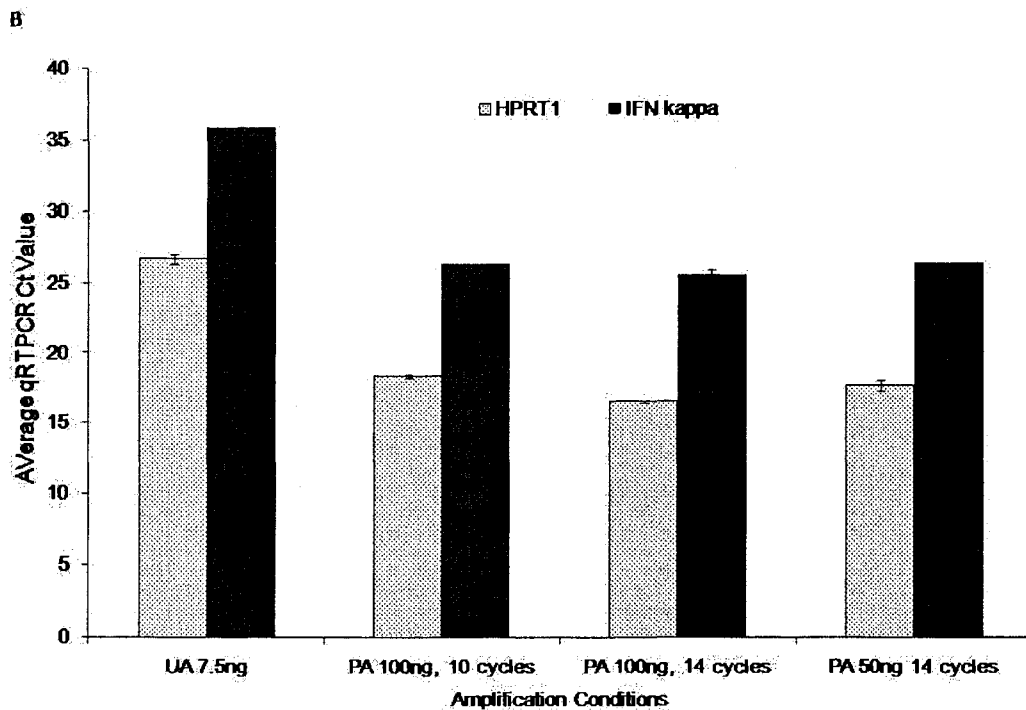


**Figure 16. Uniform cDNA amplification in cervical samples. A.** HPRT1 and PLA gene expression in NIKS, cervical biopsy sections and laser capture microdissected cervical keratinocytes was analyzed before (UA) and after (PA) cDNA amplification using qRT-PCR. Amplification uniformity was assessed using the delta delta Ct method. HPRT1 and PLA in NIKS ( $\Delta\Delta Ct = 0.03$ ), cervical sections ( $\Delta\Delta Ct = 0.93$ ) and microdissected cervical keratinocytes ( $\Delta\Delta Ct = 0.14$ ) respectively were amplified uniformly. **B.** Uniform cDNA amplification in NIKS. cDNA from NIKS was left unamplified or amplified for 10 or 14 cycles using 50 or 100ng of cDNA. qRT-PCR gene expression analysis was performed for HKG HPRT1 and target gene IFN- $\kappa$  using both unamplified and amplified cDNA. Representative cases are shown for tissue samples. 5,000 LCM captures were taken for microdissected cervical samples. Values represent raw qRT-PCR Ct value  $\pm$  SD. cDNA input concentrations were determined using the Experion<sup>TM</sup>.

and reagents for gene expression analysis, this method was used to analyze the gene expression of HKGs and target genes in samples to determine transcript input and LCM sensitivity for the detection of low-expressing IFNs. Whole biopsy sections from 3 cases of cervical dysplasia were analyzed by qRT-PCR (**Figure 17A**). Using the methods described, all IFNs were expressed within a detectable range for qRT-PCR analysis. In general, the expression level of IFNs followed the order of: IFN- $\kappa$  < IFN- $\beta$  < IFN- $\gamma$ . One thousand LCM captures (~1 ng of total RNA) were sufficient to measure HKGs and target genes present at only a moderate level, such as IFN- $\gamma$ , in cervical epithelium. However, for the detection of low expressing genes, such as IFN- $\beta$  and IFN- $\kappa$ , 5,000 LCM captures were required (~10 ng of total RNA), as illustrated in **Figure 17B**.

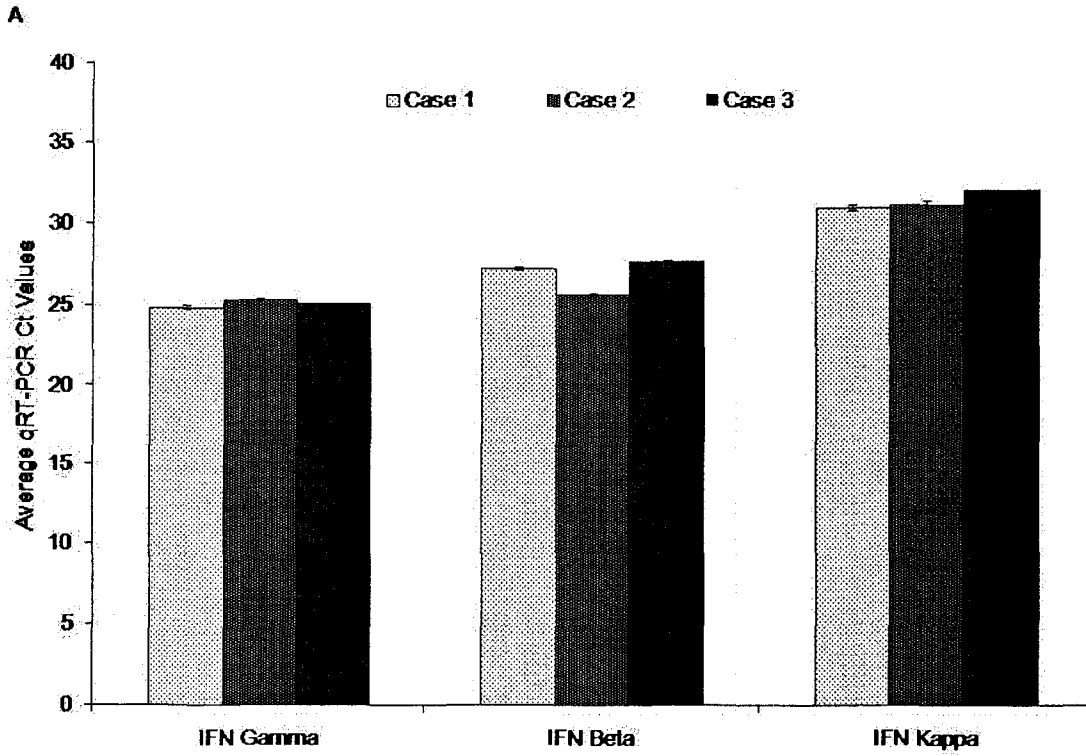
### **3.4 Interferon Gene Expression Profile in Normal, Dysplastic and Carcinoma Tissue**

#### **3.4.1 IFN- $\kappa$ Expression**

IFN- $\kappa$  gene expression in whole cervical biopsy specimens was detected more often in dysplastic tissue (10/16; 62.5%) and carcinoma tissue (2/2; 100%) (**Table 3, Figure 18**) than in normal tissue (2/8; 25%), however the prevalence was not significantly different (Fisher's exact t-test,  $p=0.50$  (ns) and  $p=0.133$  (ns), respectively). When present, the expression level of IFN- $\kappa$  was significantly higher in dysplastic tissue compared to normal HPV- tissue (REST,  $p=0.031$ ) and in carcinoma tissue compared to dysplastic tissue (student's t-test,  $p=0.022$ ) (**Table 4**). Overall, IFN- $\kappa$  gene expression prevalence increased with lesion progression, although not significantly. However, the level of IFN- $\kappa$  gene expression increased significantly as the lesion progresses from normal to invasive carcinoma (ANOVA,  $p=0.006$ ), as seen in **Figure 19**.

#### **3.4.2 IFN- $\beta$ Expression**

IFN- $\beta$  was expressed in 26/26 (100%) of all whole biopsy samples, however the IFN- $\beta$



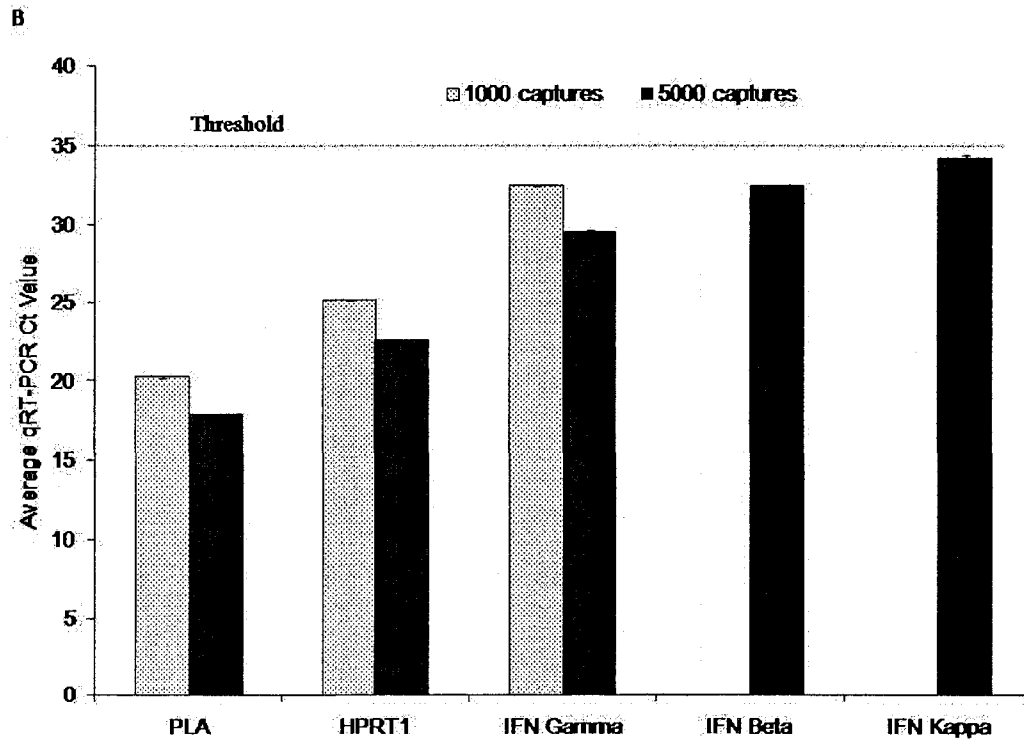


**Figure 17. Sensitivity of qRT-PCR and LCM for the detection of Interferon gene expression in dysplastic cervical tissue. A.** Three cases of cervical dysplasia were analyzed for IFN gene expression using qRT-PCR and 50ng of RNA from whole biopsy sections. cDNA input values were determined from RNA values measured using the Experion™. **B.** Housekeeping and target IFN mRNA detection using qRT-PCR and 1,000 and 5,000 LCM captures of cervical keratinocytes yielding 1 ng and 10 ng of RNA. Values represent raw qRT-PCR Ct values  $\pm$  SD. cDNA input concentrations were determined using the Experion™. The horizontal dashed line represents the upper limit for qRT-PCR detection. A representative case is shown.

**Table 3.** Summary of the prevalence of IFN- $\gamma$ , - $\beta$  and - $\kappa$  mRNA in normal (n=8), dysplastic (n=16) and cervical carcinoma(n=2) whole biopsy tissue samples.

Prevalence of IFN Expression in Whole Cervical Biopsy Tissue (%)				
Gene	Normal	LsII	HsII	Carcinoma
IFN- $\gamma$	100 (8/8)	100 (8/8)	100 (8/8)	100 (2/2)
IFN- $\beta$	100 (8/8)	100 (8/8)	100 (8/8)	100 (2/2)
IFN- $\kappa$	25 (2/8)	63 (5/8)	63 (5/8)	100 (2/2)

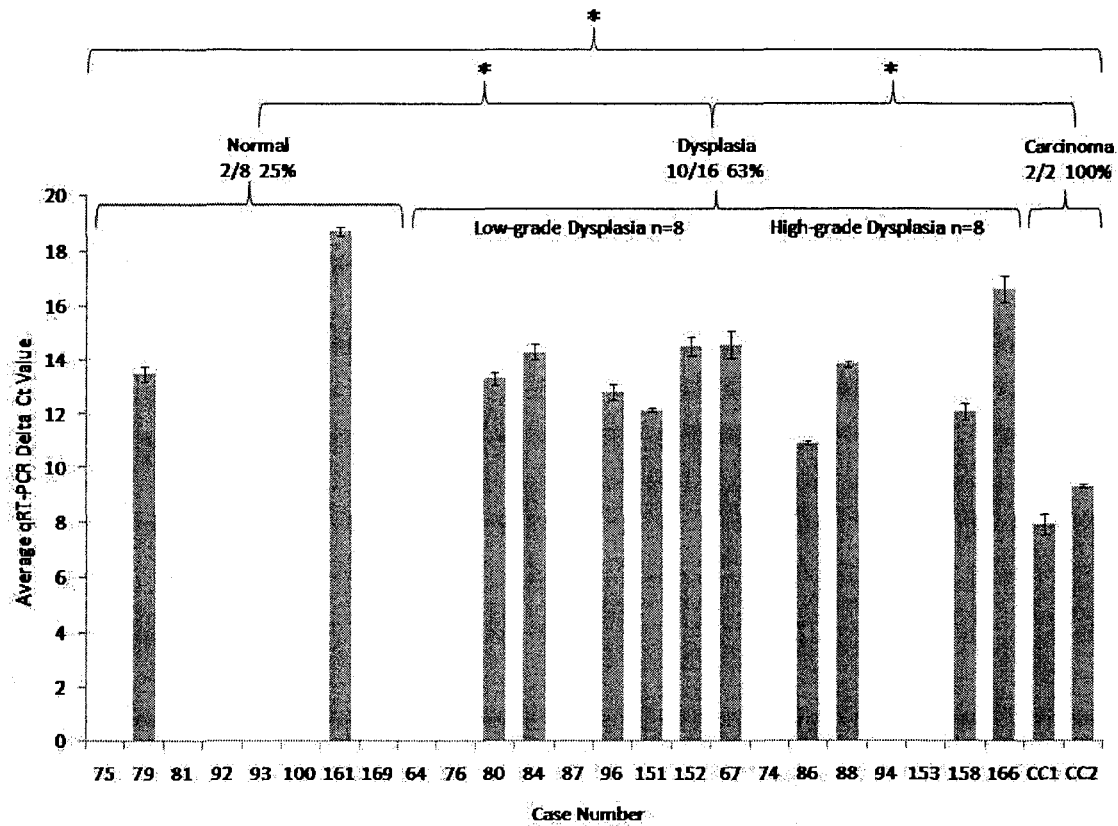


**Figure 18. IFN- $\kappa$  gene expression in cervical biopsy sections.** Full biopsy sections of normal cervical tissue (n=8), low-grade cervical dysplastic tissue (n=8), high-grade cervical dysplastic tissue (n=8) and cervical carcinoma (n=2) were analyzed for IFN- $\kappa$  mRNA levels using qRT-PCR. Vertical bars represent the average delta qRT-PCR Ct value  $\pm$  SD for each case. Percentages indicate prevalence. cDNA input concentrations were determined using the Experion<sup>TM</sup>. Asterisks indicate significant difference in expression levels between the groups.

**Table 4.** Statistical test results for IFN gene expression in normal, dysplastic cervical and carcinoma biopsy tissue. Student's t-test results are displayed at the top, REST software results are displayed in the middle and ANOVA analysis results are displayed at the bottom.

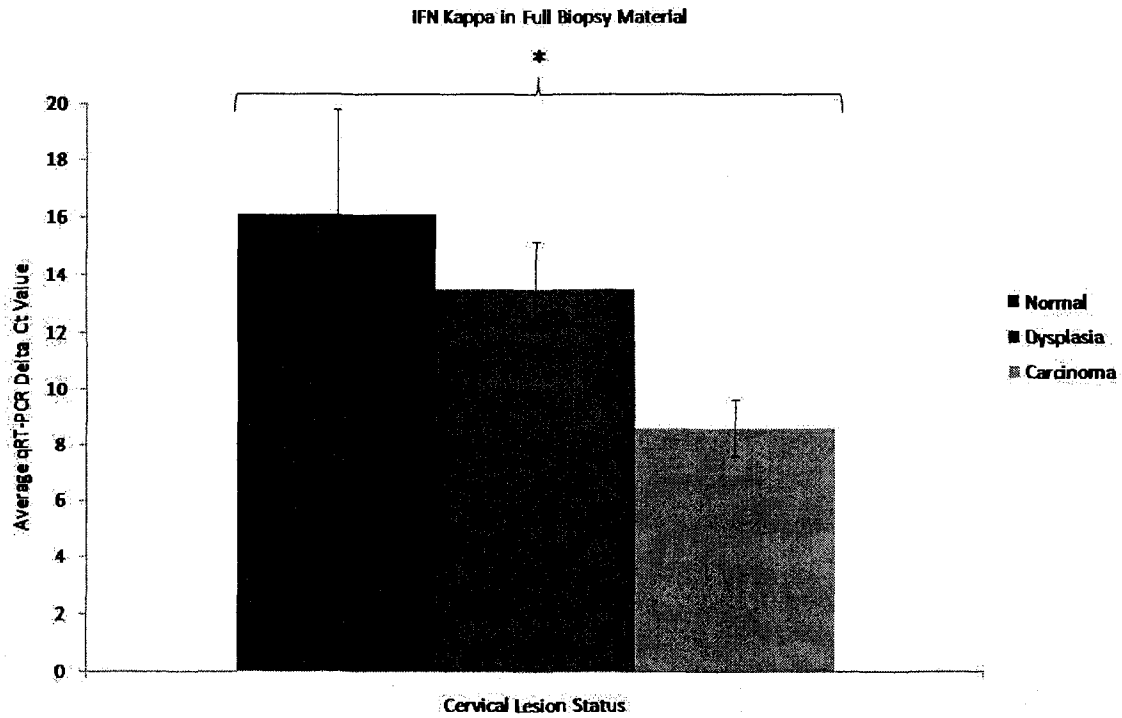
T-test p values			
Gene	Normal vs Dysplasia	Normal vs Carcinoma	Normal vs CC
IFN- $\kappa$	0.498	0.109	<b>*0.022 (<math>\uparrow</math> CC)</b>
IFN- $\beta$	<b>*0.007 (<math>\downarrow</math> Dys)</b>	0.690	0.319
IFN- $\gamma$	0.606	0.950	0.836

REST p values			
Gene	Normal vs Dysplasia	Normal vs Carcinoma	Normal vs CC
IFN- $\kappa$	<b>*0.031 (<math>\uparrow</math> Dysp)</b>	0.503	0.396
IFN- $\beta$	<b>*0.007 (<math>\downarrow</math> Dysp)</b>	0.286	<b>0.946</b>
IFN- $\gamma$	0.615	0.561	0.690

ANOVA p values	
Gene	Normal vs Dysplasia vs Carcinoma
IFN- $\kappa$	<b>*0.0006 (N &lt; D &lt; C)</b>
IFN- $\beta$	<b>*0.039 (D &lt; C &lt; N)</b>
IFN- $\gamma$	0.876



**Figure 19. Average IFN- $\kappa$  expression in normal, dysplastic and carcinoma full biopsy tissue.** Full biopsy sections of normal (n=8), dysplastic (n=16) and cervical carcinoma tissue (n=2) were analyzed for IFN- $\kappa$  mRNA levels using qRT-PCR. Vertical bars represent the average delta qRT-PCR Ct value  $\pm$  SD. cDNA input concentrations were determined using the Experion™.

gene expression level was significantly down-regulated in dysplastic tissue compared to normal HPV- tissue (REST,  $p=0.009$ , student's t-test,  $p=0.007$ ) (**Table 4, Figure 20**). Although the prevalence of IFN- $\beta$  gene expression remains unchanged with the progression of the lesion (**Table 3**), the gene expression level was significantly different in normal, dysplastic and carcinoma tissue (ANOVA,  $p=0.039$ ), as seen in **Figure 21**, where IFN- $\beta$  mRNA levels were highest in normal tissue, decreased in dysplastic tissue and then increased in carcinoma tissue.

### **3.4.3 IFN- $\gamma$ Expression**

IFN- $\gamma$  gene expression was present in 26/26 (100%) samples (**Table 3**) and its expression level remained unchanged with disease state as no significant differences in IFN- $\gamma$  mRNA levels were found between normal, dysplastic or carcinoma tissue samples (**Table 4**), as illustrated in **Figure 22**. IFN- $\gamma$  mRNA levels followed a similar trend as IFN- $\beta$  where gene expression decreased in dysplastic tissue from normal tissue and then increased in carcinoma tissue (ANOVA,  $p=0.876$  (ns)) (**Figure 23**).

### **3.4.4 Relative Expression of IFNs**

The expression of all three IFNs in relation to each other and their relative expression in whole cervical biopsy tissue are illustrated in **Figure 24** and **Figure 25** respectively. The expression levels of these IFNs follow the pattern IFN- $\kappa < \text{IFN-}\beta < \text{IFN-}\gamma$  in normal and dysplastic tissue, however in one carcinoma specimen the expression pattern was opposite; IFN- $\gamma < \text{IFN-}\beta < \text{IFN-}\kappa$ . A significant difference in expression between the two carcinoma samples was observed for IFN- $\gamma$ , - $\beta$  and - $\kappa$  (student's t-test,  $p=0.0006$ ,  $p=0.003$  and  $p=0.0008$  respectively) (**Figure 26**). There was a trend that IFN- $\kappa$  mRNA levels became closer to the expression levels of IFN- $\beta$  and IFN- $\gamma$  in carcinoma tissue compared to those found in normal and dysplastic tissue.

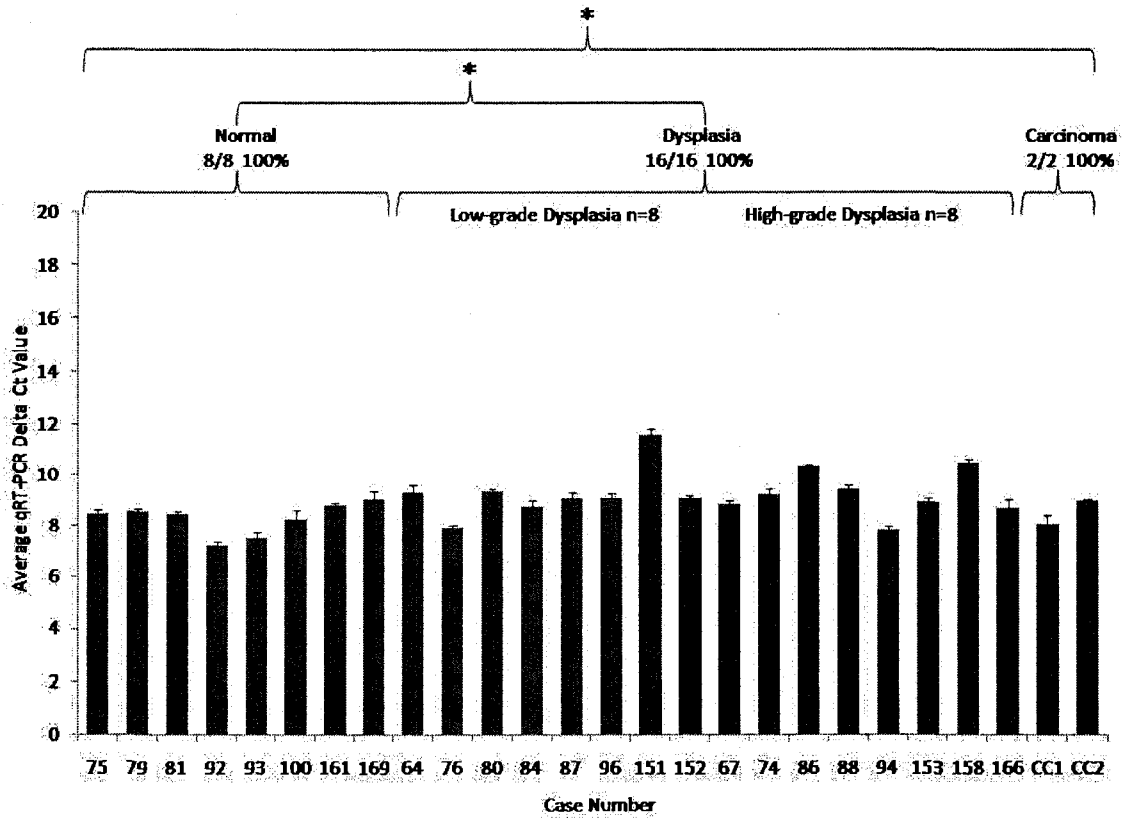


**Figure 20. IFN- $\beta$  gene expression in cervical biopsy sections.** Full biopsy sections of normal cervical tissue (n=8), low-grade cervical dysplastic tissue (n=8) and high-grade cervical dysplastic tissue (n=8) were analyzed for IFN- $\beta$  mRNA levels using qRT-PCR. Vertical bars represent the average delta qRT-PCR Ct value  $\pm$  SD for each case. Percentages indicate prevalence. cDNA input concentrations were determined using the Experion™. Asterisks indicate significant difference in expression levels between the groups.

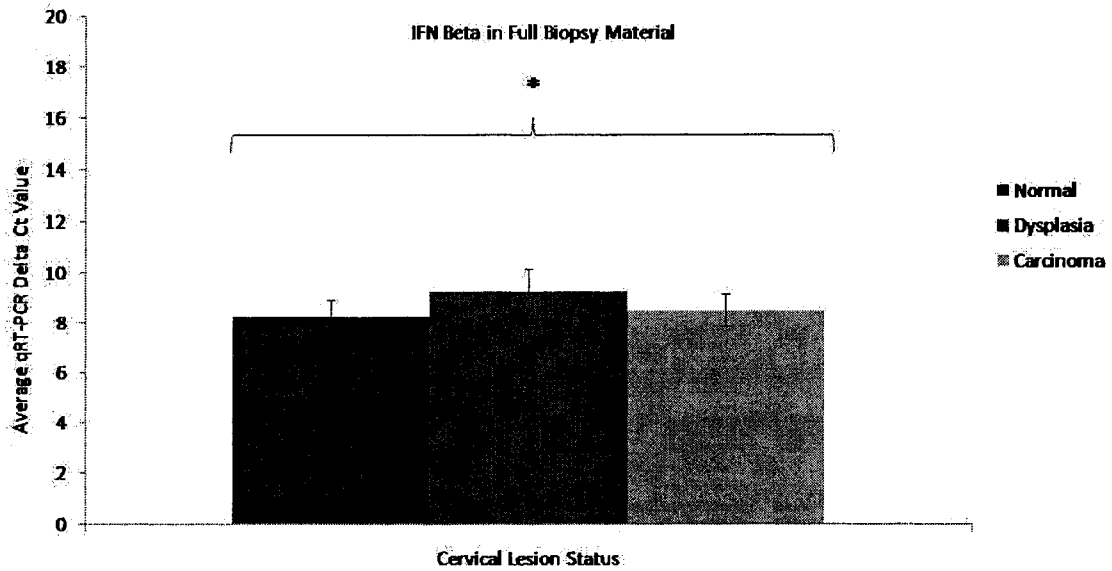


**Figure 21. Average IFN- $\beta$  expression in normal, dysplastic and carcinoma full biopsy tissue.** Full biopsy sections of normal (n=8), dysplastic (n=16) and cervical carcinoma tissue (n=2) were analyzed for IFN- $\beta$  mRNA levels using qRT-PCR. Vertical bars represent the average delta qRT-PCR Ct value  $\pm$  SD. cDNA input concentrations were determined using the Experion™.

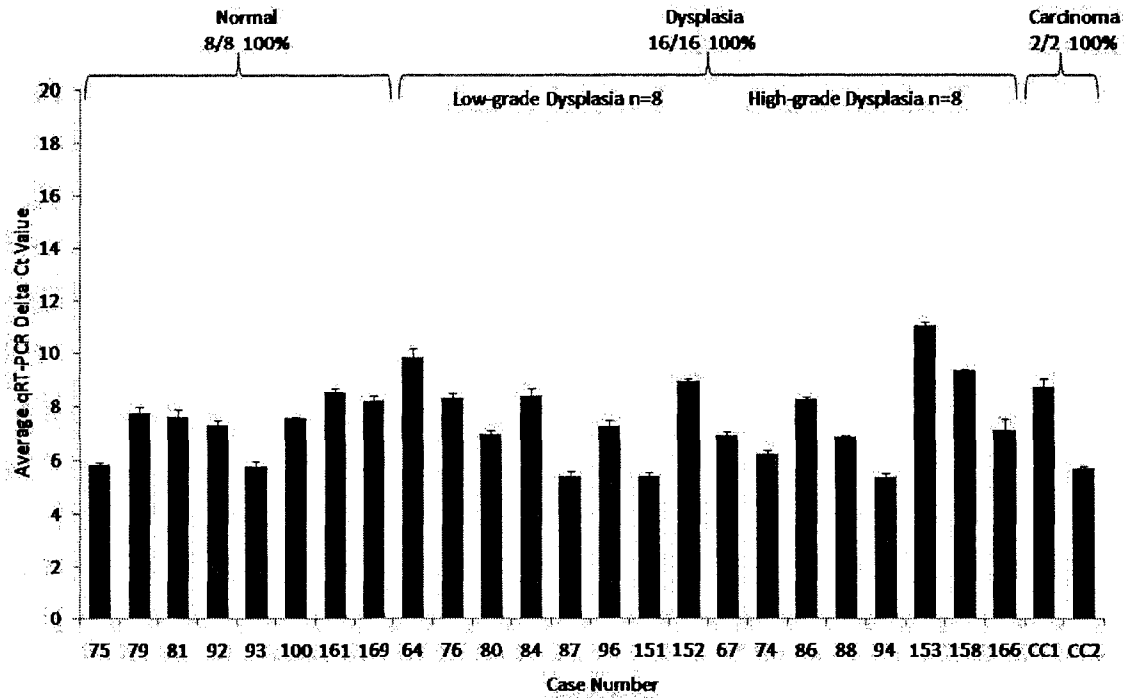


**Figure 22. IFN- $\gamma$  gene expression in cervical biopsy sections.** Full biopsy sections of normal cervical tissue (n=8), low-grade cervical dysplastic tissue (n=8) and high-grade cervical dysplastic tissue (n=8) were analyzed for IFN- $\gamma$  mRNA levels using qRT-PCR. Vertical bars represent the average delta qRT-PCR Ct value  $\pm$  SD for each case. Percentages indicate prevalence. cDNA input concentrations were determined using the Experion<sup>TM</sup>. No statistical significant difference between the groups.

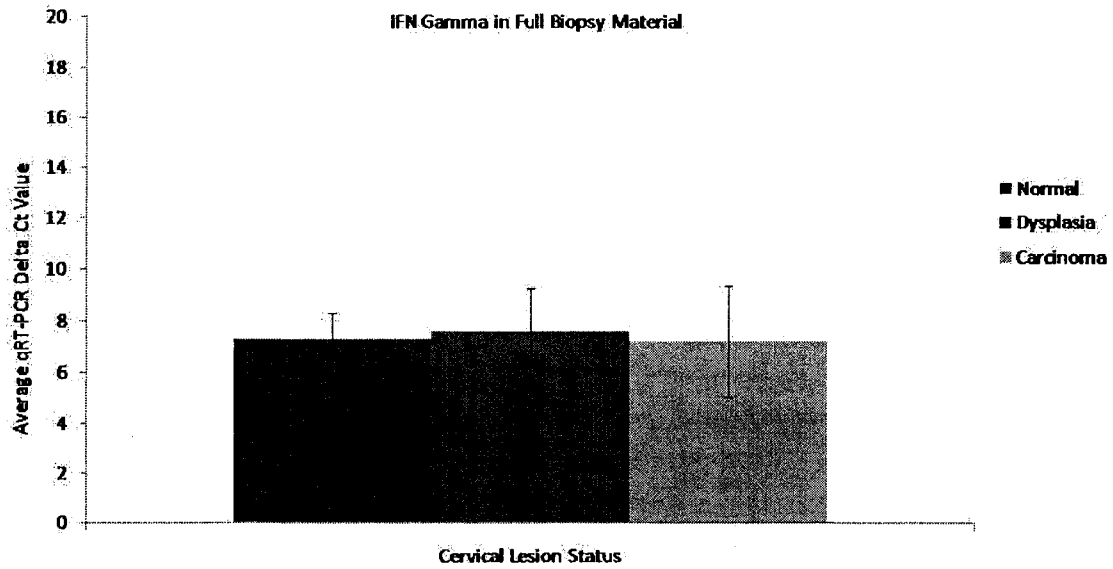


**Figure 23. Average IFN- $\gamma$  expression in normal, dysplastic and carcinoma full biopsy tissue.** Full biopsy sections of normal (n=8), dysplastic (n=16) and cervical carcinoma tissue (n=2) were analyzed for IFN- $\gamma$  mRNA levels using qRT-PCR. Vertical bars represent the average delta qRT-PCR Ct value  $\pm$  SD. cDNA input concentrations were determined using the Experion™.

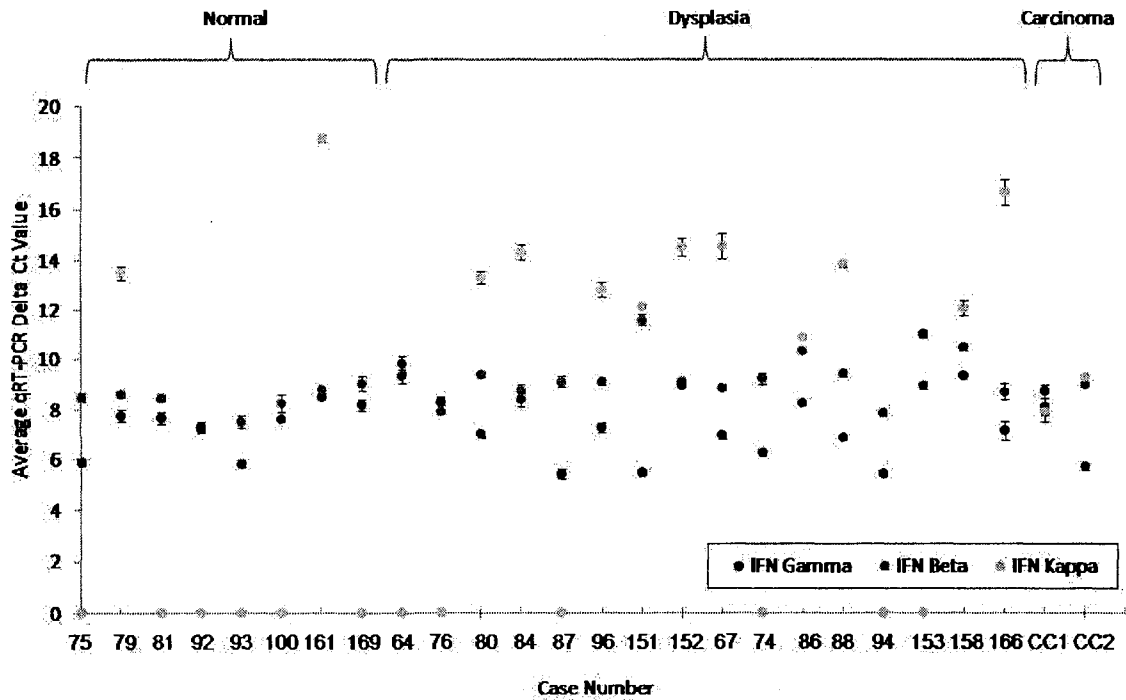


**Figure 24.** All analyzed IFNs in cervical biopsy sections. Full biopsy sections of normal cervical tissue (n=8), dysplastic tissue (n=16) and cervical carcinoma tissue (n=2) were analyzed for IFN- $\gamma$ , - $\beta$ , and - $\kappa$  mRNA levels using qRT-PCR. Values represent the average delta qRT-PCR Ct value  $\pm$  SD. cDNA input concentrations were determined using the Experion™.

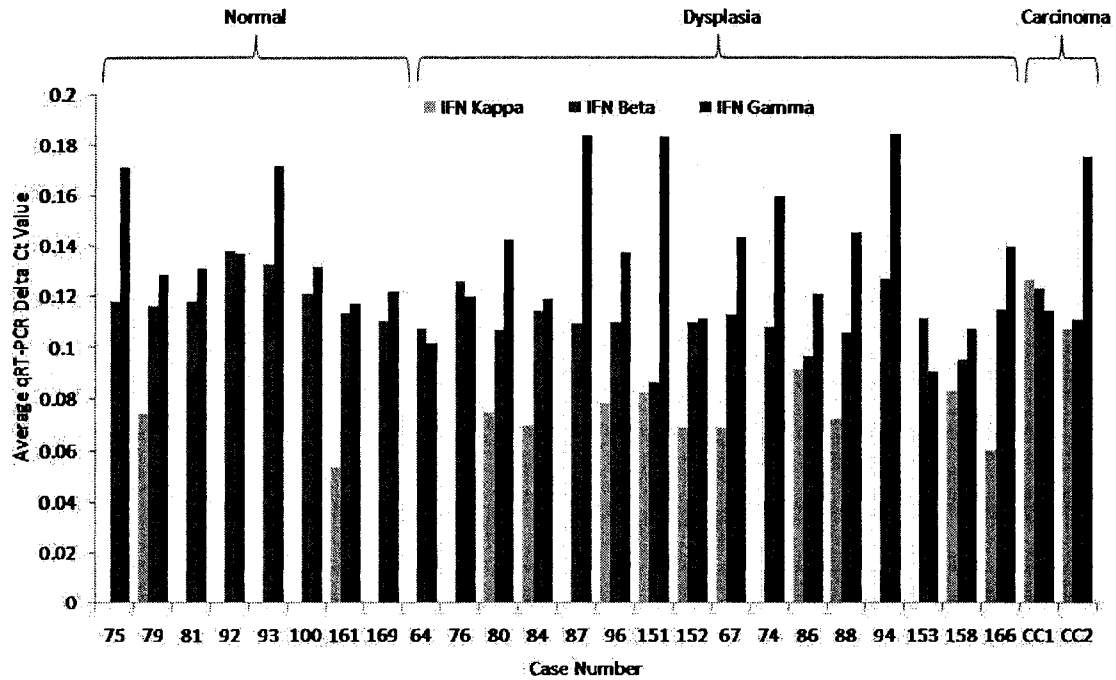


**Figure 25. Relative expression of all analyzed IFNs in cervical biopsy sections.** Full biopsy sections of normal cervical tissue (n=8) and dysplastic tissue (n=16) were analyzed for IFN- $\gamma$ , - $\beta$ , and - $\kappa$  mRNA levels using qRT-PCR. Values represent relative expression values (1/Ct). cDNA input concentrations were determined using the Experion™.

## Cervical Carcinoma Tissue

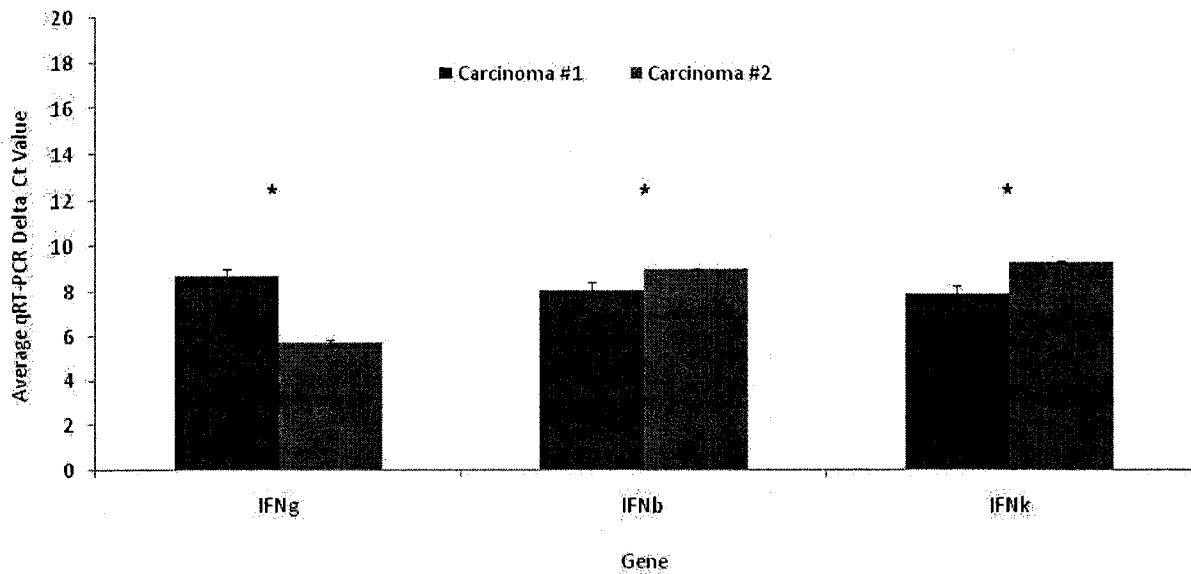


**Figure 26. IFN gene expression in whole carcinoma tissue.** Full biopsy sections of two cervical squamous carcinoma cases were analyzed for IFN- $\gamma$ , - $\beta$ , and - $\kappa$  mRNA levels using qRT-PCR. Values represent the average delta qRT-PCR Ct value  $\pm$  SD. cDNA input concentrations were determined using the Experion™. Carcinoma #1 is sample CC02 and carcinoma #2 is sample CC04. Asterisks represent significant differences in expression between samples.

### **3.5 In Vitro IFN Expression**

#### **3.5.1 Keratinocytes and Cervical Cancer-Derived Cell Lines**

Due to the low availability of cervical carcinoma tissue, cervical cancer-derived cell lines were utilized for a further investigation into IFN expression in the malignant phenotype. IFN- $\kappa$  gene expression was strong in primary keratinocytes and present in immortalized keratinocytes devoid or transduced with an HPV oncogene (**Figure 27**). However, IFN- $\kappa$  expression was lost in some carcinoma-derived cell lines, namely HeLa, SiHa and the HPV-negative C33A cell line. IFN- $\kappa$  mRNA levels were higher than IFN- $\beta$  in HPV16+ CaSki cells but found at a lower level in the Me180 cell line (**Figure 27**). IFN- $\beta$  gene expression was present in all the cell lines at a moderate level, whereas IFN- $\gamma$  was absent in almost every cell line except SiHa and C33A, notably where IFN- $\kappa$  expression was lost. A significant difference in IFN- $\kappa$  and IFN- $\beta$  expression existed between NIKS + E6 and NIKS + E7 (student's t-test,  $p = < 0.0001$  and  $p = < 0.0001$  respectively).

### **3.6 Peripheral Expression of IFNs in Patients**

#### **3.6.1 Peripheral Blood Lymphocytes**

To investigate the IFN expression profile in the periphery of patients, PBLs and monocytes, were isolated from patients who displayed IFN- $\kappa$  expression in their whole biopsy samples. IFN- $\kappa$  gene expression was not found in the PBLs of patients with normal or dysplastic cervical tissue, however IFN- $\beta$  and - $\gamma$  were found at similar levels (student's t-test,  $p = 0.643$  and  $p = 0.715$ ) in 6/6 (100%) cases, as shown in **Figure 28**. TNF- $\alpha$  gene expression was analyzed alongside the IFNs to show the expression levels of the IFNs in relation to another gene. TNF- $\alpha$  gene expression was similar in the periphery of patients with normal or dysplastic tissue (student's t-test,  $p = 0.697$ ). IFN- $\beta$  and IFN- $\gamma$  were consistently expressed at lower levels in the

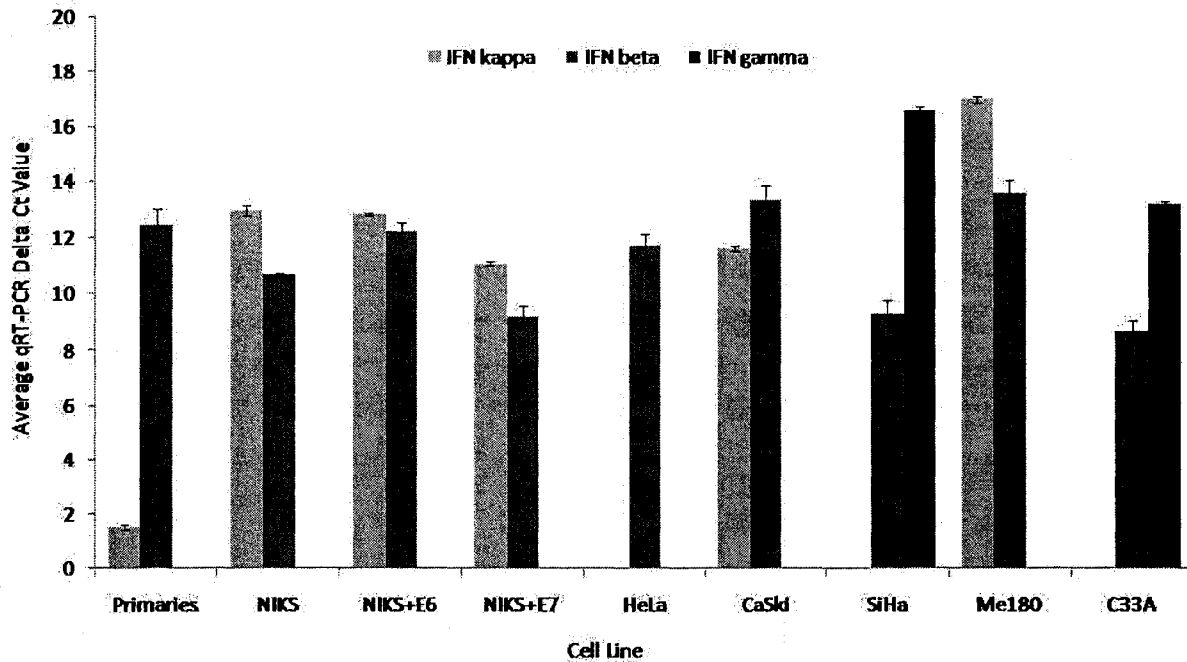


**Figure 27. IFN gene expression in cell lines.** Primary keratinocytes (n=1), immortalized keratinocytes transduced with an empty vector (n=1; NIKS) or an HPV oncogene (n=2: NIKS+ HPV16 E6; NIKS + HPV16 E7) and cervical cancer-derived cell lines (n=5: HeLa, HPV18; CaSki, HPV16; SiHa, HPV16; Me180, HPV39; C33A, HPV-) were analyzed for IFN- $\gamma$ , - $\beta$ , and - $\kappa$  mRNA levels using qRT-PCR. Values represent the average delta qRT-PCR Ct value  $\pm$  SD of two experiments. cDNA input concentrations were determined using the Experion™.

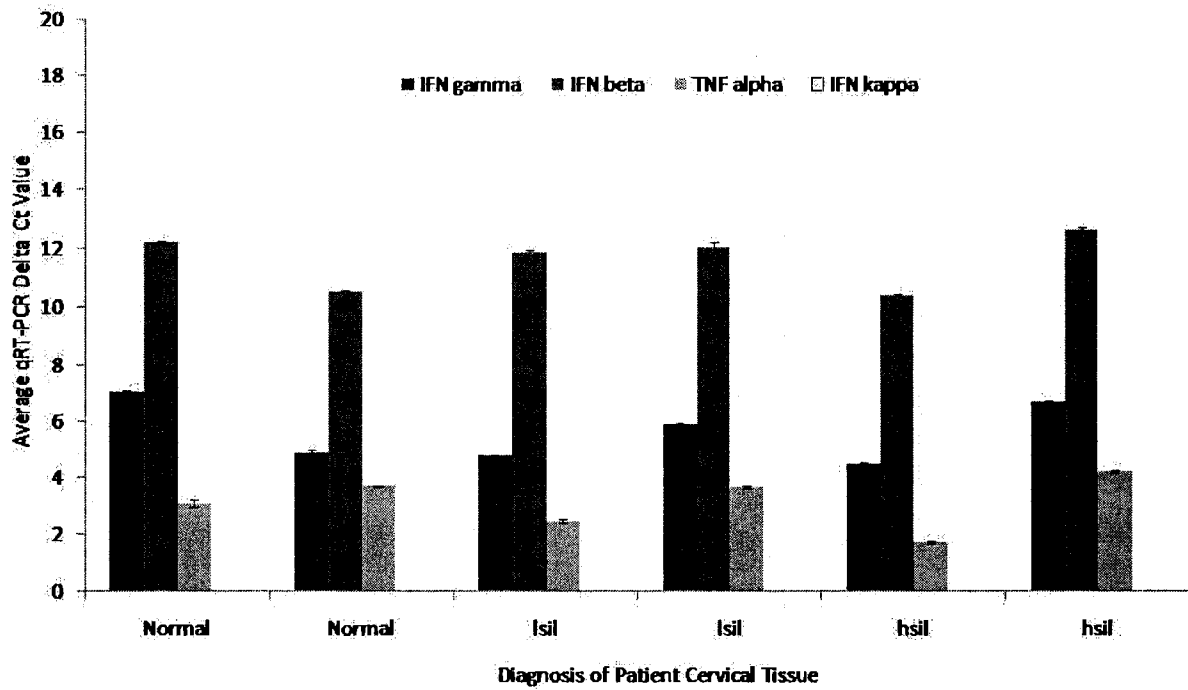


**Figure 28. IFN and TNF- $\alpha$  gene expression in peripheral blood lymphocytes.** Peripheral blood lymphocytes and monocytes were isolated from whole blood specimens obtained from patients whose full biopsy sections revealed IFN- $\kappa$  expression. PBLs were analyzed for IFN- $\gamma$ , - $\beta$ , and - $\kappa$  as well as TNF- $\alpha$  mRNA levels using qRT-PCR. Values represent the average delta qRT-PCR Ct value  $\pm$  SD. cDNA input concentrations were determined using the Experion<sup>TM</sup>.

periphery than TNF- $\alpha$ .

### 3.7 LCM Analysis of IFN Expression in Cervical Tissue

#### 3.7.1 *Microdissected Cervical Epithelium and Stroma*

To investigate the cell-specific gene expression of IFNs, cervical epithelium and stroma were isolated using laser capture microdissection. It should be noted that all excised epithelium cases did contain some infiltrating CD4/CD8+ cells, the extent of which was variable, and could not be avoided during the microdissection process. The characterization of CD4/CD8+ infiltrate in each case was documented in **Figure 8** and **Table 2**. IFN- $\kappa$  was detected in normal, dysplastic and cervical carcinoma epithelium, as seen in **Figure 29A** and in **Appendix 1: Table 5**, as well as in the stroma in 12.5 % (1/8) of dysplastic cases and in the one carcinoma sample analyzed (**Figure 29B**, **Appendix 1: Table 5**). Differences in the expression levels exist but could not be statistically analyzed due to the low sample size and expression prevalence.

IFN- $\beta$  gene expression was detected in 91.7% (11/12) of normal epithelium, 70% (7/10) of dysplastic epithelium and 100% (1/1) of carcinoma epithelium (**Appendix 1: Table 5**) and in 100% of normal (12/12) and carcinoma (1/1) stroma and in 87.5% (7/8) of dysplastic stroma. IFN- $\beta$  gene expression prevalence was not statistically different between the cases (Fisher's exact t-test,  $p > 0.05$ ). The expression levels of IFN- $\beta$  did not differ between normal and dysplastic epithelium or stroma (student's t-test,  $p=0.152$  and  $p= 0.438$  respectively) (**Appendix 1: Table 6**). The carcinoma LCM tissue could not be statistically analyzed due to the low samples size. However, a general trend existed for IFN- $\beta$ : IFN- $\beta$  gene expression was decreased in diseased cervical epithelium (**Figure 30A**), however stromal IFN- $\beta$  expression appeared to increase with HPV infection (**Figure 30B**).

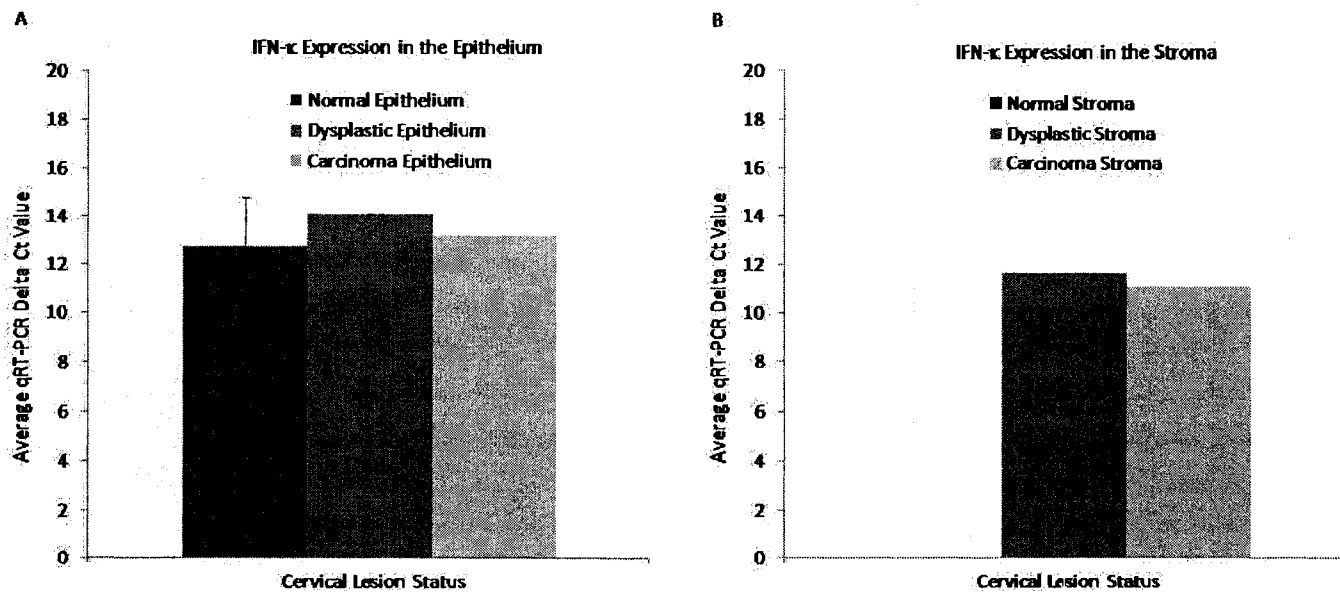


**Figure 29. Cell type-specific IFN-κ expression in normal, dysplastic and carcinoma tissue.** Cervical epithelium (A) and stroma (B) were excised from normal, dysplastic and cervical carcinoma whole biopsy samples using LCM and the mRNA levels of IFN-κ was analyzed using qRT-PCR. Vertical bars represent the average delta qRT-PCR Ct value  $\pm$  SD. Standard error bars are present when 2 or more values are available. cDNA input concentrations were determined using the Experion™.

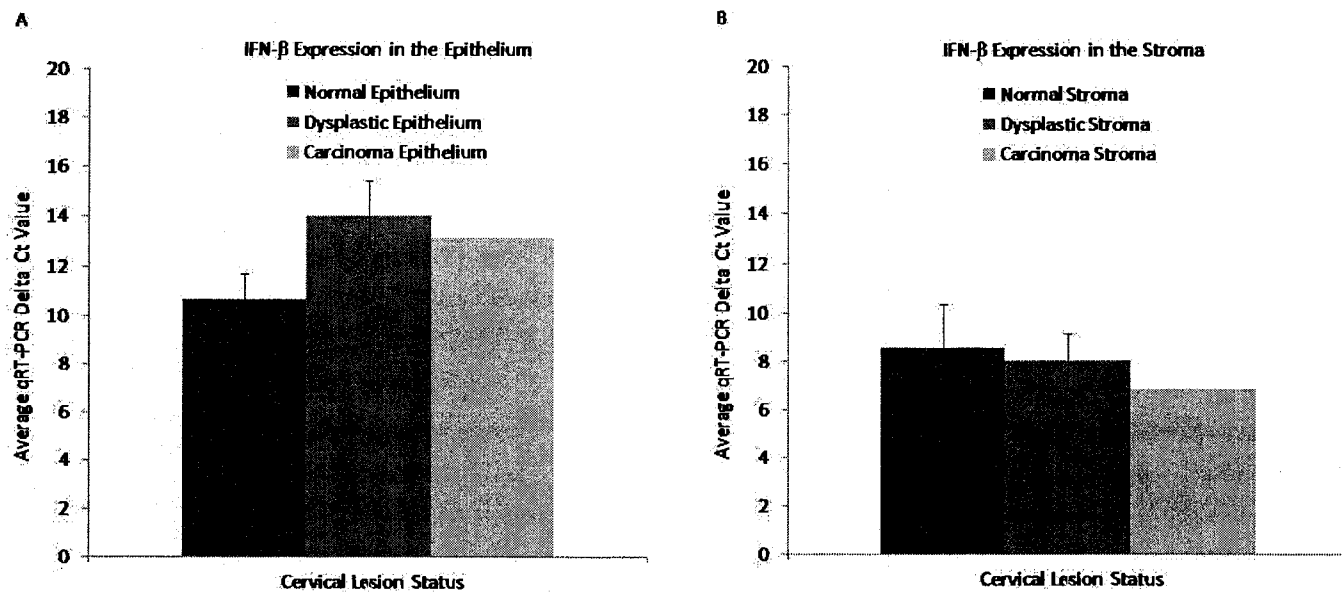


**Figure 30. Cell type-specific IFN- $\beta$  expression in normal, dysplastic and carcinoma tissue.** Cervical epithelium (**A**) and stroma (**B**) were excised from normal, dysplastic and cervical carcinoma whole biopsy samples using LCM and the mRNA levels of IFN- $\beta$  was analyzed using qRT-PCR. Vertical bars represent the average delta qRT-PCR Ct value  $\pm$  SD. Standard error bars are present when 2 or more values are available. cDNA input concentrations were determined using the Experion™.

IFN- $\gamma$  gene expression was detected in 83.3% (10/12) of normal epithelium, 90% (9/10) of dysplastic epithelium and 100% (1/1) of carcinoma epithelium (**Appendix 1: Table 5**) and in 100% of normal (12/12), dysplastic (8/8) and carcinoma (1/1) stroma. IFN- $\gamma$  gene expression prevalence was not statistically different between the cases (Fisher's exact t-test,  $p > 0.05$ ). The expression levels of IFN- $\gamma$  did not differ between normal and dysplastic epithelium or stroma (student's t-test,  $p = 0.20$  and  $p = 0.163$  respectively) (**Appendix 1: Table 6**). The carcinoma LCM tissue could not be statistically analyzed due to the low sample size. However, a general trend existed for IFN- $\gamma$ : IFN- $\gamma$  gene expression appeared to increase in diseased cervical epithelium (**Figure 31A**), yet stromal IFN- $\gamma$  expression decreased drastically in carcinoma tissue (**Figure 31B**).

### 3.8 IFN Gene Expression in Repeated LCM Samples

LCM was repeated in seven cases in different tissue layers within the same area to analyze the intra-individual distribution of gene expression present within samples (**Figure 36: Appendix 1**). IFN- $\kappa$  expression was noticeably different in 42.9% (3/7) of the LCM repeats, whereas IFN- $\beta$  and IFN- $\gamma$  expression differed noticeably in only 28.6% (2/7) of the repeated cases. Insight into the moderate focal expression of IFN- $\beta$ , IFN- $\gamma$  and, to a higher extent IFN- $\kappa$ , is illustrated in **Figure 36 A, C and G** (for IFN- $\kappa$ ), **Figure 36 E and F** (for IFN- $\beta$ ) and **Figure 36 D and E** (for IFN- $\gamma$ ) where the repeated LCM experiments result in different IFN expression profiles.

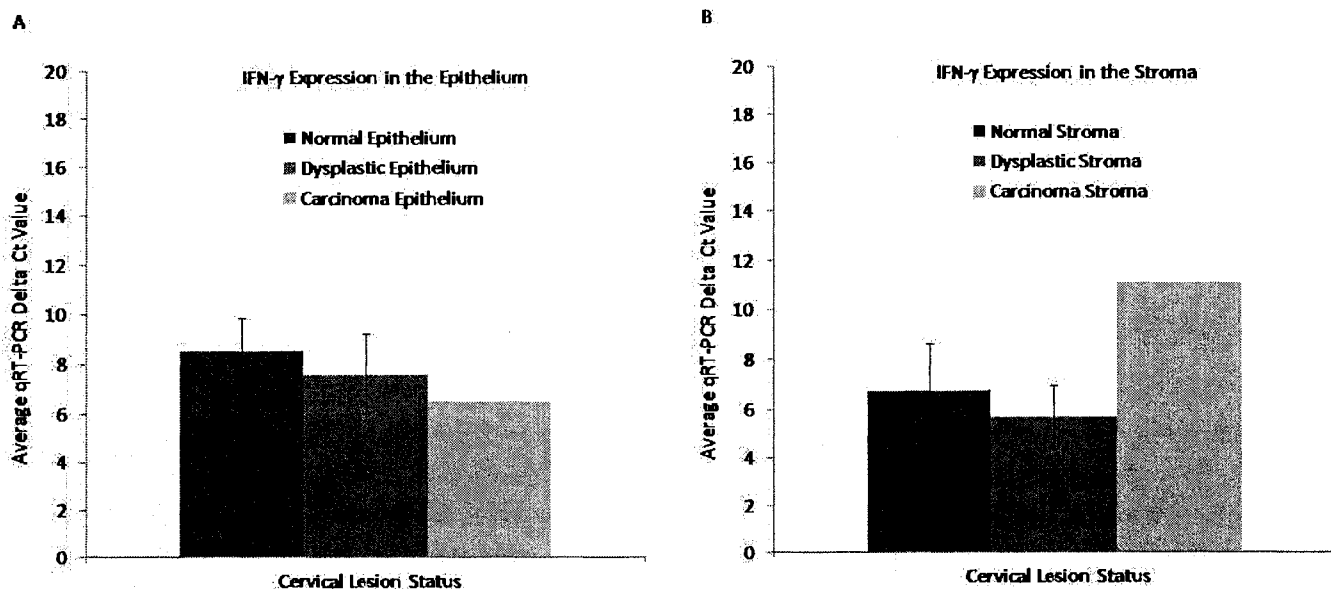


**Figure 31. Cell type-specific IFN- $\gamma$  expression in normal, dysplastic and carcinoma tissue.** Cervical epithelium (A) and stroma (B) were excised from normal, dysplastic and cervical carcinoma whole biopsy samples using LCM and the mRNA levels of IFN- $\gamma$  was analyzed using qRT-PCR. Vertical bars represent the average delta qRT-PCR Ct value  $\pm$  SD. Standard error bars are present when 2 or more values are available. cDNA input concentrations were determined using the Experion<sup>TM</sup>.

## 4.0 DISCUSSION

In this study, using cell lines, cervical tissue and microdissected cervical cells, we assessed various sample preparation and analysis techniques that can influence gene expression studies to devise optimal methods for analyzing low-abundant genes in cervical samples. Following method optimization, a thorough analysis of IFN gene expression was performed using whole cervical biopsy tissue, microdissected cervical epithelium and stroma as well as human keratinocytes and human cervical cancer-derived cell lines.

### 4.1 Method Development

The method of tissue storage was assessed for the preservation of high quality RNA in cervical biopsy specimens. In agreement with previous studies<sup>59,60,88</sup>, our data strongly suggested that FR cervical tissue was optimal for obtaining a high quality and quantity of RNA (**Figure 12A**) whereas FFPE tissue processing caused considerable degradation and low yield, possibly due to nucleic acid cross-linking with proteins, covalent modifications and strand breaks<sup>89</sup>. RNA from FFPE tissue was not suitable for gene expression analysis. For the detection of quality and quantity of RNA in the range of 20-40 ng/ $\mu$ l, the Experion<sup>TM</sup> high sensitivity kit produced more reliable results than the standard kit.

Published methods for extracting RNA differ with respect to reagents, filter columns and the amount of sample required. Furthermore, many published techniques claiming high quality RNA isolation from FR tissue either relied only on expression of HKGs<sup>59,60</sup>,  $A_{260} / A_{280}$  ratios<sup>90,91</sup> or did not perform RNA quality assessment at all<sup>66,68,92</sup>. Here we show that contrary to previous results with FR tissue<sup>62,93-95</sup>, the modified Arcturus RNA extraction method was optimal for the extraction of high quality RNA compared to the Ambion and Sigma methods for cervical biopsy sections (**Figure 12B**). Although limited material prohibited a direct comparison of all

techniques with the same sample, representative images are shown for each extraction method (**Figure 12B**). The Trizol extraction method had previously been shown to produce poorer RNA quality when using small amounts of cervical cells<sup>66</sup>. Small amounts of sample material may limit RNA yield for some extraction methods. Although the amount of tissue used was in the range specified by the Ambion and Sigma kits, high quality RNA was only obtained using the Arcturus kit, which is designed for extraction from microdissected samples. This indicates that for extraction from small amounts of cervical tissue, as seen previously in prostate tissue<sup>82</sup>, methods optimized for extraction from microdissected samples produced favorable results.

Tissue preparation protocols for LCM and FR tissue often differ in many respects, including the dehydration procedure and the staining solutions. Recent evidence suggests that inclusion of an RNase inhibitor<sup>82</sup> as well as a prolonged 100% (v/v) ethanol incubation<sup>68,82</sup> generated higher quality RNA from microdissected samples. It was previously argued that the protocol described in the Arcturus Histogene™ Frozen Section Staining Kit is not adequate for obtaining high quality RNA from FR LCM samples<sup>68</sup>. This could be due to active RNases present in the tissue and/or improper dehydration leading to RNA degradation. Together with recent results utilizing similar methodology and FR specimens<sup>64,82</sup>, our data demonstrate that a modified version of the Arcturus staining method combined with the Arcturus extraction method was highly suitable for morphological assessment and high quality RNA extraction from LCM-obtained cervical keratinocytes (**Figure 13**). This finely-tuned technique is a significant advancement, as obtaining intact RNA from LCM samples is often challenging, and our modification may be extended for the preparation of other FR tissues for LCM. RNAlater®-ICE (Ambion), tested for its impact on RNA integrity preservation, rendered the biopsy specimen difficult to section and had no impact on sample RNA integrity (data not shown). In addition,

cervical tissue scraped off the slide displayed similar HKG expression compared to LCM-obtained cervical material from the same specimen (data not shown), indicating that the microdissection process did not compromise RNA integrity.

The type of primers used for RNA RT is critical for the quality of cDNA produced<sup>96</sup> and depending on the type of primers utilized, differences exist in the calculated mRNA copy numbers<sup>97</sup>. Oligo(dT) primers are widely used for priming cDNA reactions, however, recent evidence suggests they are markedly less sensitive than random primers for the RT process<sup>96</sup>. Although random primers may present considerable problems for detecting transcripts present at low levels within a sample<sup>98</sup>, this method may introduce less bias in the resulting cDNA compared to oligo(dT) primers or target-specific primers due to the exclusion of hairpins or RNA secondary structures<sup>99</sup>. Random hexamer primers were chosen for RT of RNA to cDNA as these primers resulted in minimal differences in HKG expression between samples and slightly higher mRNA levels compared to RT using oligo(dT) primers (**Figure 14**). Random hexamer primers are thus preferred when preparing samples for the comparison of low-expressing gene levels between pathologic conditions.

HPRT is a commonly used reference gene, previously utilized for the study of low-level cytokine expression<sup>74</sup> and cervical cancer<sup>100</sup>. HPRT has been verified as an optimal normalizer between samples in colon, prostate, breast, skin and bladder tissue<sup>101</sup> but had not been established as a suitable normalizer between normal and diseased cervical tissue. We demonstrated that HPRT1 is the optimal HKG for normalization compared to  $\beta$ -actin, B2M, 18S and PLA in NIKS transduced or devoid of the HPV16 E6 oncogene (**Figure 15A**) as well as in cervical tissue in the presence or absence of HPV (**Figure 15B**). Relatively constant expression of HKGs in specimens is also indicative of sample integrity at this stage of sample processing.

We found that PLA was also a suitable HKG in cervical tissue, though its expression may vary in the presence of high IFN protein<sup>102</sup> and therefore may change in virus-infected tissue. HPRT was reported to represent the mean expression of many commonly used normalizing genes<sup>101</sup>, eliminating the need to use multiple genes for normalization. It is suitable for use with sensitive detection methods<sup>103</sup> and, similar to our data, HPRT has been shown to exhibit a low expression level suitable for the measurement of low expressing genes<sup>101</sup>, such as IFN- $\kappa$ .

While several methods exist for transcript amplification, they are often tedious and time-consuming. cDNA amplification is comparatively simple but its utility has never been reported in cervical samples for the analysis of multiple low-expressing target genes. Our data demonstrated that cDNA amplification significantly increased the expression level of target genes within NIKS, whole biopsy specimens and laser capture microdissected samples versus the expression levels obtained using unamplified cDNA (**Figure 16A**). Furthermore, determining the optimal amplification conditions (**Figure 16B**) (i.e., the number of cycles and the least amount of input cDNA required for target mRNA detection using qRT-PCR) greatly increased the ability of our techniques to measure target genes in limited amounts of cervical samples. We have shown that a reasonable amount of RNA isolated from cervical specimens, with the aid of cDNA amplification, permitted detection of all IFNs within a suitable qRT-PCR level ( $\leq 35$  Ct) in both whole cervical sections (**Figure 17A**) and microdissected cervical keratinocytes (**Figure 17B**). IFN- $\kappa$  gene transcripts were not detectable in cervical biopsy tissue or microdissected keratinocytes using unamplified cDNA (data not shown) and, along with IFN- $\beta$ , was not detected in microdissected cervical keratinocytes using amplified cDNA from 1,000 LCM captures (**Figure 17B**). This is a significant sensitivity advancement and, to our knowledge, this is the first time IFN- $\kappa$  detection has been demonstrated in cervical keratinocytes from human

cervical biopsy specimens.

The development of precise methodology for measurement of cell-specific targets is instrumental for experimental pathologists to investigate the molecular profile of disease. The methods described herein were crucial for the comprehensive analysis of interferons in cervical tissue and likely could be extended to other keratinocyte-based investigations. Combined with high-throughput gene expression technologies, such as cDNA microarrays, these methods could lead to improvements in immunological profiling and disease diagnosis.

#### **4.2 Interferon Expression in Patients**

To our knowledge, this study is the first of its kind to show IFN- $\kappa$  gene expression in cervical tissue, with respect to HPV as well as in microdissected cervical keratinocytes and dermal stroma using qRT-PCR. Further, this study has characterized the regulation of IFN- $\kappa$  gene expression in response to HPV infection and cervical disease progression and also provided insight into specific cell types implicated in this observed change in expression within the cervical microenvironment. Additionally, this study is the first to demonstrate the relationship between three IFNs, with respect to novel IFN- $\kappa$ , in cervical tissue. The distinct relative expression levels of these IFNs, regardless of HPV infection, illustrates the differences between the subclasses of IFNs. Further, the expression of IFN- $\kappa$  in relation to IFN- $\beta$ , in terms of relative expression and HPV-induced expression, highlights the uniqueness of IFN- $\kappa$  as a type I IFN. A relationship exists between decreased IFN- $\beta$  expression and increased IFN- $\kappa$  expression with cervical disease progression, suggesting an alternate expression of the type I IFNs, a relationship which, to our knowledge, has also never been documented previously.

Our results demonstrate that the mRNA levels of IFN- $\kappa$ , a novel type I IFN, are significantly increased in dysplastic and carcinoma tissue compared to normal HPV- cervical

tissue (**Figure 19**). Similarly, IFN- $\kappa$  mRNA levels have previously been detected in resting primary keratinocytes and upregulated in virus-induced keratinocytes<sup>11</sup>. In contrast to our results, IFN- $\kappa$  protein expression was not detected in healthy skin tissue<sup>29</sup>. However the post-transcriptional regulation of IFN- $\kappa$  has not been characterized in cervical tissue. Further, in other studies IFN- $\kappa$  expression has shown variable results with respect to viral infection. For example, in the central nervous system, levels of IFN- $\kappa$  were unaffected by infection with Theiler's virus, a picornavirus, or a mutant La Crosse virus, an arbovirus<sup>104</sup>, however IFN- $\kappa$  was capable of mediating anti-viral protection against two families of RNA viruses, encephalomyocarditis, a picornavirus, and vesicular stomatitis, a virus of the Rhabdoviridae family, in human dermal fibroblasts<sup>11</sup> and against a hepatitis C virus replicon cell line<sup>28</sup>. Our study is the first to analyze IFN- $\kappa$  expression response upon infection by a DNA virus. The consequences of DNA viral infection are infrequently discussed in the scientific literature, as most studies involving a viral inducer focus on RNA viruses and associated ligands. This study demonstrates that DNA viruses can have a similar effect on innate immune system regulation as RNA viruses with regard to IFN- $\kappa$ , as the effects of HPV in cervical tissue is similar to that of dsRNA-treated keratinocytes<sup>11</sup>.

IFN- $\kappa$  exhibits similar antiviral activity<sup>28</sup> and utilizes the same type I IFN receptor and regulatory element as other type I IFNs<sup>11</sup> but differs in its expression and signalling characteristics<sup>28</sup>. Along with differences in expression and signaling, the IFN- $\kappa$  gene is located adjacent to the type I IFN cluster<sup>11</sup> and its sequence is structurally different than all other IFNs<sup>11</sup>. Although the pathways involved in the activation of IFN- $\beta$  and - $\gamma$  are known, the transcriptional regulation of IFN- $\kappa$  is unknown. Our data indicate that, while IFN- $\beta$  mRNA levels decrease with HPV infection and progression to cancer, IFN- $\kappa$  gene expression is upregulated in diseased

tissue. We reason that because the IFN- $\kappa$  gene harbors structural differences from other type I IFNs, the observed differences in gene expression patterns between IFN- $\beta$  and IFN- $\kappa$  could be due to distinct pathways/transcription factors governing IFN- $\kappa$  gene regulation which may not be inhibited by HPV, as is seen with IFN- $\beta$ . Instead, the effect of HPV on IFN- $\kappa$  in cervical tissue is likely gene transcription promoting, as seen in dsRNA induced keratinocytes<sup>11</sup>. Further studies are required to investigate post-translational IFN- $\kappa$  expression to determine the biological effects, if any, of the observed increase in IFN- $\kappa$  gene expression in HPV-infected cervical tissue.

In contrast to IFN- $\kappa$ , IFN- $\beta$ , another type I IFN, was detected at the mRNA level in all tissue specimens, and, as previously shown using RT-PCR<sup>105</sup>, its expression is down-regulated in virally-infected tissue in the present study (**Figure 21**). Similarly, IFN- $\beta$  and IFN- $\alpha$  transcription was shown to be downregulated in keratinocytes infected with HPV16 using RT-PCR analysis<sup>42</sup>. The down-regulation of IFN- $\beta$  gene expression is consistent with the known inhibitory effects of HPV on transcription factors governing IFN expression. HPV E6 and E7 oncoproteins bind to transcription factors critical for mediating IFN signaling in response to a viral infection. For example, HPV type 16 E6 binds and inactivates the transcription factor IRF-3<sup>48</sup> while HPV16 E7 inactivates IRF-1<sup>47</sup>; both of which result in a reduction in IFN- $\beta$  gene expression during HPV infection. The observed increase in IFN- $\beta$  gene expression in cervical carcinoma tissue compared to dysplastic tissue could be attributed to changes in immunogenicity common to the cervical malignant phenotype. The decreased expression of HPV early gene E2, which is associated with viral genome integration in severe cervical lesions, leads to a substantial increase in HPV E6 and E7 expression. The increase in expression of E6 and E7 could alter the immunogenicity of HPV viral proteins<sup>106</sup> leading to a host-generated immune response against

the virus which could trigger, for instance, an increase in IFN- $\beta$  gene expression, as shown in carcinoma tissue in the present study. However, HPV has been shown to inhibit proteins involved in IFN-elicited anti-viral pathways, such as ISGF<sup>46</sup> and JAK-STAT<sup>53</sup>, which may prevent the generation of a beneficial IFN- $\beta$  response and which may explain why increased IFN- $\beta$  mRNA levels were associated with cervical carcinoma.

IFN- $\gamma$ , a type II IFN, has previously been demonstrated to be decreased in cervical dysplasia compared to normal tissue<sup>56</sup> and expressed at lower frequencies in invasive carcinoma compared to dysplastic tissue<sup>55</sup>. In contrast, results of the present study indicate no significant difference in IFN- $\gamma$  gene expression levels or prevalence between normal, dysplastic and cervical carcinoma biopsy tissue (**Figure 23**). A trend exists where IFN- $\gamma$  does decrease in dysplastic compared to normal tissue; however, intra-individual variability for this gene was too high to enable statistical significance. IFN- $\gamma$  up-regulation has been implicated as a possible prognostic marker for the oncogenic potential of HR HPV<sup>107</sup>. The results of the current study indicate that decreased IFN- $\gamma$  expression does not represent a specific marker for HR HPV infection. However, there is a high prevalence of HR HPV infection in the dysplastic group of the present study (66.7%; 12/18), therefore the infectious HPV type could be a possible contributor to the high variability found in IFN- $\gamma$  gene expression levels in this study. IFN- $\gamma$  stimulation has previously been shown to induce IFN- $\kappa$  expression in monocytes<sup>30</sup> and in human keratinocytes *in vitro*<sup>11,29</sup>. This relationship was not found *ex vivo* in the present study using cervical whole tissue biopsies (**Figure 25**). Tissue exhibiting high IFN- $\gamma$  levels did not display noticeably different IFN- $\kappa$  levels. This disparity further illustrates the uniqueness of IFN- $\kappa$  expression in the cervical microenvironment.

Using normal, dysplastic and cervical carcinoma full biopsy specimens, we have shown

the gene expression levels of three prominent IFNs with respect to HPV infection using qRT-PCR. While IFN- $\beta$  gene expression decreases with HPV infection, IFN- $\kappa$  mRNA levels substantially increase and IFN- $\gamma$  shows no significant change in expression. Although trends exist with the analysis of whole cervical biopsy tissue, multiple cell-types within the tissue sample may affect the analysis. Using microdissection to isolate cervical keratinocytes and stroma, which consist of a wide variety of different cell types including, dendritic cells, fibroblasts and monocytes, can provide insight into the cell-specific IFN response within the cervical microenvironment.

The isolation of cervical epithelium and stroma using LCM has allowed for the discrimination of specific cell populations involved in the observed change in gene expression. LCM revealed a correlation between gene expression of IFN- $\kappa$  in stromal cells and cervical disease progression. Epithelial IFN- $\kappa$  expression was present in normal, dysplastic and carcinoma tissue (**Figure 29A**). However, stromal expression of IFN- $\kappa$  was only present in dysplastic and carcinoma tissue (**Figure 29B**), indicating that HPV infection induces IFN- $\kappa$  expression in the dermal stroma. These results are similar to previous findings that the ISRE upregulation by IFN tau, another type I IFN, was found in the stroma in ovine endometrium<sup>108</sup>. An increase in stromal gene expression of IFN- $\kappa$  in response to HPV-infected cervical epithelium could be indicative of a host-generated immune response against HPV infection. While recruited infiltrating leukocytes may exhibit IFN- $\kappa$  expression, the consequences of the increase in IFN- $\kappa$  gene expression in these cells remains to be explored. Further experiments are required to identify the specific stromal cells responsible for this expression. Previous studies have shown IFN- $\kappa$  expression in resting monocytes and dendritic cells<sup>11</sup>, but our data suggest that in the cervical microenvironment these innate immune cells do not inherently express IFN- $\kappa$

in normal stroma because CD4/CD8 + infiltrating cells were present in the majority (91.7%) of cases devoid of stromal IFN- $\kappa$  expression. While no differences were found in IFN- $\beta$  (**Figure 30**) or IFN- $\gamma$  (**Figure 31**) gene expression in isolated normal or dysplastic epithelium or stroma, this study demonstrates that, unlike previously shown<sup>11</sup>, IFN- $\beta$  mRNA levels are detected in resting keratinocytes.

### 4.3 Interferon Expression in Cell Lines

IFN- $\kappa$  expression was very high in primary keratinocytes compared to immortalized keratinocytes and cervical cancer-derived cell lines (**Figure 27**). This demonstrates the intrinsic difference in the immune response present in skin versus the uterine cervix and further demonstrates the importance of developing sensitive techniques for the detection of IFN- $\kappa$  transcripts in cervical tissue. High levels of IFN- $\kappa$  expression relative to IFN- $\beta$  in HPV16+ CaSki cells substantiates the evidence that IFN- $\kappa$  levels were higher than other IFNs in an HPV16+ cervical carcinoma specimen (**Figure 26, CC02**). These data indicate that perhaps HPV type 16, once integrated into the host genome, leads to a preferential induction of IFN- $\kappa$ . The HPV-negative cell line, C33A, shows no IFN- $\kappa$  gene expression and substantiates our claim that HPV is associated with an induction of IFN- $\kappa$  gene expression in cervical cells. However, IFN- $\kappa$  mRNA levels were undetectable in SiHa cells, which also contain one copy of integrated HPV16, and HeLa cells, containing HPV18; results of which cannot be explained at present. While cell lines are useful for preliminary analyses of cell-signaling pathways, confirmation using *ex vivo* tissue, mouse models or an *in vitro* organotypic raft culture system is necessary. Further, given that previous studies have shown slight differences in IFN- $\beta$  gene expression regulation between the HPV type 16 E6 and E7 oncoproteins<sup>47,48</sup>, we analyzed IFN- $\kappa$  gene expression in NIKS transduced with only HPV16 E6 or HPV16 E7. A significant difference in

IFN- $\kappa$  mRNA levels was found between NIKS+E6 and NIKS+E7 (**Figure 27**). NIKS + E7 displayed a significantly higher expression of IFN- $\kappa$  than NIKS + HPV16 E6 and even NIKS + empty vector, indicative of a possible role of HPV16 E7 in IFN- $\kappa$  gene activation. The promoting role of HPV16 E7 for IFN- $\kappa$  gene expression indicates the involvement of unique factors governing IFN- $\kappa$  transcription that may be selectively activated by HPV E7.

#### **4.4 Conclusions and Future Studies**

The worldwide impact of HPV is significant as thousands of women succumb to HPV-associated cervical cancer each year. The recently approved prophylactic vaccine against common HR HPVs is not a treatment for cervical or any other HPV-associated cancer and is not beneficial to people already infected with HR HPV or immunocompromised patients. As a consequence, there is a great need for studies which characterize the effects of HPV on the immune system to aid in the development of patient-tailored treatment regimes. This study, describing the optimized methods for low-expressing gene detection combined with the HPV-associated upregulation of a novel type I IFN in human cervical tissue, represents novel technological advancements and insight for the area of immunological regulation of HPV-associated cervical disease.

IFNs are innate immunity mediators vital to the generation of an immune response against invading pathogens. Type I and II IFNs differ vastly in biological function and thus it was important to characterize the differences in biological expression levels of the two classes within HPV-infected cervical tissue. Although present at low levels within the normal, physiological cervical microenvironment, IFN- $\kappa$  gene expression is profoundly influenced by HPV infection, demonstrating the biological relevance of detecting this IFN at low levels. LCM has isolated a probable cause of the observed increase in IFN- $\kappa$  gene expression, shedding light

on the importance of the entire microenvironment in anti-viral defense. We have indicated an opposing relationship between the two type I IFNs analyzed in this study. This relationship emphasizes the unique expression pattern of IFN- $\kappa$  in cervical tissue and outlines a novel relationship between type I IFNs. Cell line and carcinoma tissue data indicate a possible role of HPV16 E7 in promoting IFN- $\kappa$  gene activation. Lack of IFN- $\kappa$  expression in C33A cells further substantiates our data indicating the gene promoting effects of HPV in cervical cells.

As a result of this research, questions about the relevance of IFN- $\kappa$  gene expression now remain. Why is the expression of IFN- $\kappa$ , a potent anti-viral mediator, high in dysplastic and carcinoma tissue? What happens following IFN- $\kappa$  gene transcription that permits the disease to progress despite high active gene levels? Does IFN- $\kappa$  play a role in anti-papillomaviral activity? Do mRNA levels correlate with protein expression? What is the specific cell type responsible for the upregulation of IFN- $\kappa$  expression in the stroma? The question of the biological relevance of high gene transcription levels could be answered by evaluating IFN- $\kappa$  expression on the protein level in cervical tissue. However, to date, multiple IFN- $\kappa$  antibodies exist, all of which have been unsuccessful in specifically targeting IFN- $\kappa$  protein expression using immunohistochemistry for this study (data not shown). Furthermore, *in situ* hybridization along with staining for cell-specific markers in the stroma would be the most precise method to elucidate the responsible cell type.

In this study, we have made significant strides in characterizing the effects of HPV on IFN-mediated innate immunity. However, although characterizing the effects of HPV in *ex vivo* human tissue has its value, the effects on IFN- $\kappa$  during the full viral life cycle cannot be studied in this context. Mechanistic studies involving the active viral life cycle is an important step in the analysis of the effect of HPV on IFN- $\kappa$  and *in vitro* studies are now in progress which mimic the

active HPV viral life cycle. Using an organotypic raft culture system with NIKS transfected with full length HPV16, the effect of HPV on IFN- $\kappa$  can be analyzed during both the productive and non-productive stages of the viral life cycle. The organotypic raft culture system will provide insight into the biological significance of IFN- $\kappa$  gene activation by permitting investigations during the active viral life cycle that eventually can be correlated with our *ex vivo* results using cervical biopsies. Furthermore, gene analysis in *ex vivo* cervical tissue may be influenced by co-infections with other HPV types or other microbial agents residing in the female uterine tract, such as cocci, fungi or other sexually transmitted infections that can be controlled for using the raft culture system.

This study has presented a thorough analysis of IFN- $\kappa$  gene expression in *ex vivo* cervical material and we now possess the necessary tools to further investigate the mechanistic role HPV plays in IFN- $\kappa$  gene regulation.

## 5.0 REFERENCES

1. H. Zur Hausen, W. Meinhof, W. Scheiber, G.W. Bornkamm, Attempts to detect virus-specific DNA sequences in human tumors: I. Nucleic acid hybridizations with complementary RNA of human wart virus, *Int. J. Cancer*. 13 (1974) 650-656.
2. H. zur Hausen, Papillomaviruses and cancer: from basic studies to clinical application, *Nature*. 2 (2002) 342-350.
3. E.R. Flores, P.F. Lambert, Evidence for a switch in the mode of human papillomavirus type 16 FNA replication during the viral life cycle, *J. Virol.* 71 (1997) 7167-7179.
4. P.M. Howley, The viruses and their replication, *Papillomavirinae*, In "Fields Virology", B.N. Fields and D.M. Knipe, Eds, 3<sup>rd</sup> Ed., (1996) 2045-2076.
5. M. Durst, A. Kleinheinz, M. Holta, L. Gissmann, The physical state of human papillomavirus type 16 DNA in benign and malignant genital tumours, *J. Gen. Virol.* 66 (1985) 1515-1522.
6. H. zur Hausen, Human papillomaviruses in the pathogenesis of anogenital cancer, *Virology*. 184 (1991) 9-13.
7. M. von Knebel Doeberitz, C. Rittmuller, H. zur Hausen, M. Durst, Inhibition of tumorigenicity of cervical cancer cells in nude mice by HPV E6-E7 anti-sense RNA, *Int. J. Cancer*. 51 (1992) 831-834.
8. A. Takaoka, S. Hayakawa, H. Yanai, H. Negishi, H. Kikuchi, S. Sasaki, et al., Integration of interferon- $\alpha/\beta$  signalling to p53 responses in tumor suppression and antiviral defense, *Nature*. 424 (2003) 516-523.
9. A. Isaacs and J.J. Lindemann, Virus interference. I. The Interferon, *Proc. R. Soc. London Ser. B*. 147 (1957) 258-267.
10. U. Boehm, T. Klamp, M. Groot, J.C. Howard, Cellular responses to interferon-gamma, *Ann. Rev. Immunol.* 15 (1997) 749-795.
11. D.W. Lafleur, B. Nardelli, T. Tsareva, D. Mather, P. Feng, M. Semenuk, Interferon- $\kappa$ , a novel type I Interferon expressed in human keratinocytes, *J. Biol. Chem.* 276 (2001) 39765-39771.

12. E.A. Bach, M. Aguet, R.D. Schreiber, The IFN gamma receptor: a paradigm for cytokine receptor signalling, *Annu. Rev. Immunol.* 15 (1997) 563-591.
13. D. Novick, B. Cohen, M. Rubinstein, The human interferon alpha/beta receptor: characterization and molecular cloning, *Cell.* 77 (1994) 391-400.
14. K. Tanaka, M. Kasahara, The MHC class I ligand-generating system: roles of immunoproteasomes and the interferon-gamma-inducible proteasome activator PA28, *Immunol. Rev.* 163 (1998) 161-176.
15. M. Revel, J. Chebath, Interferon activated genes, *Trends. Biochem. Sci.* 11 (1986) 166-170.
16. A.C. Issekutz, T.B. Issekutz, Quantitation and kinetics of blood monocytes migration to acute inflammatory reactions and IL-1, tumor necrosis factor, and IFN- $\gamma$ , *J. Immunol.* 151 (1993) 2105-2115.
17. W. Barchet, A. Blasius, M. Cella, M. Colonna, Plasmacytoid dendritic cells: in search of their niche in immune responses, *Immunol. Res.* 32 (2005) 75-84.
18. V. Gerein, E. Rastorguev, J. Gerein, P. Jecker, H. Pfister, Use of interferon-alpha in recurrent respiratory papillomatosis: 20 year follow-up, *Ann. Otol. Rhinol. Laryngol.* 114 (2005) 463-471.
19. N. Scheinfeld, D.S. Lehman, An evidence-based review of medical and surgical treatment of genital warts, *Dermatol. Outline J.* 12 (2006) 5.
20. C.H. Polman, P.W. O'Conner, E. Havrdova, M. Hutchinson, L. Kappos, D. H. Miller, J.T. Phillips, F.D. Lublin, M.A. Panzara, A.W. Sandrock, A randomized, placebo-controlled trial of natalizumab for relapsing multiple sclerosis, *N. Engl. J. Med.* 354 (2006) 899-933.
21. E. Maeyer, J. Maeyer-Guignard, *The cytokine handbook*, In: Thompson A., ed. CA: Academic Press (1994) 265-288.
22. J. Vilcek, Adverse effects of interferon in virus infections, autoimmune diseases and acquired immunodeficiency, *Prog. Med. Virol.* 30 (1984) 62-77.
23. G.M. Lauer, B.D. Walker, Hepatitis C virus infection. *N. Engl. J. Med.* 345 (2001) 41-52.
24. M.P. Manns, J.G. McHutchison, S.C. Gordon, V.K. Rustgi, M. Shiffman, R. Reindollar, Z.D. Goodman et al., Interferon alfa-2b plus ribavirin compared with interferon alfa2b plus

- ribavirin for initial treatment of chronic hepatitis C: a randomised trial, *Lancet*. 358 (2001) 958-965.
25. A. Muggiano, C. Mulas, B. Fiori, G. Liciardi, M. Pintus, L. Tanca, A. Tedde, Feasibility of high-dose interferon-alpha2b adjuvant therapy for high-risk resected cutaneous melanoma, *Melanoma Res.* 2 (2004) S1-7.
  26. A.L. Radin, H.T. Kim, B.W. Grant, J.M. Bennett, J.M. Kirkwood, J.A. Stewart, R.G. Hahn et al., Phase II study of alpha2 interferon in the treatment of the chronic myeloproliferative disorders (E5487): a trial of the Eastern Cooperative Oncology Group, *Cancer*. 98 (2003) 100-109.
  27. P.M. Pitha, W.C. Au, W. Lowther, Y.T. Juang, S.L. Schafer, L. Burysek, J. Hiscott, P.A. Moore, Role of the interferon regulatory factors (IRFs) in virus-mediated signaling and regulation of cell growth, *Biochimie*. 80 (1998) 651-658.
  28. P.J. Buontempo, R.G. Jubin, C.A. Buontempo, N.E. Wagner, G.R. Reyes, B.M. Baroudy, Antiviral activity of transiently expressed IFN- $\kappa$  is cell-associated, *J. Inter. Cyto. Res.* 52 (2006) 40-52.
  29. C. Scarponi, B. Nardelli, D.W. LaFleur, P.A. Moore, S. Madonna, O. De Pita, G. Girolomoni, et al., Analysis of IFN- $\kappa$  expression in pathological skin conditions: downregulation in psoriasis and atopic dermatitis, *J. Inter. Cyto. Res.* 26 (2006) 133-140.
  30. B. Nardelli, L. Zaritskaya, M. Semenuk, Y.H. Cho, D. LaFleur, D. Shah, S. Ulrich, G. Girolomoni, C. Albanesi, P.A. Moore, Regulatory effect of IFN- $\kappa$ , a novel type I IFN, on cytokine production by cells of the innate immune system, *J. Immunol.* 169 (2002) 4822-4830.
  31. H. Hemmi, O. Takeuchi, T. Kawai, T. Kaisho, S. Sato, H. Sanjo, M. Matsumoto, et al., A toll-like receptor recognizes bacterial DNA, *Nature*. 408 (2000) 740-745.
  32. M. Yoneyama, M. Kikuchi, T. Natsukawa, N. Shinobu, T. Imaizumi, M. Miyagishi, K. Taira, The RNA helicase RIG-1 has an essential function in double-stranded RNA-induced innate antiviral responses, *Nat. Immunol.* 5 (2004) 730-737.
  33. T. Kawai, K. Takahashi, S. Sato, C. Coban, H. Kumar, H. Kato, K.J. Ishii, et al., IPS-1, an

- adaptor triggering RIG-1 and Mda5-mediated type I IFN induction, *Nat. Immunol.* 6 (2005) 981-988.
34. P.M. Pitha, M.S. Kunzi, Type I interferon: the ever unfolding story, *Curr. Top. Microbiol. Immunol.* 316 (2007) 41-70.
  35. M. Sato, S. Suemori, N. Hata, M. Asagiri, K. Ogasawara, K. Nakao, T. Nakaya, Distinct and essential roles of transcription factors IRF-3 and IRF-7 in response to viruses for IFN- $\alpha/\beta$  gene induction, *Immunity.* 13 (2000) 539-548.
  36. S.A. Veals, C. Schindler, D. Leonard, X.Y. Fu, R. Aebersold, J.E. Jr. Darnell, D.E. Levy et al., Subunit of alpha-interferon-responsive transcription factor is related to interferon regulatory factor and Myb families of DNA-binding proteins, *Mol. Cell. Biol.* 12 (1992) 3315-3324.
  37. M. Myamoto, T. Fujita, Y. Kimura, M. Maruyama, H. Harada, Y. Sudo, T. Miyata et al., Regulated expression of a gene encoding a nuclear factor, IRF-1, that specifically binds to IFN-beta gene regulatory elements, *Cell.* 54 (1988) 903-913.
  38. A. Bachmann, B. Hanke, R. Zawatzky, U. Soto, J. van Riggelen, H. zur Hausen, F. Rosl, Disturbance of tumor necrosis factor alpha-mediated beta interferon signalling in cervical carcinoma cells, *J. Virol.* 76 (2002) 280-291.
  39. G. Uze, G. Lutfalla, I. Gresser, Genetic transfer of a functional human interferon alpha receptor into mouse cells: cloning and expression of its cDNA, *Cell.* 60 (1990) 225-234.
  40. A.R. Bluysen, J.E. Durbin, D.E. Levy, ISGF3 gamma p48, a specificity switch for interferon activated transcription factors, *Cytokine Growth Factor Rev.* 7 (1996) 11-17.
  41. T. Decker, D.J. Lew, J. Mirkovitch, J.E. Jr. Darnell, cytoplasmic activation of GAF, an IFN- $\gamma$ -regulated DNA\_binding factor, *The EMBO Journal.* 10 (1991) 927-932.
  42. M. Nees, J.M. Geoghegan, T. Hyman, S. Frank, L. Miller, C.D. Woodworth, Papillomavirus type 16 oncogenes downregulate expression of interferon-responsive genes and upregulate proliferation-associated and NF-kB-responsive genes in cervical keratinocytes, *J. Virol.* 75 (2001) 4283-4296
  43. M. Dey, B. Trieselmann, E.G. Locke, J. Lu, C. Cao, A.C. Dar, et al. PKR and GCN2

- kinases and guanine nucleotide exchange factor eukaryotic translation initiation factor 2B (eIF2B) recognizes overlapping surfaces on eIF2alpha, *Mol. Cell. Biol.* 25 (2005) 3063-3075.
44. M.J. Clemens, B.R. Williams, Inhibition of cell-free protein synthesis by pppA2'p5'A2'p5'A: a novel oligonucleotide synthesized by interferon-treated L cell extracts, *Cell.* 13 (1978)565-572.
  45. O. Haller, G. Kochs, Interferon-induced Mz proteins: dynamin-like GTPases with antiviral activity, *Traffic.* 3 (2002) 710-717.
  46. P. Barnard, N.A. McMillan, The human papillomavirus E7 oncoprotein abrogates signalling mediated by interferon-alpha, *Virology.* 259 (1999) 305-313.
  47. J.S. Park, E.J. Kim, H.J. Kwon, E.S. Hwang, S.E. Namkoong, S.J. Um, Inactivation of interferon regulator factor-1 tumor suppressor protein by HPV E oncoprotein, *J. Biol. Chem.* 275 (2000) 6764-6769.
  48. L.V. Ronco, A.Y. Karpova, M. Vidal, P.M. Howley, Human papillomavirus 16 E6 oncoprotein binds to interferon regulatory factor-3 and inhibits its transcriptional activity, *Genes and Dev.* 12 (1998) 2061-2072.
  49. M. Scheffner, J.M. Huibregtse, R.D. Vierstra, P.M. Howley, The HPV-16 E6 and E6-AP complex functions as a ubiquitin-protein ligase in the ubiquitination of p53, *Cell.* 75 (1993) 495-505.
  50. V. Dulic, W.K. Kaufmann, S.J. Wilson, T.D. Tlsty, E. Lees, J.W. Harper, *et al.*, p53-dependent inhibition of cell-dependent kinase activities in human fibroblasts during radiation-induced G1 arrest, *Cell.* 76 (1994) 1013-1023.
  51. T.D. Kessis, R.J. Slebos, W.G. Nelson, M.B. Kastan, B.S. Plunkett, S.M. Han, *et al.*, Human papillomavirus 16 E6 expression disrupts the p53-mediated cellular response to DNA damage. *Proc. Natl. Acad. Sci.* 90 (1993) 3988-3992.
  52. H. Zimmerman, R. Degenkolbe, H.U. Bernard, M.J. O'Connor, The human papillomavirus type 16 E6 oncoprotein can down-regulate p53 activity by targeting the transcriptional coactivator CBP/p300, *J. Virol.* 73 (1999) 6209-6219.

53. S. Li, S. Labrecque, M.C. Gauzzi, A.R. Cuddihy, A.H.T. Wong, S. Pellegrini, G.J. Matlashewski, A. Kromilas, The human papilloma virus (HPV)-18 E6 oncoprotein physically associates with Tyk2 and impairs Jak-STAT activation by interferon- $\alpha$ , *Oncogene*. 18 (1999) 5727-5737.
54. K.Y. Kim, L. Blatt, M.W. Taylor, The effects of interferon on the expression of human papillomavirus oncogenes, *J. Gen. Virol.* 81 (2000) 695-700.
55. T.D. de Gruijl, H.J. Bontkes, A.J. van den Muysenberg, J.W. van Oostveen, M.J. Stukart, R.H. Verheijen, N. Van der Vange, et al, Differences in cytokine mRNA profiles between premalignant and malignant lesions of the uterine cervix, *Eur. J. Cancer*. 35 (1999), 490-497.
56. A.M. El-Sherif, R. Seth, P.J. Tighe, D. Jenkins, Quantitative analysis of IL-10 and IFN-gamma mRNA levels in normal cervix and human papillomavirus type 16 associated cervical precancer, *J. Pathol.* 195 (2001) 179-185.
57. A. Gey, P. Kumari, A. Sambandam, F. Lecuru, L. Cassard, C. Badoual, C. Fridman, B. et al., Identification and characterization of group of cervical carcinoma patients with profound downregulation of intratumoral type I (IFN $\gamma$ ) and type 2 (IL-4) cytokine mRNA expression, *Eur. J. Cancer*. 39 (2003) 595-603.
58. N.T. Holland, M.T. Smith, B. Eskenazi, M. Bastaki, Biological sample collection and processing for molecular epidemiological studies, *Mutat Res.* 543 (2003) 217-234.
59. S.L. Karsten, V.M.D. Van Deerlin, C. Sabatti, L.H. Gill, D.H. Geschwind, An evaluation of tyramide signal amplification and archived fixed and frozen tissue in microarray gene expression analysis, *Nucleic Acids Res.* 30 (2002) 2e4.
60. T. Hiller, L. Snell, P.H. Watson, Microdissection RT-PCR analysis of gene expression in pathologically defined frozen tissue sections, *Biotechniques* 21 (1996) 38-44.
61. M.J. Wallard, C.J. Pennington, A. Veerakumarasivam, G. Burt, I.G. Mills, A. Warren *et al*, Comprehensive profiling and localization of the matrix metalloproteinases in urothelial carcinoma, *Br. J. Cancer*. 94 (2006) 569-577.
62. A.D. Strand, A.K. Aragaki, Z.C. Baquet, A. Hodges, P. Cullingham, P. Holmans,

Conservation of regional gene expression in mouse and human brain, *PLoS Genet.* 3 (2007) e59.

63. D.B. Krizman, R.F. Chuaqui, P.S. Meltzer, J.M. Trent, P.H. Duray, W.M. Linehan, Construction of a representative cDNA library from prostatic intraepithelial neoplasia, *Can. Res.* 56 (1996) 5380-5383.
64. Y.X. Wang, B. Martin-McNulty, A.D. Freay, D.A. Sukovich, M. Halks-Miller, W.W. Li, Angiotensin II increases urokinase-type plasminogen activator expression and induces aneurysm in the abdominal aorta of apolipoprotein E-deficient mice, *Am. J. Pathol.* 159 (2001) 1455-1464.
65. J.E. Kendrick, M.G. Conner, W.K. Huh, Gene expression profiling of women with varying degrees of cervical intraepithelial neoplasia, *J. Low. Genit. Tract. Dis.* 11 (2007) 25-28.
66. L. Lamarq, J. Deeds, D. Ginzinger, J. Perry, S. Padmanabha, K. Smith-McCune, Measurements of human papillomavirus transcripts by real-time quantitative reverse transcription-polymerase chain reaction in samples collected for cervical cancer screening, *JMD* 4 (2002) 97-102.
67. H. Futakuchi, M. Ueda, K. Kanda, K. Fujino, H. Yamaguchi, S. Noda, Transcriptional expression of survivin and its splice variants in cervical carcinomas, *Int. J. Gynecol. Cancer.* 17 (2007) 1092-1098.
68. M. Morrogh, N. Olvera, F. Bogomolny, P.I. Borgen, T.A. King, Tissue preparation for laser capture microdissection and RNA extraction from fresh frozen breast tissue, *Biotechniques* 43 (2007) 41-48.
69. H. Wang, J.D. Owens, J.H. Shih, M.C. Li, R.F. Bonnerm J.F. Mushinski, Histological staining methods preparatory to laser capture microdissection significantly affect the integrity of the cellular RNA, *BMC Genomics* 7 (2006) 97-104.
70. A.H. Kihara, A.S. Moriscot, P.J. Ferreira, D.E. Hamassaki, Protecting RNA in fixed tissue: an alternative method for LCM users, *J. Neurosci. Methods* 148 (2005) 103-107.
71. J. Zhang, C.D. Byrne, Differential priming of RNA templates during cDNA synthesis markedly affects both accuracy and reproducibility of quantitative competitive reverse-transcriptase PCR, *Biochem J.* 337 (1999) 231-241.

72. W.H. 3rd. Karge, E.J. Schaefer, J.M.Ordovas, Quantification of mRNA by polymerase chain reaction (PCR) using an internal standard and a nonradioactive detection method, *Methods in Mol. Biol.* 110 (1998) 43-61.
73. T. Suzuki, P.J. Higgins, D.R. Crawford, Control selection for RNA quantitation, *Biotechniques* 29 (2000) 332-337.
74. K. Dheda, J.F. Huggett, S.A. Bustin, M.A. Johnson, G. Rook, A. Zumla, Validation of housekeeping genes for normalizing RNA expression in real-time PCR, *Biotechniques* 37 (2004) 112-119.
75. S.D. Ginsberg, S. Che, RNA amplification in brain tissues, *Neurochem .Res.* 27 (2002) 981-992.
76. R.C. Day, L. McNoe, R.C. Mcknight, Evaluation of global RNA amplification and its use for high-throughput transcript analysis of laser microdissected endosperm, *Int. J. Plant Genomics* (2007) 61028:17 pages.
77. K. Kurimoto, Y. Yabuta, Y. Ohinata, M. Saitou, Global single-cell cDNA amplification to provide a template for representative high-density oligonucleotide microarray analysis, *Nat. Protoc.* 2 (2007) 739-752.
78. M. Noutsias, M. Rohde, A. Block, K. Klippert, O. Lettau, K. Blunert, Preamplication techniques for real-time RT-PCR analyses of endomyocardial biopsies, *BMC Mol. Biol.* 9 2(2008) 3.
79. E.R. Flores, B.L. Allen-Hoffmann, D. Lee, C.A. Sattler, P.F. Lambert, Establishment of the Human Papillomavirus type 16 (HPV-16) life cycle in an immortalized human foreskin keratincocyte cell line, *Virology* 262 (1999) 344-354.
80. H. Lichtiq, M. Alqrisi, L.E. Botzer, T. Abadi, Y. Verbitzky, A. Jackman, HPV16 E6 natural variants exhibit different activities in functional assays relevant to the carcinogenic potential of E6, *Virology* 350 (2006) 216-227.
81. C.F.A. Culling, .T. Allison, W.T. Barr (4 Eds.), *Cellular Pathology Techniques*, Butterworths, London, 1984 pp. 55-59.
82. D.M. Kube, C.D. Savci-Hejjink, A.F. Lamblin, F. Kosari, G. Vasmatzis, J.C. Cheville,

- Optimization of laser capture microdissection and RNA amplification for gene expression profiling of prostate cancer, *BMC Mol. Biol.* 8 (2007) 25-38.
83. A. Schroeder, O. Mueller, S. Stocker, R. Salowsky, M. Leiber, M. Gassmann, The RIN: an RNA integrity number for assigning integrity values to RNA measurements, *BMC Mol. Biol.* 7 (2006) 3.
  84. V. Marx, RNA quality: Defining the good, the bad and the ugly, *Genomics and proteomics*, 4 (2004) 14-21.
  85. M.W. Pfaffl, G.W. Horgan, L. Dempfle, Relative expression software tool (REST©) for group-wise comparison and statistical analysis of relative expression results in real-time PCR, *Nucleic Acids Res* 9 (2002) e36.
  86. M.W. Pfaffle, A new mathematical model for relative quantification in real-time RT-PCR, *Nucleic Acids Res.* 29 (2001) e45.
  87. M.W. Pfaffl, A. Tichopad, C. Prgomet, T.P. Neuvians, Determination of stable housekeeping genes, differentially regulated target genes and sample integrity: Bestkeeper-excel based tool using pari-wise correlations, *Biotechnol. Lett.* 26 (2004) 509-515.
  88. Y. Qin, V.M. Heine, H. Karst, P.J. Lucassen, M. Joels, Gene expression patterns in rat dentate granule cells: comparison between fresh and fixed tissue, *J. Neurosci. Methods.* 131 (2003) 205-211.
  89. T. Inoue, K. Nabeshima, H. Kataoka, M. Koono, Feasibility of archival non-buffered formalin-fixed and paraffin-embedded tissues for PCR amplification: an analysis of resected gastric carcinoma, *Pathol. Int.* 46 (1996) 997-1004.
  90. L.V. Madabusi, G.T. Latham, B.F. Andruss, RNA extraction for arrays, *Methods Enzymol.* 411 (2006) 1-13.
  91. S.A. Bustin, Absolute quantification of mRNA using real-time reverse transcription polymerase chain reaction assays, *J. Mol. Endocrinol.* 25 (2000) 169-193.
  92. M.E. Moreau, P. Dubreuil, G. Molinaro, M. Chagnon, W. Muller-Esterl, Y. Lepage, Expression of metalloproteinases and kinin receptors in swine oropharyngeal tissues: effects of angiotensin I-converting enzyme inhibition and inflammation, *J. Pharmacol. Exp. Ther.*

315 (2005) 1065-1074.

93. D.K. Gaffney, K. Winter, C. Fuhrman, R. Flinner, K. Greven, J. Ryu, Feasibility of RNA collection for micro-array gene expression analysis in the treatment of cervical carcinoma: A scientific correlate of RTOG C-0128, *Gynecol. Oncol.* 97 (2005) 607-611.
94. P. Micke, M. Ohshima, S. Tahmasebpour, Z.P. Ren, A. Ostman, F. Ponten, Biobanking of fresh frozen tissue: RNA is stable in nonfixed surgical specimens, *Lab. Invest.* 86 (2006) 202-211.
95. S. Akilesh, S. Petkova, T.J. Sproule, D.J. Shaffer, G.J. Christianson, D. Roopenian, The MHC class I-like Fc receptor promotes humorally mediated autoimmune disease, *J. Clin. Invest.* 113( 2004) 1328-1333.
96. Leparc GG, Mitra RD. A sensitive procedure to detect alternatively spliced mRNA in pooled-tissue samples. *Nucl Acid Res* 2007;1-8.
97. Zhang J, Byrne CD. Differential priming of RNA templates during cDNA synthesis markedly affects both accuracy and reproducibility of quantitative competitive reverse-transcriptase PCR. *Biochem J* 1999;337:231-241
98. Bustin SA, Nolan T. Pitfalls of quantitative real-time reverse-transcription polymerase chain reaction. *J Biomol Tech* 2004;15:155-166.
99. Ginzinger DG. Gene quantification using real-time quantitative PCR: An emerging technology hits the mainstream. *Exp Hematol* 2002;30:503-512.
100. Y. Zhai, R. Kuick, B. Nan, I. Ota, S.J. Weiss, C.L. Trimble, Gene expression analysis in preinvasive and invasive cervical squamous cell carcinomas identifies HOXC10 as a key mediator of invasion, *Cancer Res.* 67 (2007) 10163-10172.
101. J.B. de Kok, R.W. Roelofs, B.A. Giesendorf, J.L. Pennings, E.T. Waas, T. Feuth, Normalization of gene expression measurements in tumor tissues: comparison of 13 endogenous control genes, *Lab. Invest.* 85 (2005) 154-159.
102. J. Lindbom, A.G. Ljungman, M. Lindahl, C. Tagesson, Increased gene expression of novel cytosolic and secretory phospholipase A(2) types in human airway epithelial cells induced by tumor necrosis factor-alpha and IFN-gamma, *J Interferon Cytokine Res.* 22 (2002) 947-

955.

103. D.L. Foss, M.J. Baarsch, M.P. Murtaugh, Regulation of hypoxanthine phosphoribosyltransferase, glyceraldehyde-3-phosphate dehydrogenase and beta-actin mRNA expression in porcine immune cells and tissues, *Anim. Biotechnol.* 9 (1998) 67-78.
104. S. Delhaye, S. Paul, G. Blakqori, M. Minet, F. Weber, P. Staeheli, T. Michiels, Neurons produce type I interferon during viral encephalitis, *Proc. Natl. Acad. Sci. U.S.A.* 103 (2006) 7835-7840.
105. S.J. Um, J.W. Rhyu, E.J. Kim, K.C. Jeon, E.S. Hwang, J.S. Park, Abrogation of IRF-1 response by high-risk HPV E7 protein in vivo, *Cancer Letters.* 179 (2002) 205-212.
106. C. Natale, T. Giannini, A. Lucchese, D. Kanduc, Computer-assisted analysis of molecular mimicry between human papillomavirus 16 E7 oncoprotein and human protein sequences, *Immunol Cell Biol.* 78 (2000) 580-585.
107. S.H. Song, J.K. Lee, O.S. Sek, H.S. Saw, The relationship between cytokines and HPV-16, HPV-16 E6, E7, and high-risk HPV viral load in the uterine cervix, *Gyne. Oncol.* 104 (2007) 732-738.
108. C. Youngsok, G.A. Johnson, R.C. Burghardt, L.R. Berghman, M.M. Joyce, K.M. Taylor, M.D. Stewart, Interferon regulatory factor-two restricts expression of interferon-stimulated genes to the endometrial stroma and glandular epithelium of the ovine uterus. *Biol. of Repro.* 65 (2001) 1038-1049.

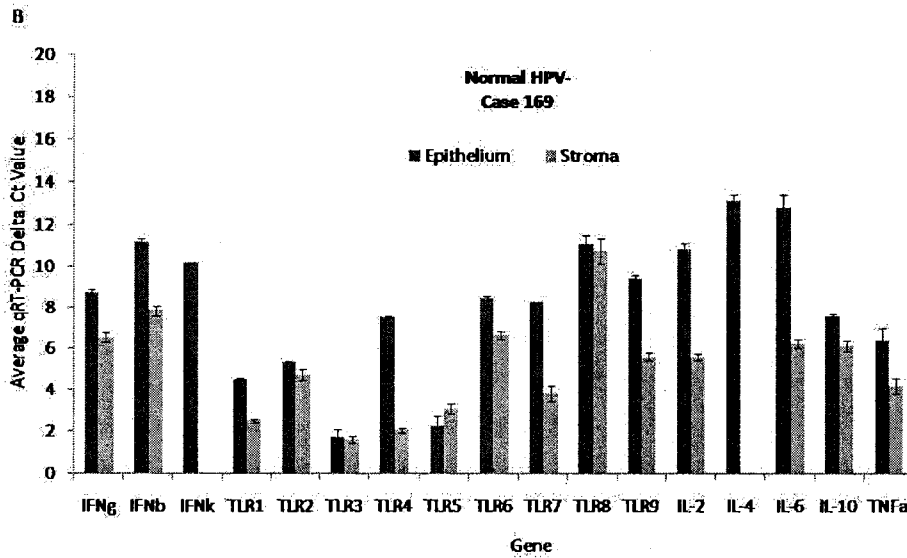
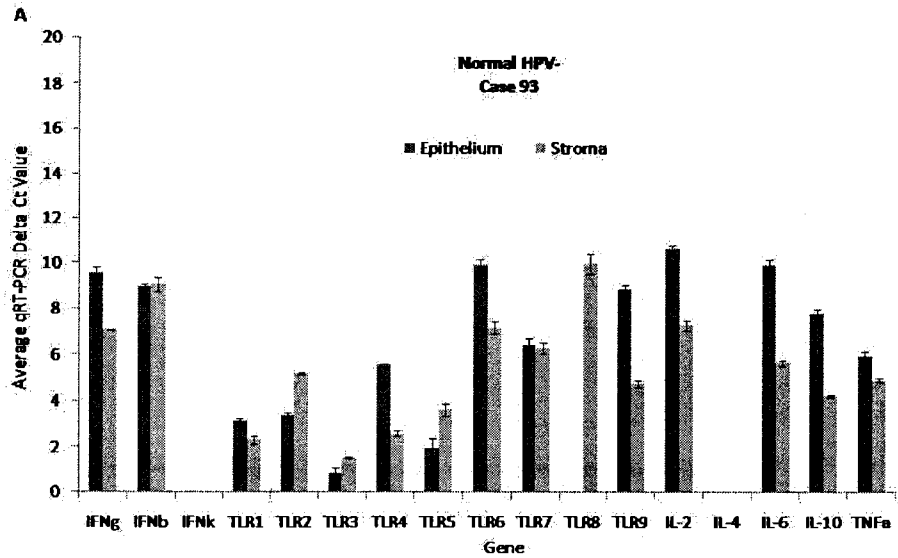
#### FIGURE REFERENCES

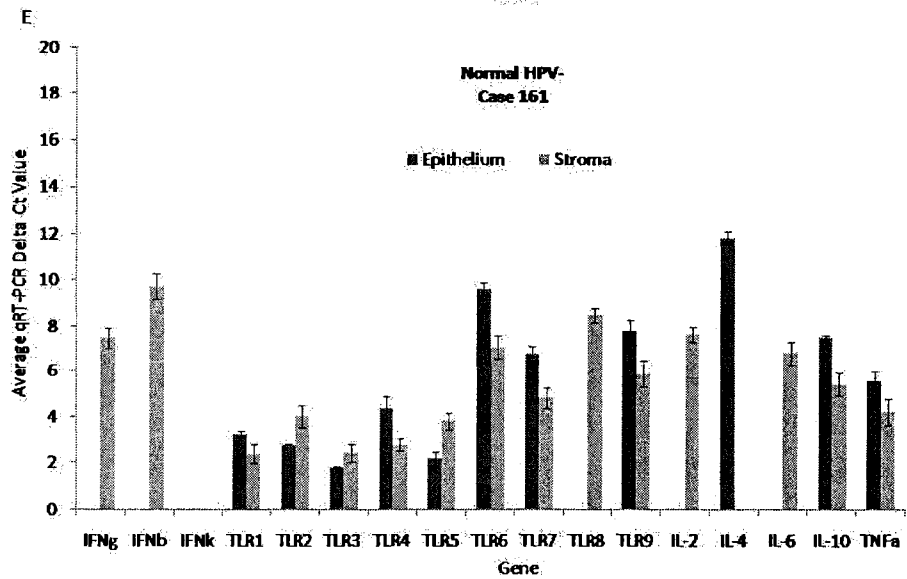
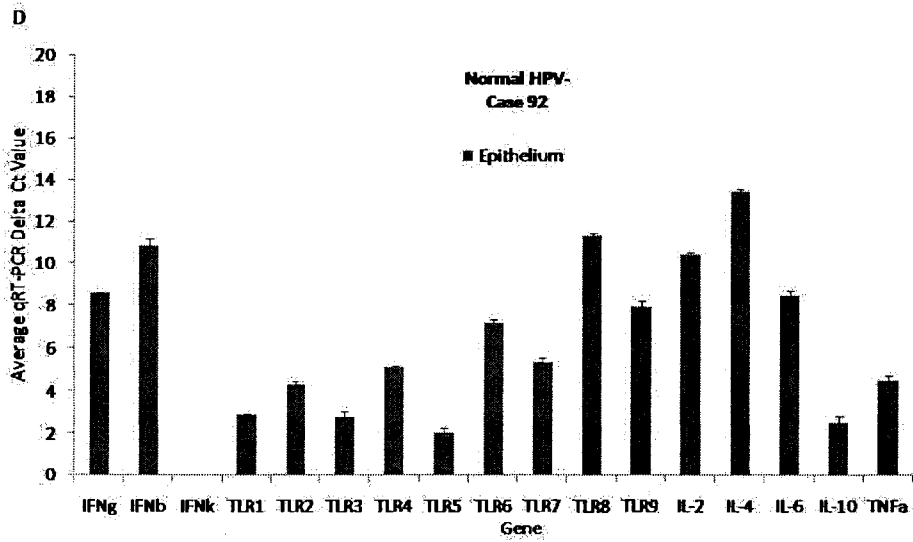
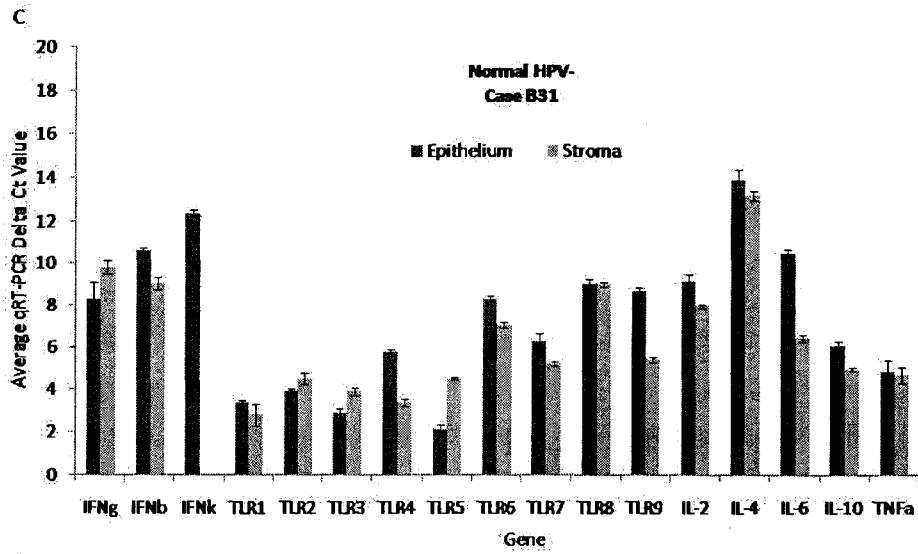
109. A. Garcia-Sastre, C.A. Biron, Type I interferons and the virus-host relationship: a lesson in détente, *Science.* 312 (2006) 879-882.
110. M. Benevolo, M. Mottolese, F. Marandino, G. Vocaturo, R. Sindico, G. Piperno, L. Mariani, I. et al., Immunohistochemical expression of p16(INK4a) is predictive of HR-HPV infection in cervical low-grade lesions, *Mod. Pathol.* 19 (2006) 384-391.

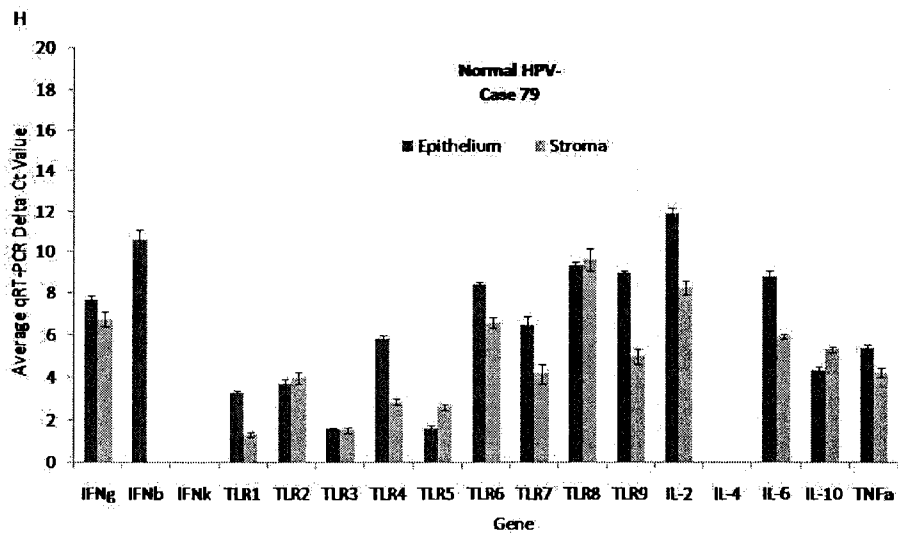
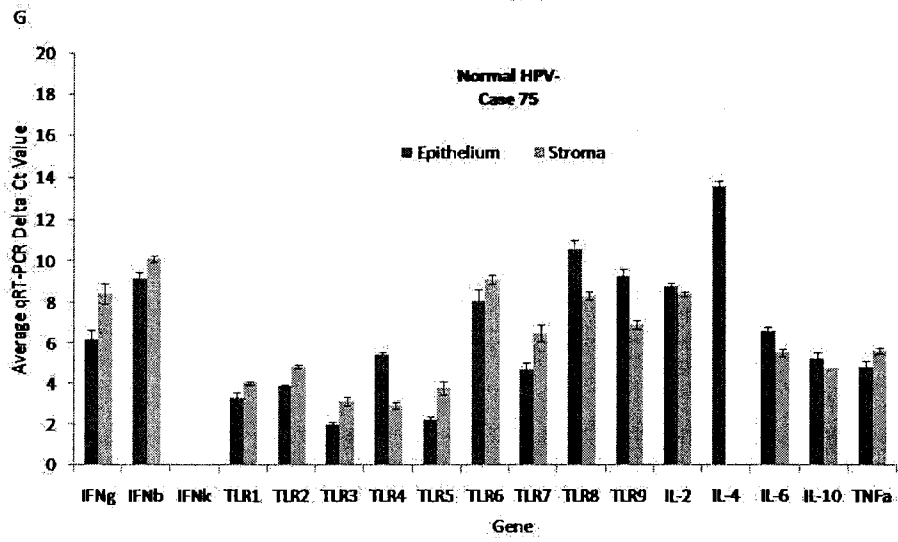
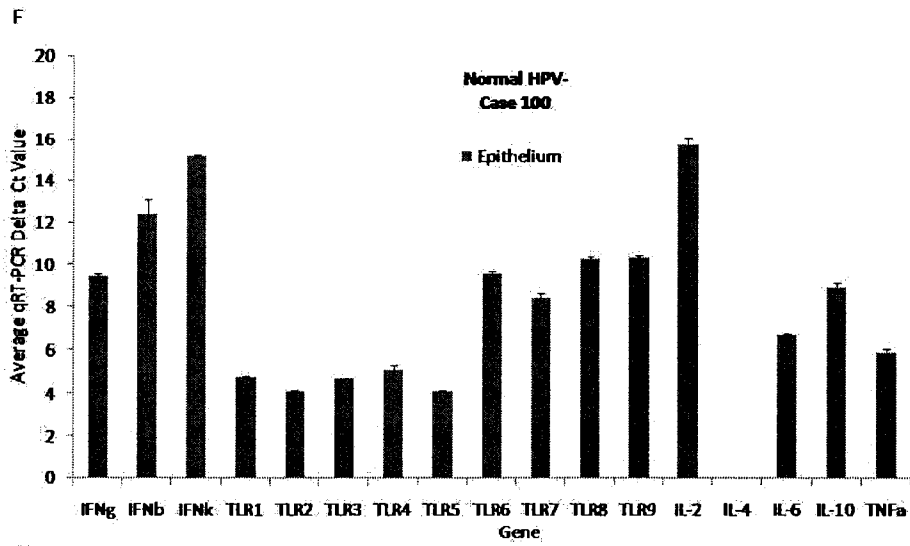
## 6.0 APPENDIX A

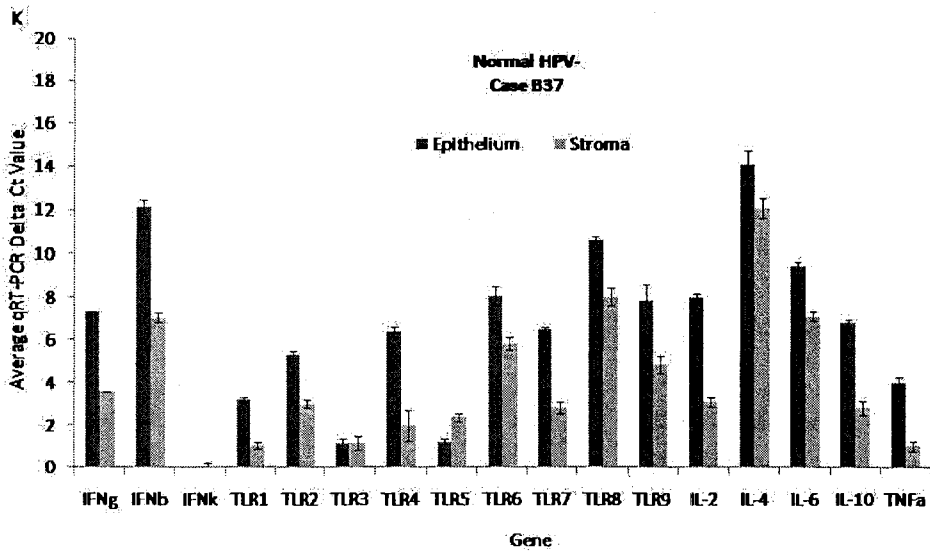
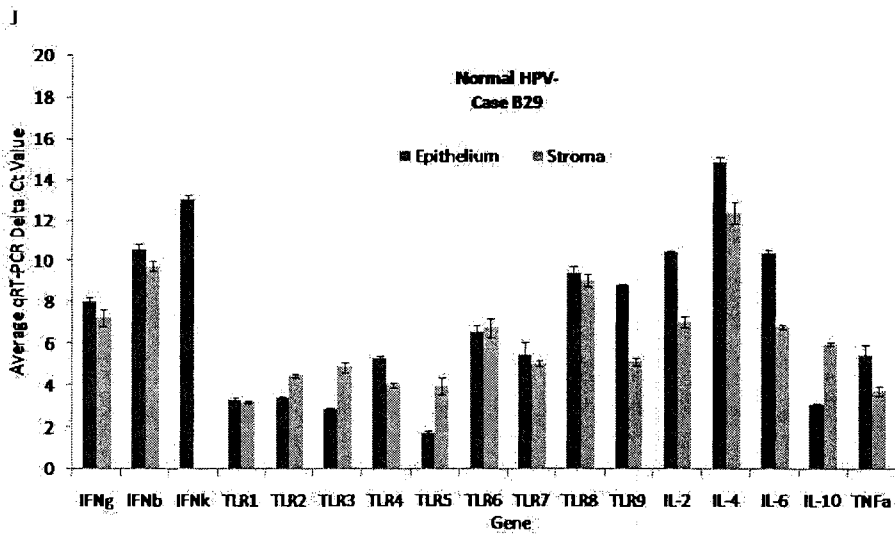
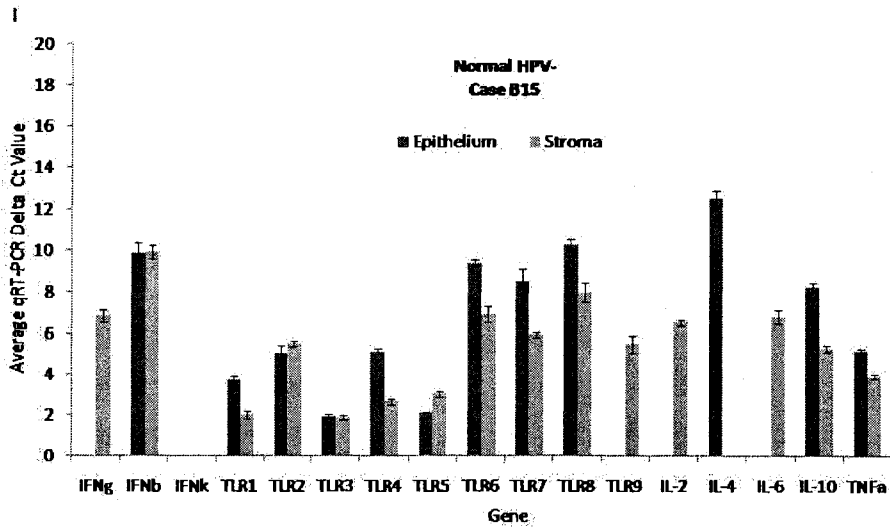
### 6.1 Survey of Innate Immune Response in Microdissected Cervical Material

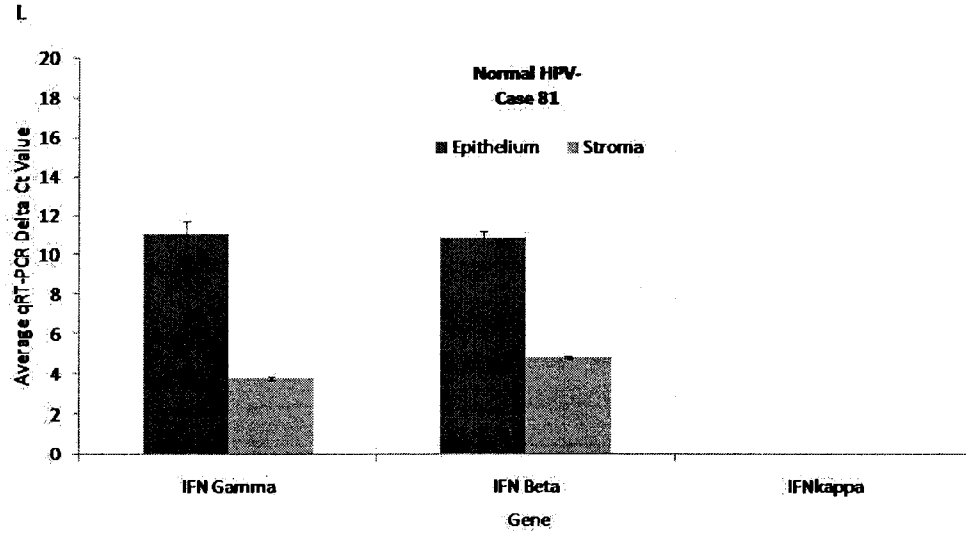
#### 6.1.1 Individual Normal Cases (n=12)





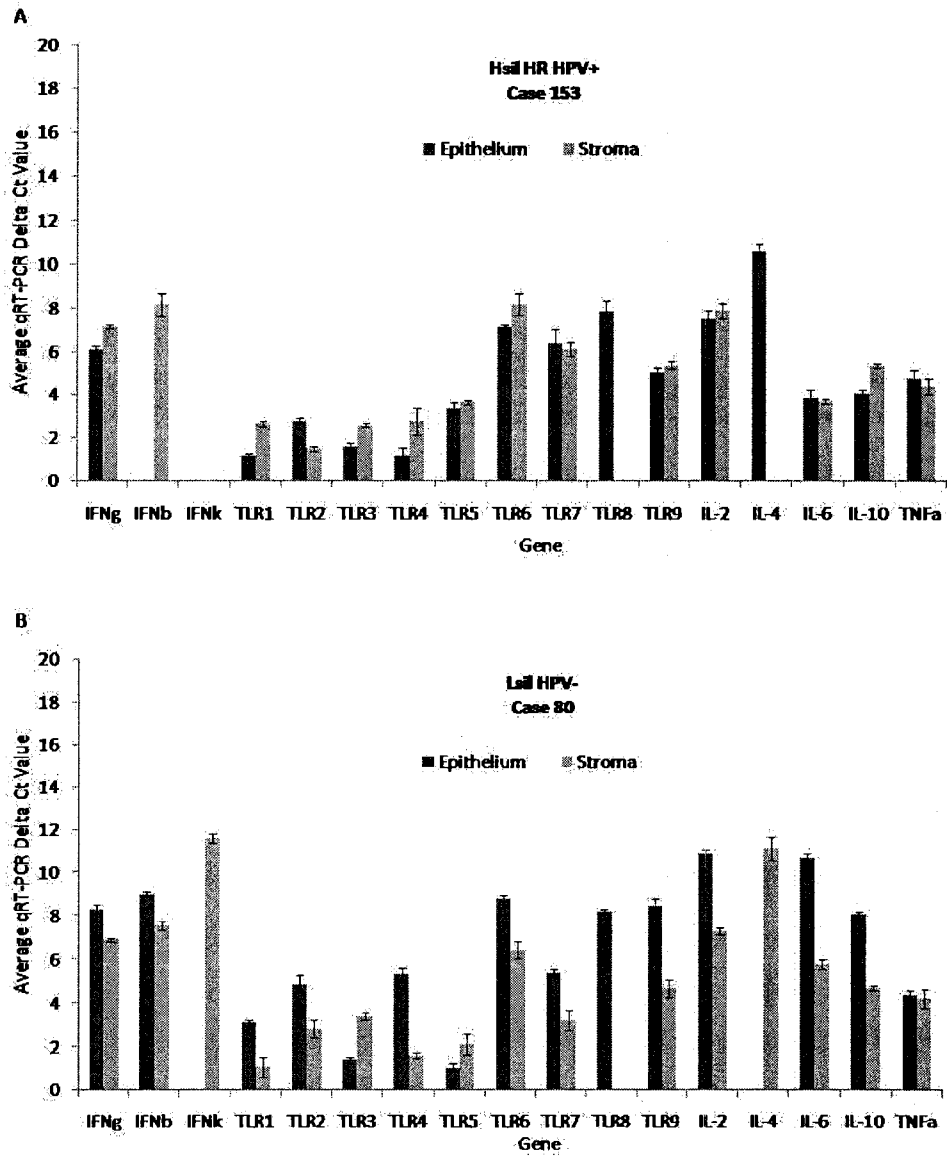


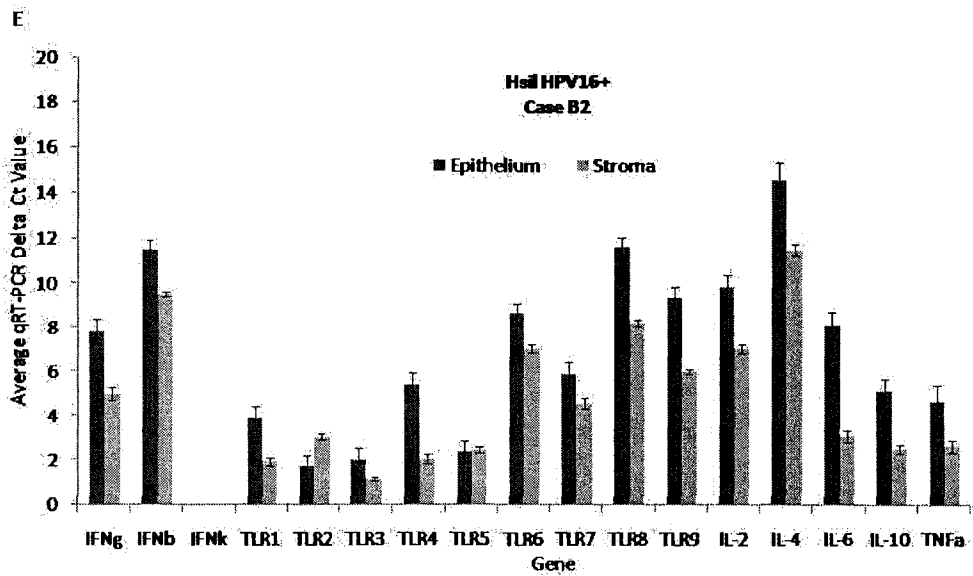
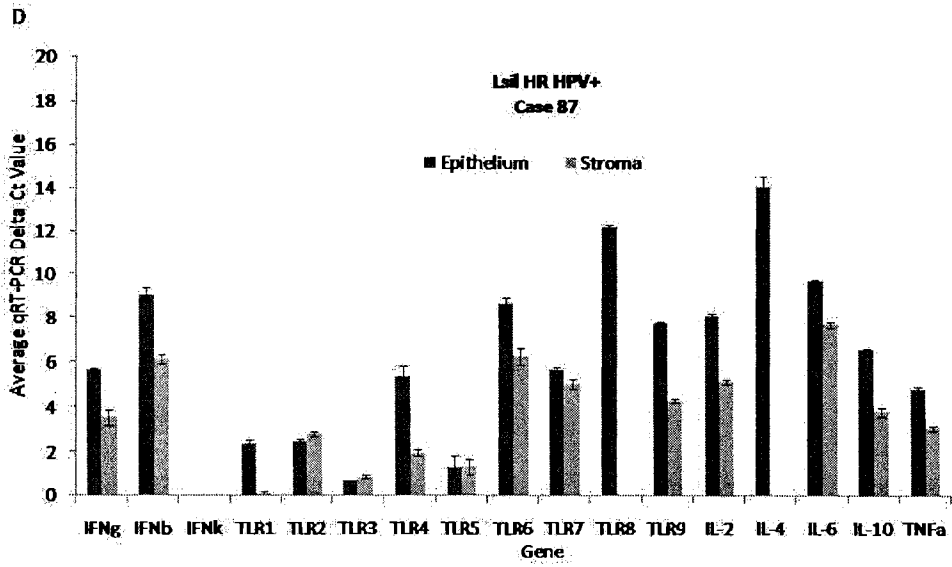
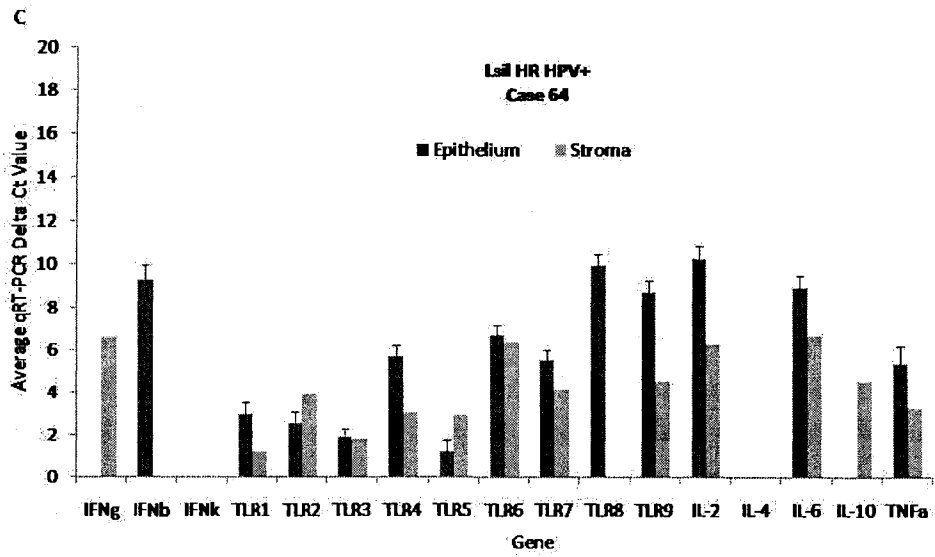


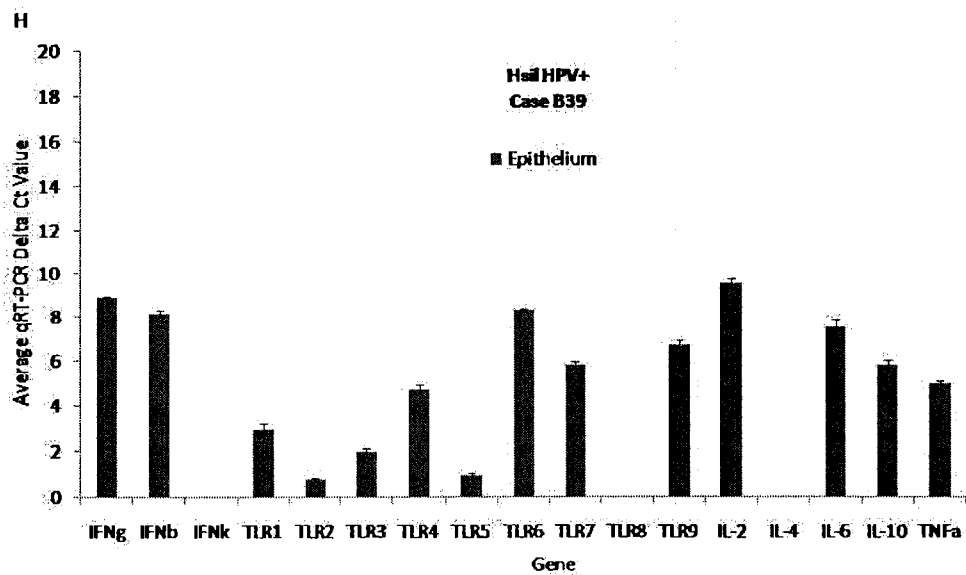
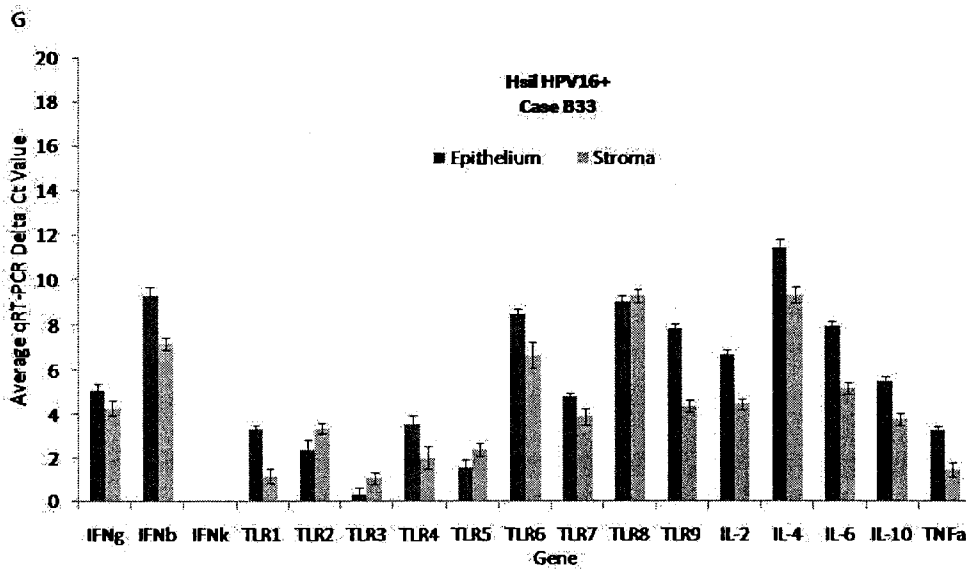
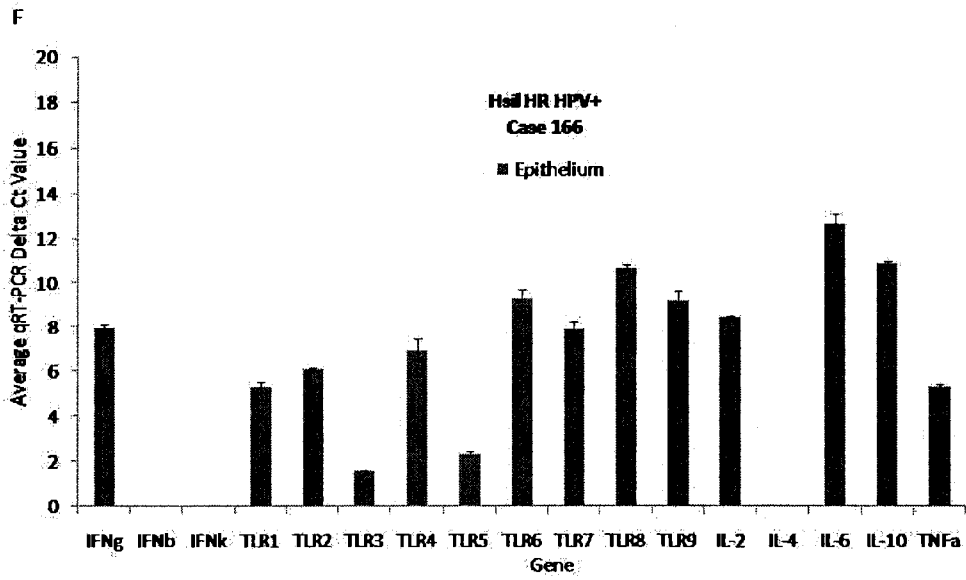


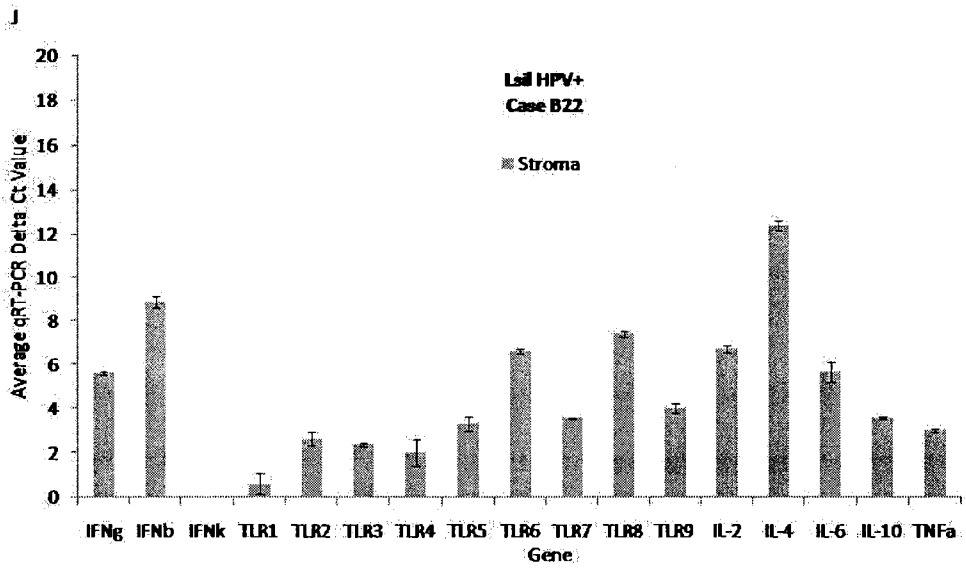
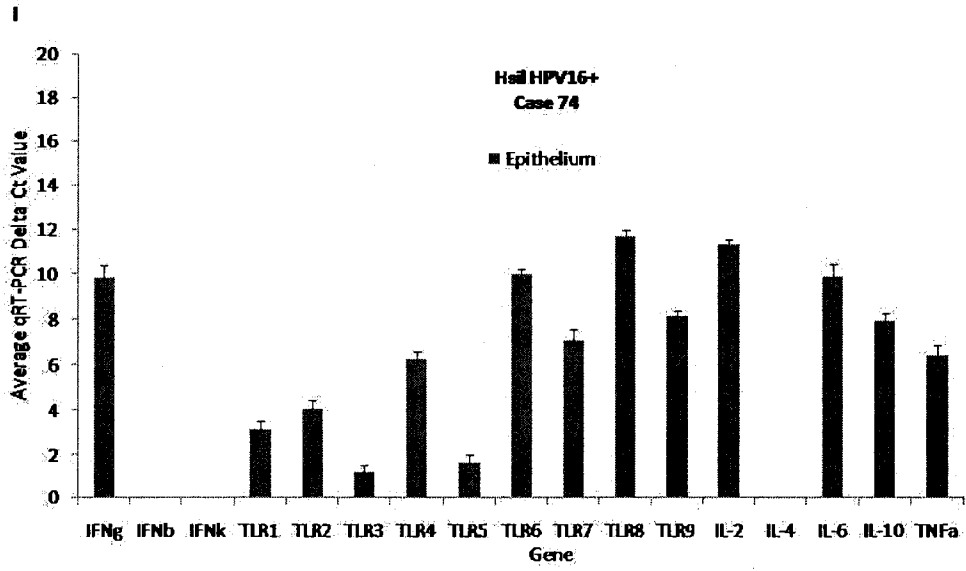
**Figure 32. Cell type-specific gene expression of IFNs and genes involved in innate immunity in individual normal HPV- cervical tissue samples.** Cervical epithelium (dark grey bars) and stroma (light grey bars) were excised from whole cervical samples using LCM and the mRNA levels of 16 genes were analyzed using qRT-PCR. Samples A-K were analyzed for all 16 genes, while sample L was analyzed just for IFN expression. Ten cases involved both epithelium and stromal analysis, while 2 samples do not include stromal gene expression analysis. Values represent the average delta qRT-PCR Ct value  $\pm$  SD. cDNA input concentrations were determined using the Experion™.

### 6.1.2 Individual Dysplastic Cases (n=11)









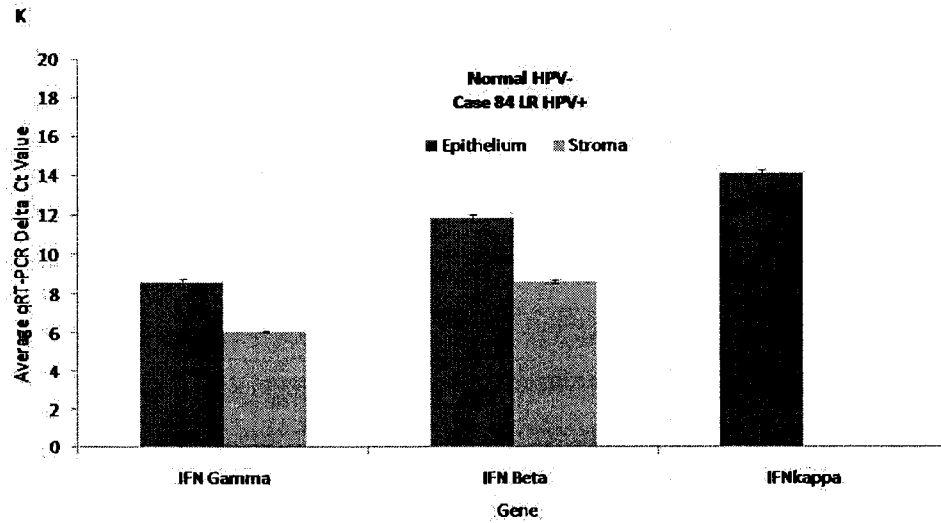


**Figure 33. Cell type-specific gene expression of IFNs and genes involved in innate immunity in individual dysplastic cervical tissue samples.** Cervical epithelium (dark grey bars) and stroma (light grey bars) were excised from whole cervical samples using LCM and the mRNA levels of 16 genes were analyzed using qRT-PCR. Samples A-J were analyzed for all 16 genes, while sample K was analyzed just for IFN expression. Seven cases involved both epithelium and stromal analysis, while 4 cases include either epithelium or stromal gene expression analysis only. Values represent the average delta qRT-PCR Ct value  $\pm$  SD. cDNA input concentrations were determined using the Experion™.

## 6.2 Prevalence of Gene Expression in LCM Cohort

**Table 5.** Summary of the prevalence of genes expressed in normal and dysplastic cervical epithelium and stroma

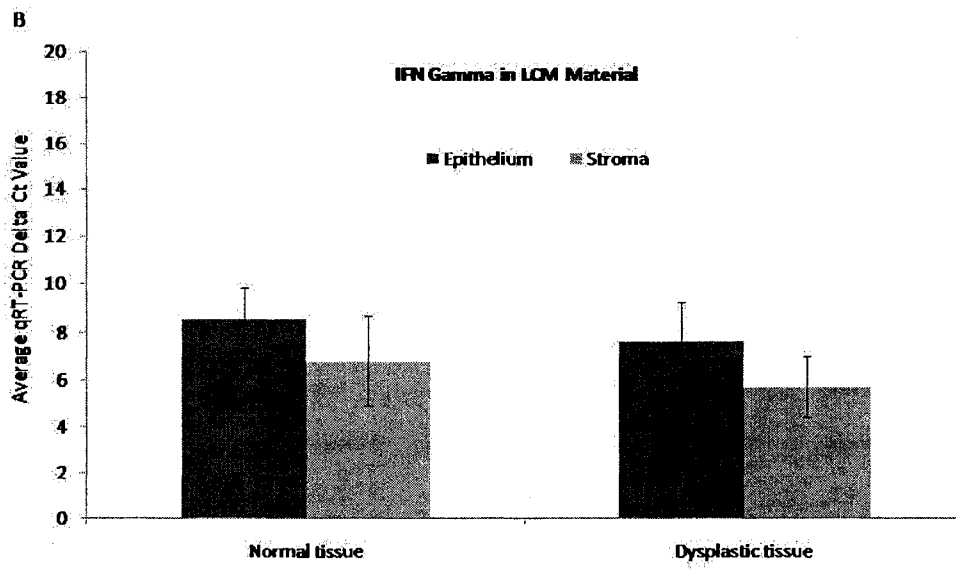
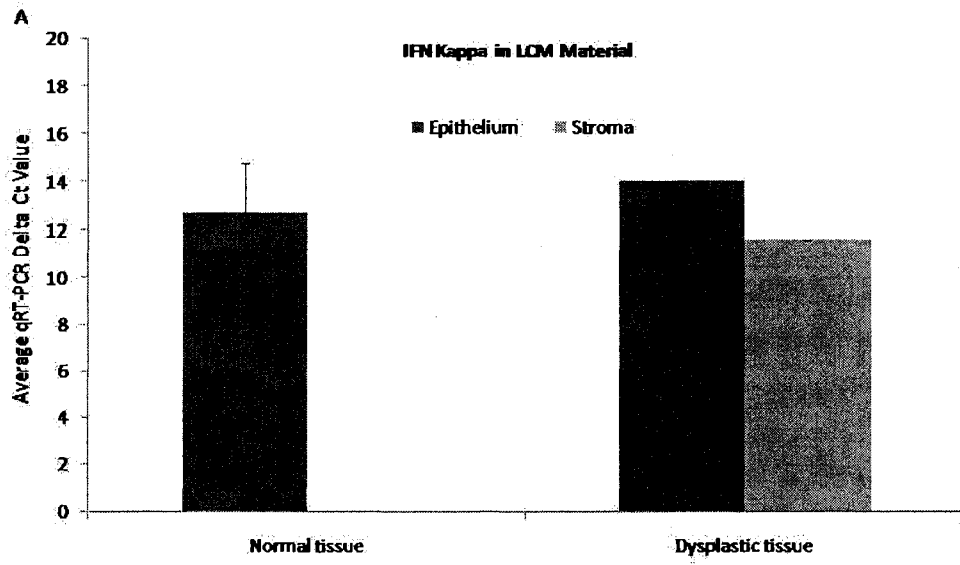
Gene	Normal		Dysplastic		Carcinoma	
	Epithelium	Stroma	Epithelium	Stroma	Epithelium	Stroma
IFN- $\gamma$	83.3 (10/12)	100 (10/10)	90 (9/10)	100 (8/8)	100 (1/1)	100 (1/1)
IFN- $\beta$	91.7 (11/12)	100 (10/10)	70 (7/10)	87.5 (7/8)	100 (1/1)	100 (1/1)
IFN- $\kappa$	33.3 (4/12)	0 (0/10)	10 (1/10)	12.5 (1/8)	100 (1/1)	100 (1/1)
TLR1	100 (11/11)	100 (9/9)	100 (9/9)	100 (7/7)	100 (1/1)	100 (1/1)
TLR2	100 (11/11)	100 (9/9)	100 (9/9)	100 (7/7)	100 (1/1)	100 (1/1)
TLR3	100 (11/11)	100 (9/9)	100 (9/9)	100 (7/7)	100 (1/1)	100 (1/1)
TLR4	100 (11/11)	100 (9/9)	100 (9/9)	100 (7/7)	100 (1/1)	100 (1/1)
TLR5	100 (11/11)	100 (9/9)	100 (9/9)	100 (7/7)	100 (1/1)	100 (1/1)
TLR6	100 (11/11)	100 (9/9)	100 (9/9)	100 (7/7)	100 (1/1)	100 (1/1)
TLR7	100 (11/11)	100 (9/9)	100 (9/9)	100 (7/7)	100 (1/1)	100 (1/1)
TLR8	81.8 (9/11)	100 (9/9)	88.9 (8/9)	42.9 (3/7)	100 (1/1)	100 (1/1)
TLR9	90.9 (10/11)	100 (9/9)	100 (9/9)	100 (7/7)	100 (1/1)	100 (1/1)
IL-2	81.8 (9/11)	100 (9/9)	100 (9/9)	100 (7/7)	100 (1/1)	100 (1/1)
IL-4	72.7 (8/11)	33.3 (3/9)	44.4 (4/9)	57.1 (4/7)	0 (0/1)	100 (1/1)
IL-6	81.8 (9/11)	100 (9/9)	100 (9/9)	100 (7/7)	100 (1/1)	100 (1/1)
IL-10	100 (11/11)	100 (9/9)	88.9 (8/9)	100 (7/7)	100 (1/1)	100 (1/1)
TNF- $\alpha$	100 (11/11)	100 (9/9)	100 (9/9)	100 (7/7)	100 (1/1)	100 (1/1)
TGF- $\beta$	100 (11/11)	100 (9/9)	100 (9/9)	100 (7/7)	100 (1/1)	100 (1/1)

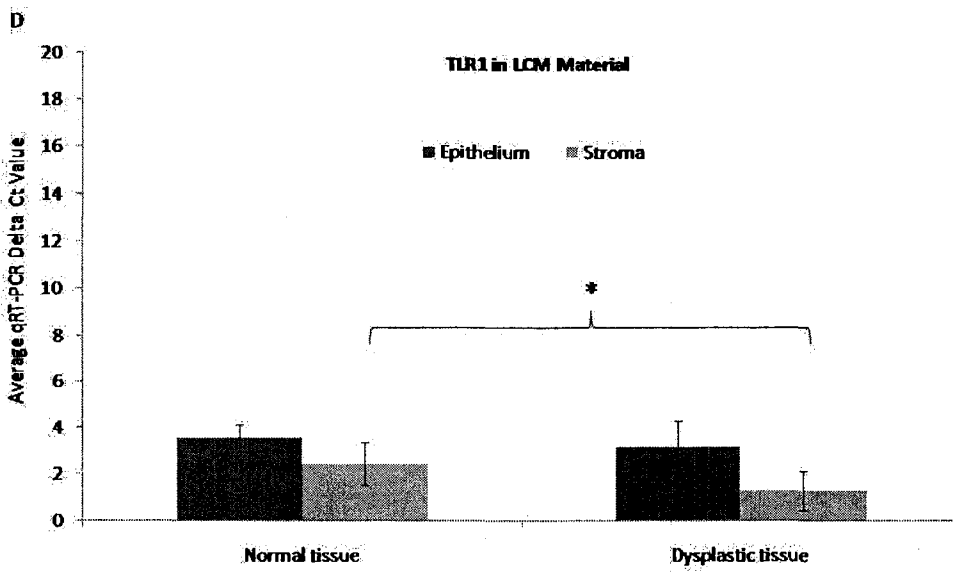
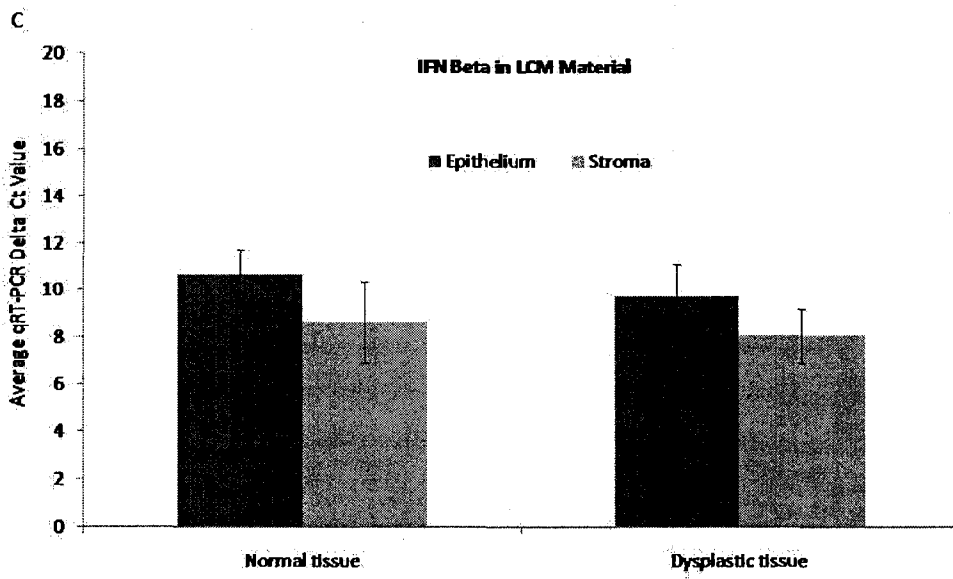
### 6.3 Statistical Differences in Gene Expression in LCM cohort

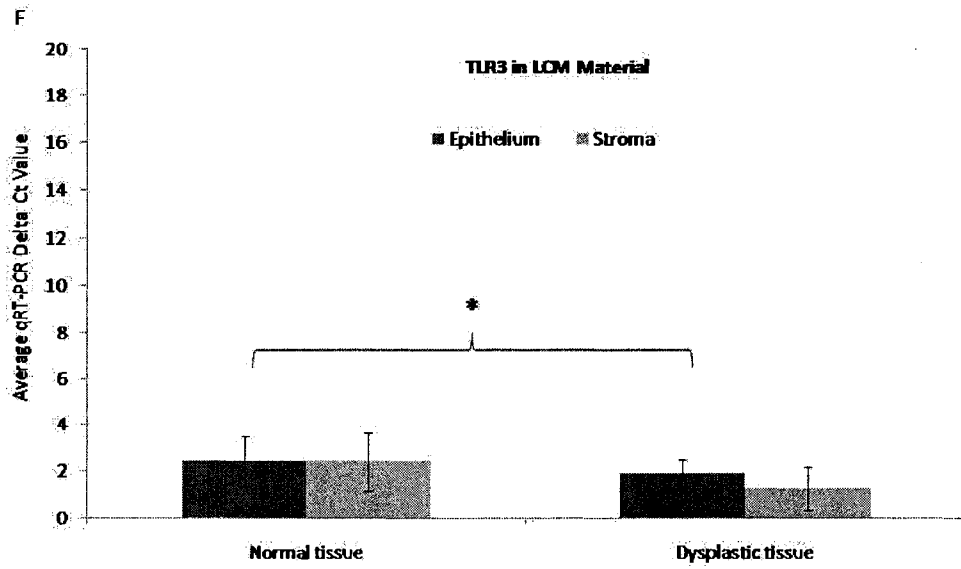
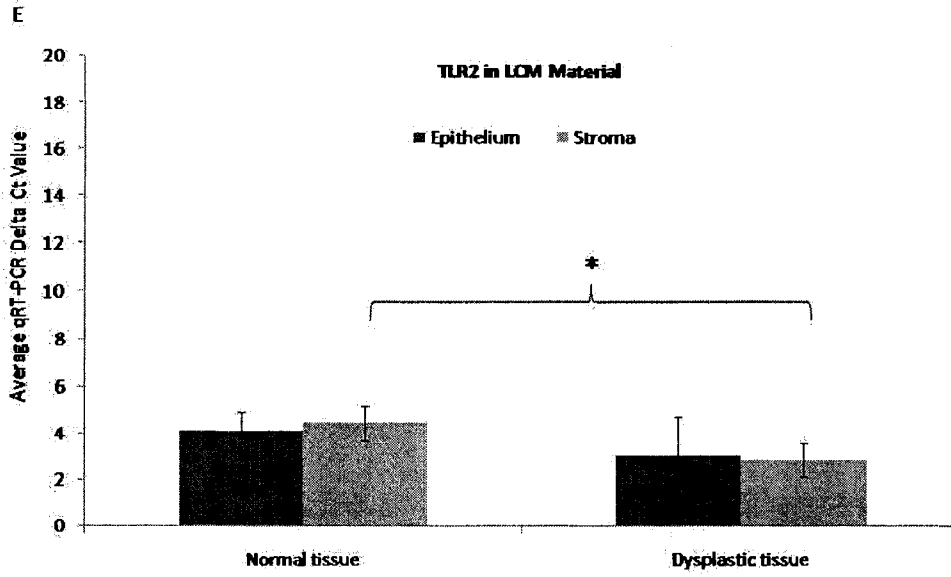
**Table 6.** Statistical significance in gene expression in LCM samples: A comparison of innate immunity gene expression between normal and dysplastic epithelium and stroma

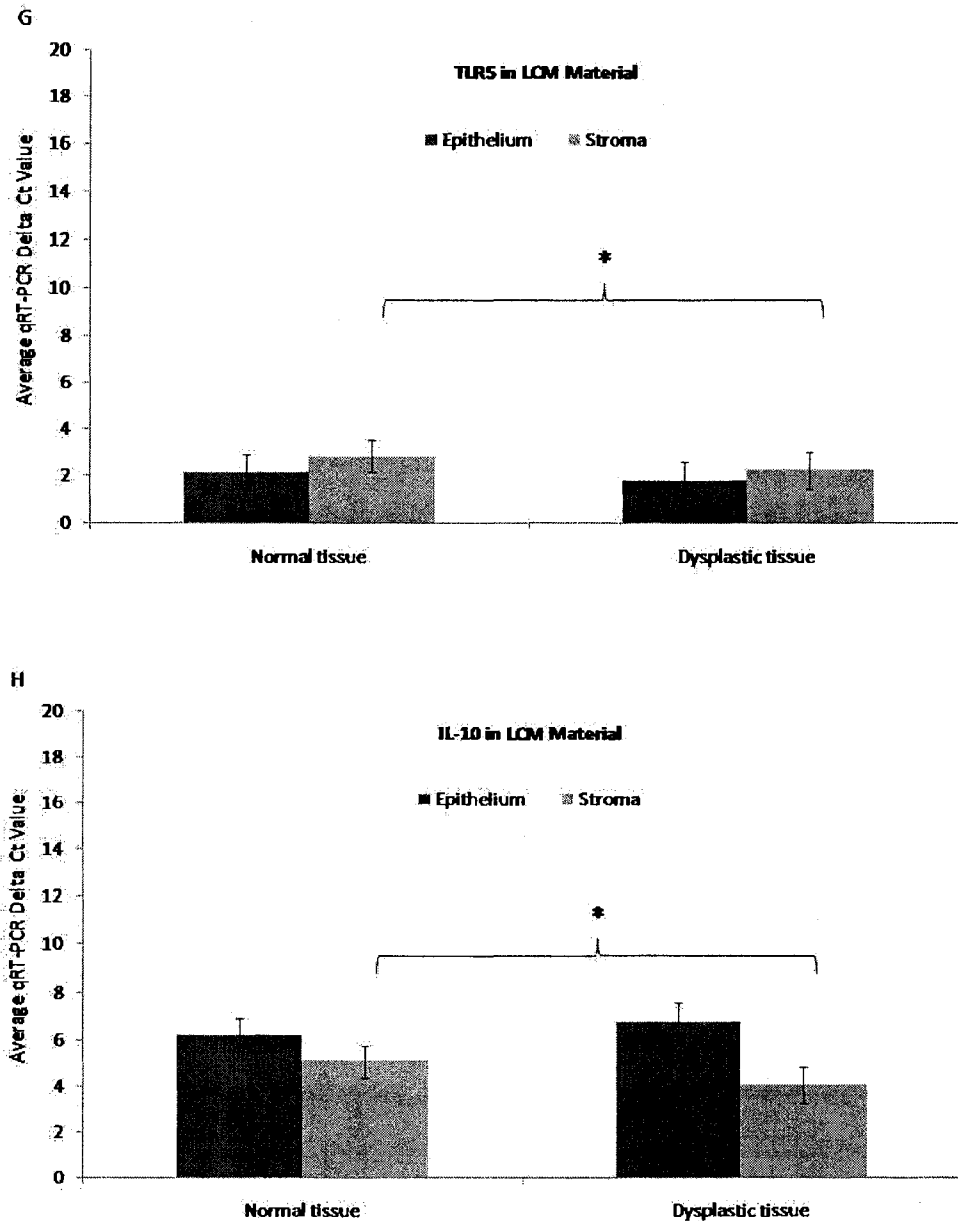
Gene	Epithelium		Stroma		Normal		Dysplastic	
	Normal	Dysplastic	Normal	Dysplastic	Epithelium	Stroma	Epithelium	Stroma
IFN- $\gamma$	0.20		0.163		<b>*0.027</b>		<b>*0.016</b>	
IFN- $\beta$	0.152		0.438		<b>*0.008</b>		<b>*0.026</b>	
IFN- $\kappa$	-		-		-		-	
TLR1	0.363		<b>*0.022</b>		<b>*0.007</b>		<b>*0.002</b>	
TLR2	0.118		<b>*0.0009</b>		0.326		0.729	
TLR3	<b>*0.052</b>		0.337		0.650		0.253	
TLR4	0.310		0.060		<b>*&lt;0.0001</b>		<b>*0.001</b>	
TLR5	0.289		<b>*0.049</b>		0.0008e		<b>&lt;0.0001e</b>	
TLR6	0.919		0.69		<b>*0.003</b>		<b>*0.002</b>	
TLR7	0.247		0.295		<b>*0.007</b>		<b>*0.012</b>	
TLR8	0.899		0.325		<b>*0.009</b>		0.057	
TLR9	0.115		0.068		<b>*&lt;0.0001</b>		<b>*&lt;0.0001</b>	
IL-2	0.123		0.535		<b>*0.0008</b>		<b>*0.001</b>	
IL-4	0.506		0.104		0.111		0.225	
IL-6	0.855		0.166		<b>*0.0005</b>		<b>*0.005</b>	
IL-10	0.583		<b>*0.053</b>		0.138		<b>*0.009</b>	
TNF- $\alpha$	0.293		0.135		<b>*0.0014</b>		0.125	
TGF- $\beta$	0.456		0.353		<b>*0.0017</b>		<b>*0.030</b>	

\* Results significantly higher for dysplastic or stroma tissue (where applicable) unless otherwise stated  
**Bold values** = statistically significant (-) = could not be analyzed (e) = epithelium  
 Carcinoma material not included (n=1)



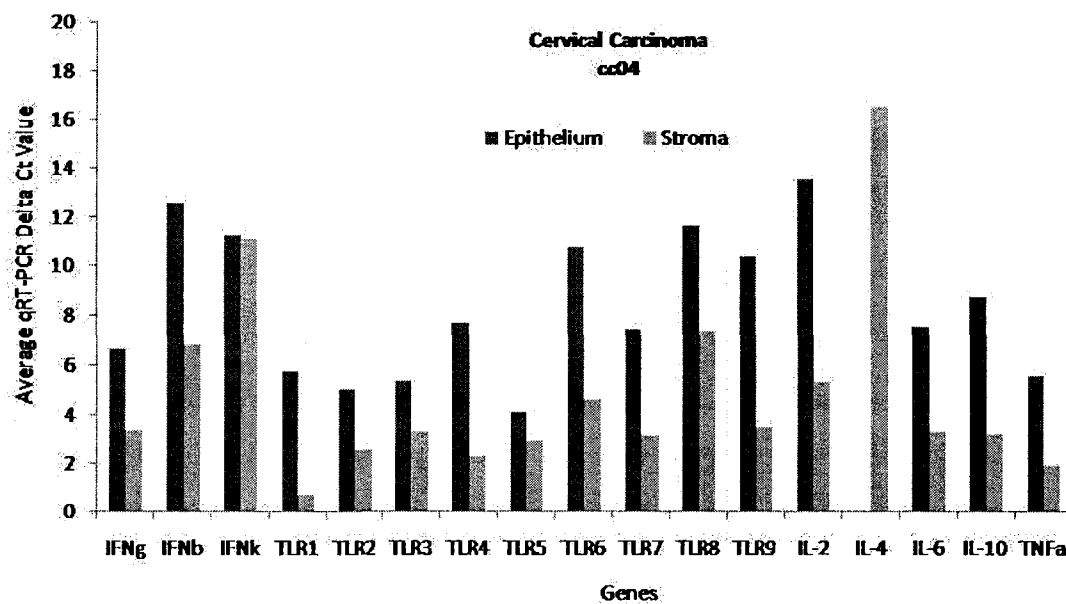






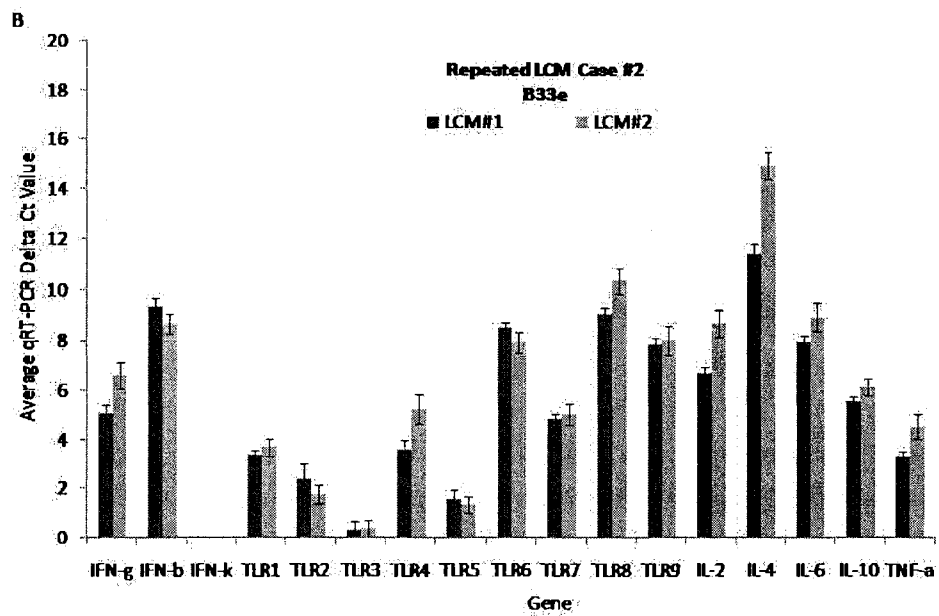
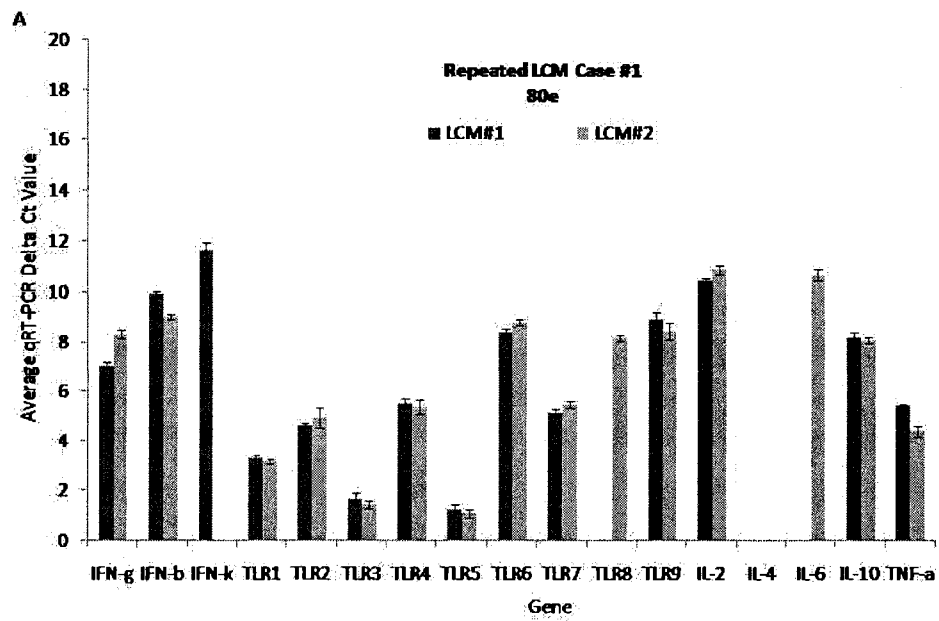
**Figure 34.** Summary of IFN gene expression as well as genes displaying significant differences in expression between normal HPV- and dysplastic cervical tissue. IFN- $\kappa$  (A), - $\gamma$  (B), - $\beta$  (C), TLR 1 (D), 2 (E), 3 (F), 5 (G) and IL-10 (H) gene expression was measured separately in the epithelium and stroma of cervical tissue using laser capture microdissection. The mRNA levels of genes were analyzed using qRT-PCR. Values represent the average delta qRT-PCR Ct value  $\pm$  SD. cDNA input concentrations were determined using the Experion<sup>TM</sup>. Asterisks indicate significant differences.

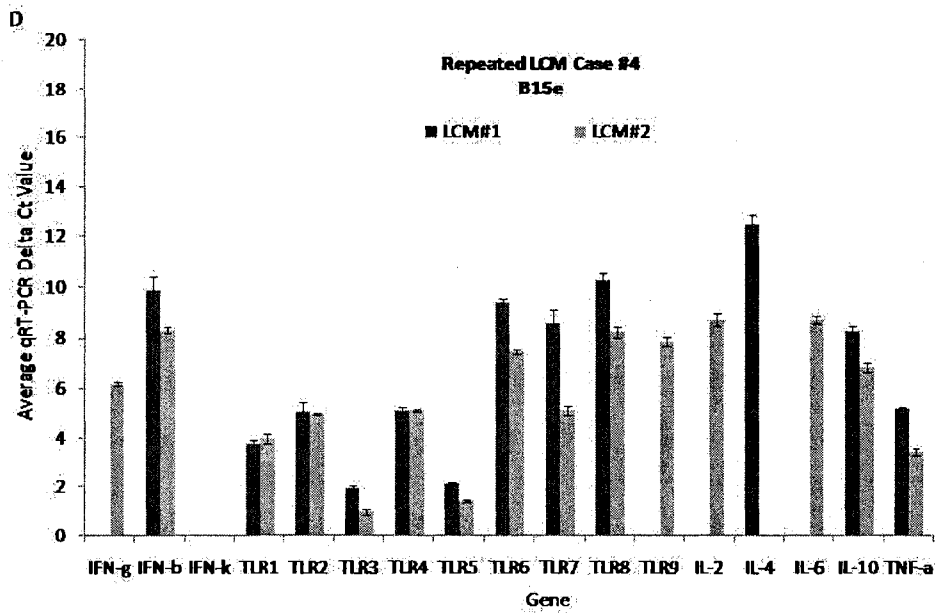
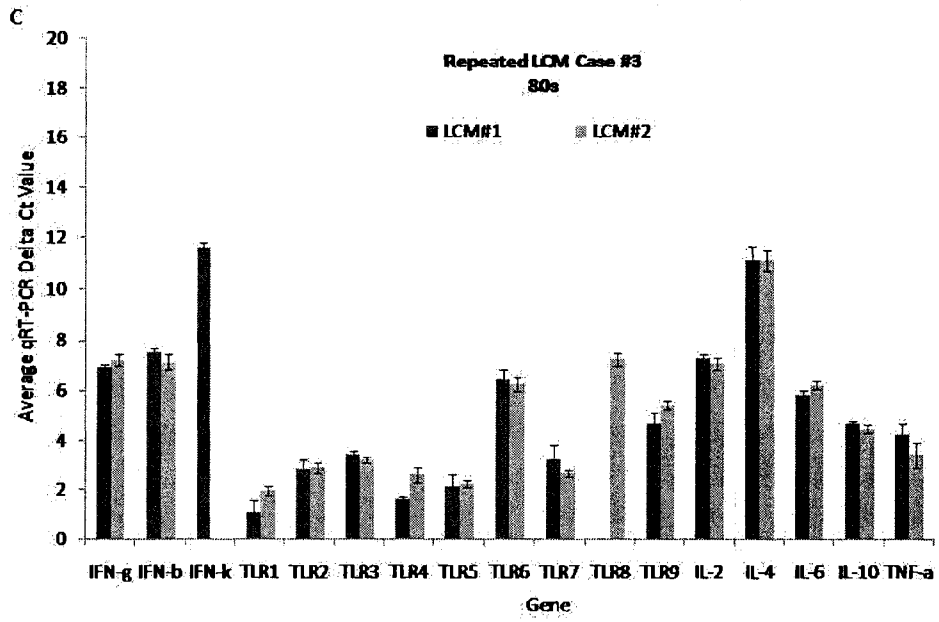
## 6.4 Cell-specific Gene Expression in Cervical Carcinoma epithelium and Stroma

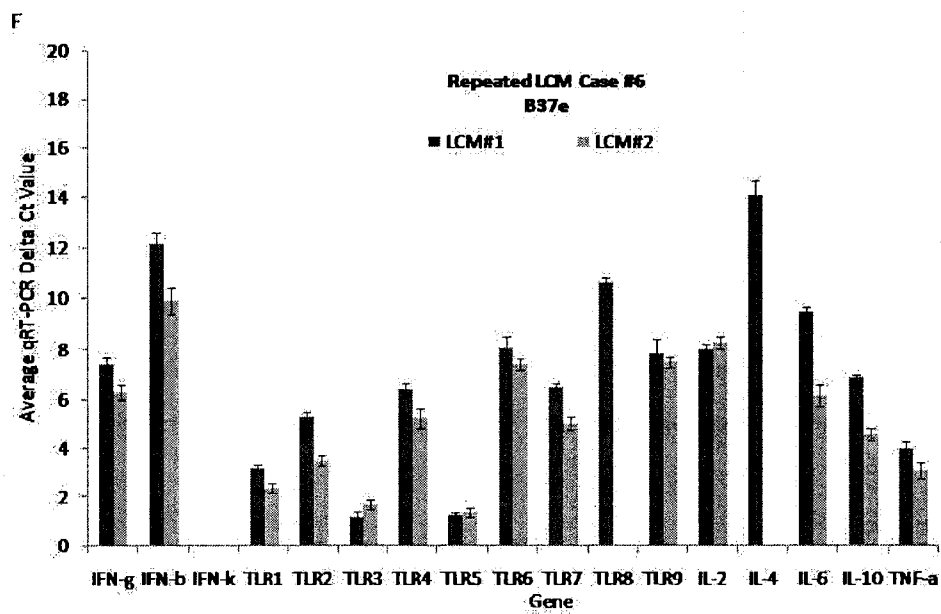
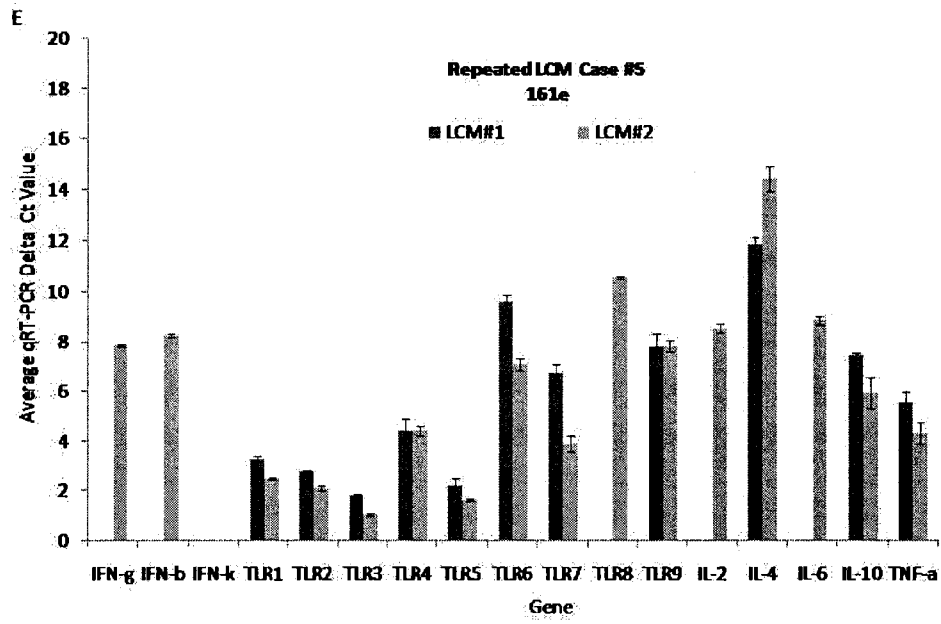


**Figure 35. IFN expression in cervical carcinoma epithelium and stroma.** . IFN- $\kappa$ , - $\gamma$ , - $\beta$ , TLR1-9, IL-2,-4,-6,-10, and TNF- $\alpha$  gene expression was measured separately in the epithelium and stroma of cervical carcinoma tissue using laser capture microdissection. The mRNA levels of genes were analyzed using qRT-PCR. Vertical bars represent the average delta qRT-PCR Ct value  $\pm$  SD. cDNA input concentrations were determined using the Experion™.

## 6.5 Inter-Individual Distribution of Innate Immunity Gene Expression







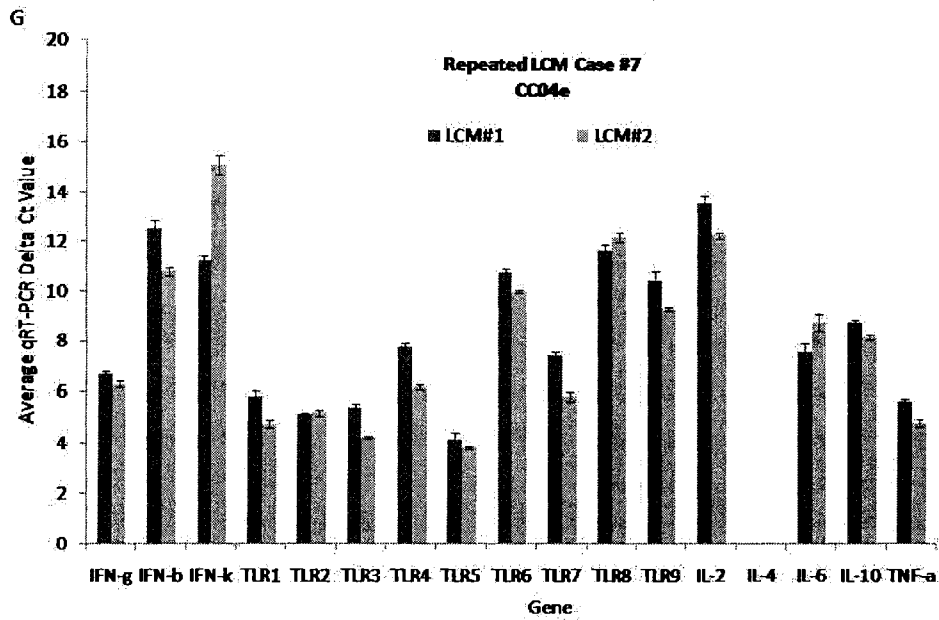


**Figure 36.** A survey of gene expression in different tissue layers within 7 individual tissue samples. Cervical epithelium and stroma were excised from tissue samples separately on two occasions in the same region using LCM and the mRNA levels of 16 genes were analyzed using qRT-PCR. Dark grey bars indicate the first microdissection experiment and the light grey bars indicate the second microdissection experiment. Vertical bars represent the average delta qRT-PCR Ct value  $\pm$  SD. cDNA input concentrations were determined using the Experion™.